Application of Shrimp Waste Based Biomass for Removal of Heavy Metals (Cadmium(II), Copper(II), Nickle(II)) from Aqueous Phase

Zeinab Hejazi

Thesis submitted to the University of Ottawa
in partial Fulfillment of the requirements for the
Master of Applied Science

Department of Civil Engineering
Faculty of Engineering
University of Ottawa

Supervisor: Dr. Majid Sartaj

Abstract

Finding economical and environmentally friendly processes to remove heavy metals (HMs) from industries' influent is a research priority to move toward sustainability. Shrimp shell waste (SSW) could be converted to an efficient adsorbent for HM uptake from aqueous solutions. In this study, two methods – the conventional method and the deep eutectic solvents (DESs) method – are assessed for the removal of proteins and minerals from SSW and the extraction of chitin.

Chitin extracted by the conventional method (Ch-C) and extracted by the DES method (Ch-DES) prepared to remove Cu(II), Cd(II) and Ni(II) from single-component aqueous solution in the first phase. The effect of experimental factors, including the pH, adsorbent dosage, initial concentration, and temperature on removal efficiency and adsorption uptake of Ch-C in a single-component system was evaluated to optimize the adsorption conditions. SEM, FT-IR and BET of the synthesized Ch-C confirmed the removal of protein and mineral components, increased surface area and pore volume, and uptake of HMs after adsorption. The isotherm study showed that Langmuir isotherm was the best fit to the experimental data of Cu(II), Cd(II) and Ni(II) adsorption on Ch-C and thermodynamic studies showed all the adsorption reactions were exothermic, physical and spontaneous. Then, Ch-C and Ch-DES were used for Cu(II), Cd(II) and Ni(II) adsorption from competitive aqueous media in the second phase. The Langmuir model showed that the maximum adsorption capacity of chitin in a multi-component system is for Cu(II), with maximum adsorption capacity of 42.20 mg/g for Ch-DES versus 32.88 mg/g for Ch-C, showing an improvement of approximately 28% for q_{max} under same experimental conditions. The q_{max} of Cd(II) and Ni(II) were 29.85 and 19.71 mg/g onto Ch-C, 38.25 and 23.48 mg/g onto Ch-DES. The pseudo-second-order best fitted all the experimental data and the thermodynamic study showed that all the adsorption reactions were exothermic, physical and spontaneous. While DESs were utilized as a green extraction medium for chitin, a comprehensive assessment should be conducted for the potential impacts to disposal or reuse, especially in large-scale applications

Keywords: Heavy metals, adsorption, DES, Kinetics study, Thermodynamic study, Characterization.

Dedication

To my dear parents, Maryam and Bahram,

My sister, Darya

&

My beloved partner, Amir

Acknowledgements

First and foremost, I would like to express my deepest gratitude to my supervisor, Dr. Majid Sartaj, for his invaluable guidance, support, and constant encouragement throughout my journey. His kindness, positivity, and belief in me have been a true source of motivation. I am especially grateful for the financial support that made this work possible and for creating an environment where I could grow both professionally and personally. I am also deeply thankful to Soroor (Fatemeh) Bagh, Ph.D., EIT, for her generous time, insightful guidance, and support throughout my thesis. Working alongside her has been an incredible learning experience that I will always cherish.

My deepest appreciation goes to my family, whose endless emotional and financial support and unwavering belief in my abilities have carried me through every chapter of my life. To my friends in Iran and Canada, thank you for always believing in me, no matter the distance.

Lastly, to my love, Amir – you've been by my side through every step of this journey. From starting our master's program together to facing every challenge and celebrating every success hand in hand – your presence has made this path meaningful.

This success is not mine alone. It belongs to all of you who stood by me with love, patience, and faith.

Thank you!

Table of Contents

Abstract ii
Dedication iii
Acknowledgements iv
List of Figures ix
List of Tables x
List of Abbreviations xii
Chapter 1 : Introduction 2
1.1 General Background 2
1.2 Research Objectives 4
1.3 Thesis Organization and Outline 5
1.4 References 6
Chapter 2 : Literature Review 8
2.1 Water Resources Pollution 8
2.2 HMs – Properties and Impact 8
2.2.1 Cadmium (Cd) 10
2.2.2 Copper (Cu) 10
2.2.3 Nickel (Ni) 11
2.3 Methods of HMs' Removal 11
2.3.1 Membrane Filtration 11
2.3.1.1 Microfiltration (MF) 12
2.3.1.2 Ultrafiltration (UF) 13
2.3.1.3 Nanofiltration (NF) 13
2.3.1.4 Reverse osmosis 13
2.3.1.5 Electrodialysis 13
2.3.2 Chemical Precipitation 15
2.3.2.1 Hydroxide Precipitation 15
2.3.2.2 Sulfide Precipitation 16
2.3.2.3 Carbonate Precipitation 16
2.3.2.4 Chelating Agent Precipitation 16
2.3.2.5 Disadvantages and Drawbacks 16
2.3.3 Ion-Exchange 19
2.3.4 Adsorption 22

2.4 Shrimp Shell Waste (SSW), Chitin and Chitosan 24
2.4.1 Chitin and Chitosan production 27
2.4.1.1 Conventional Method 27
2.4.1.2 Ionic Liquids (ILs) 29
2.4.1.3 Deep Eutectic Solvents (DESs) 31
2.4.1.4 DESs Synthesis 33
2.4.1.5 Chitin Extraction with DES 34
2.5 SSW, Chitin, and Chitosan adsorption uptake 36
2.6 Adsorption mechanisms and influencing parameters 37
2.6.1 Solution pH 39
2.6.2 Adsorbent Dosage 40
2.6.3 Metal Initial Concentration 40
2.6.4 Temperature 40
2.6.5 Contact Time 42
2.7 Summary and Research gap 43
2.8 References 43
Chapter 3 : Materials & Methods 45
3.1 Reagents and Chemicals 45
3.2 Preparation of Shrimp Shells 45
3.3 DES Synthesis 46
3.4 Chitin Extraction using Conventional Method 46
3.5 Chitin Extraction using DES Method 47
3.6 Ch-C and Ch-DES Characterization 48
3.8 Kinetic Study 50
3.9 Thermodynamic Study 50
3.10 References 50
Chapter 4 : Technical Paper 52
4.1 Abstract 52
4.2 Introduction 53
4.3 Materials & Methods 56
4.3.1 Reagents and Chemicals 56
4.3.2 Preparation of Shrimp Shells 57
4.3.3 DES Synthesis 57
4.3.4 Chitin Extraction using Conventional Method 57

4.3.5 Chitin Extraction using DES Method 58
4.3.6 Ch-C and Ch-DES Characterization 59
4.3.7 Batch adsorption isotherm 59
4.3.8 Adsorption isotherm models 61
4.3.9 Thermodynamic Study 61
4.3.10 Kinetic Study 62
4.4 Results & Discussion 62
4.4.1 Chitin Yield% 62
4.4.2 Effect of Experimental factors on Adsorption in Single Component System 64
4.4.2.1 Ch-C dosage 64
4.4.2.2 pH 67
4.4.3 Adsorption isotherm models in single component system (Ch-C) 70
4.4.4 Thermodynamic analysis 74
4.4.5 Kinetics Study 77
4.4.6 Multi-Component adsorption mechanisms 78
4.4.6.1 Isotherm Study 78
4.4.6.2 Thermodynamic Study 81
4.4.6.3 Kinetic Study 83
4.5 Chitin Characterization 85
4.5.1 BET Analysis – Surface Area and Total pore volume 85
4.5.2 SEM Analysis 86
4.5.3 SEM-EDS Analysis 87
4.5.4 FT-IR Analysis 88
4.6 Comparison with other adsorbents derived from SSW 90
4.7 Conclusion 93
4.8 References 93
Chapter 5 : Conclusion & Future Works 95
5.1 Conclusion 95
5.2 Recommendations for future work 96
References 97
Appendices 117
Appendix A: Complementary Results 117
A1: Kinetic study 117
A2: Freundlich Isotherm study of multi-component systems onto Ch-C and Ch-DES 121

A3: FT-IR analysis of Ch-C and SSW in a single-component system 123
A4: SEM-EDS analysis on Ch-DES in a single-component system 124

List of Figures

Figure 2-1 Adsorption process used for removing HMs [56] 22
Figure 2-2 Structure of Chitin and Chitosan [26][92] 25
Figure 2-3 Chitin and Chitosan chemical extraction procedure 28
Figure 2-4 General properties of ILs [114]. 29
Figure 2-5 Schematic representation of a eutectic point on a two-component. 32
Figure 2-6 Structures of various halide salts and HBDs involved in the synthesis of DESs [123]. 33
Figure 2-7 Comparing Conventional method and DES method for extracting chitin from crustacean shells (e.g., in this study SSW). 34
Figure 3-1 The process of preparing Shrimp Shells Powder. 46
Figure 3-2 Schematic representation of chitin extraction by; (a) Conventional method (Ch-C), (b) DES method (Ch-DES). 47
Figure 4-1 Schematic representation of chitin extraction by; (a) Conventional method (Ch-C), (b) DES method (Ch-DES). 58
Figure 4-2 Adsorption uptake (mg/g) of chitin for Cd, Cu, and Ni using different synthesized DESs. 63
Figure 4-3 Effect of Ch-C dosage on removal efficiency (%) and adsorption uptake (mg/g) of Cd(II), Cu(II), and Ni(II). 66
Figure 4-4 Effect of pH on removal efficiency (%) of Cd(II), Cu(II) and Ni(II), onto Ch-C. 68
Figure 4-5 Effect of pH on adsorption uptake (mg/g) of Cd(II), Cu(II) and Ni(II), onto Ch-C. 70
Figure 4-6 Langmuir and Freundlich isotherm models of the adsorption of Cd(II), Cu(II) and Ni(II) on a single-component solution by Ch-C. 72
Figure 4-7 Experimental data and Langmuir model for initial concentration 2.5, 10, 50, 75 and 100 ppm of Cu(II), Cd(II) and Ni(II) on Ch-C and Ch-DES with dosage 2.5 g/L at 20 ℃ in a competitive environment. 80
Figure 4-8 PSO kinetics of the adsorption of Cu(II), Cd(II), and Ni(II) in a multi-component system by Ch-C and Ch-DES. 85
Figure 4-9 Plots of SEM analysis Virgin SSW; Virgin Ch-C; Ch-C loaded with Ni(II), Cd(II) and Cu(II). 87
Figure 4-10 SEM-EDS analysis of (a) Ch-C and (b) Ch-DES after adsorption of Cu(II), Cd(II), and Ni(II). 88
Figure 4-11 FT-IR analysis for SSW, Ch-C and Ch-DES before and after adsorption of HMs. 90

List of Tables

Table 2-1 Chemical properties and Characteristics common HMs along with maximum contamination in drinking water (mg/L) [38-42]. 9
Table 2-2 Various types of membrane technologies involved in Cd, Cu and Ni removal. 12
Table 2-3 Comparison of the performance of different membrane filtration methods [17][46][47][56]. 15
Table 2-4 Removal of HMs by different precipitation methods. 18
Table 2-5 Removal of HMs by ion exchange. 20
Table 2-6 Finding on studies of various bio-sorbents, zeolites and clay minerals. 24
Table 2-7 Some physical and chemical properties of chitin and chitosan [26]. 26
Table 2-8 Chemical extraction methods for recovery of chitin [24]. 28
Table 2-9 Conditions applied in research on chitin extraction by DES and conditions for DES synthesis. 35
Table 2-10 Cd, Cu and Ni adsorption on chitin, chitosan and SSW. 36
Table 2-11 Frequently used adsorption isotherms models for single-component system. 38
Table 2-12 Thermodynamic equations and their parameters. 41
Table 2-13 The kinetic models used for HM adsorption. 43
Table 3-1 The different molar ratios that were examined in this study for DES. 46
Table 4-1 The different molar ratio that were examined in this study for DES. 57
Table 4-2 Chitin yield (%) using different DESs synthesized under given conditions. 63
Table 4-3 Initial pH (before adsorption) and final pH (after adsorption). 69
Table 4-4 Langmuir and Freundlich results for adsorption of Cd(II), Cu(II), and Ni(II) on a single-component solution by Ch-C. 73
Table 4-5 The studied desorption media for Cu(II), Cd(II) and Ni(II) onto Ch-C and Ch-DES in a single-component system. 73
Table 4-6 Thermodynamic parameters for HMs adsorption onto Ch-C at pH 6 for Cd(II) and 5 for Cu(II) and Ni(II), dosage 2.5 g/L and HM concentration 2.5 mg/L. 75
Table 4-7 Thermodynamic parameters for HMs adsorption onto Ch-DES at pH 6 for Cd(II) and 5 for Cu(II) and Ni(II), dosage 2.5 g/L and HM concentration 100 mg/L. 76
Table 4-8 Results of kinetic study after fitting the models to equilibrium curve. 78
Table 4-9 Isotherm parameters for adsorption of HMs onto Ch-C and Ch-DES in a multi-component system. 78

Table 4-10 The studied desorption media for Cu(II), Cd(II) and Ni(II) onto Ch-DES in a multi-component system. 81
Table 4-11 Thermodynamic parameters for HMs adsorption onto Ch-C at pH 5.5, dosage 2.5 g/L and HMs' concentration 100 mg/L in a multi-component system..... 82
Table 4-12 Thermodynamic parameters for HMs adsorption onto Ch-DES at pH 5.5, dosage 2.5 g/L and HMs' concentration 100 mg/L in a multi-component system..... 83
Table 4-13 Results of kinetic study after fitting the models to equilibrium curve. 83
Table 4-14 BET surface area and total pore volume of SSW, Ch-C and Ch-DES..... 86
Table 4-15 Comparison of Ch-C and Ch-DES with different adsorbents derived from SSW in a single-component and multi-component system. 91

List of Abbreviations

DA	Degree of Acetylation
DD	Degree of Deacetylation
DES	Deep Eutectic Solvent
HBA	Hydrogen Bond Acceptor
HBD	Hydrogen Bond Donor
HM	Heavy Metal
IL	Ionic Liquid
MF	Microfiltration
MW	Molecular Weight
NF	Nanofiltration
PFO	Pseudo-First-Order
PSO	Pseudo-Second-Order
SSA	Specific Surface Area
SSW	Shrimp Shell Waste
UF	Ultrafiltration
WR	Water Resources

Chapter 1

Introduction

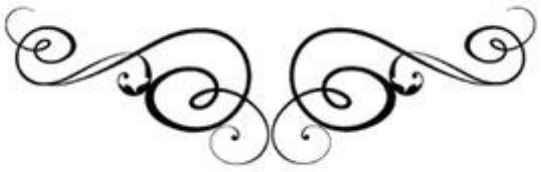

Chapter 1: Introduction

1.1 General Background

The global population is steadily increasing, and it is projected to reach 9.7 billion in 2050 [1]. As a result of population growth, natural resources are decreasing rapidly due to higher consumption rates and anthropogenic activities. Advancements in technology and industrialization further accelerate resource exploitation by driving higher energy demands, large-scale production, and intensive raw material extraction, which results in ever-increasing generation of solid wastes [2], [3], [4]. In addition, the increasing population and industrialization contribute to the higher disposal rates of a variety of contaminants into the environment, leading to pollution of natural resources, including water resources (WRs). The contamination of freshwater systems poses a significant challenge, as these resources are inherently limited [5]. Addressing these challenges requires a shift towards sustainable development and circular economy principles, which focus on minimizing waste, optimizing resource use, and promoting the reuse and recycling of materials. One promising approach involves the application of solid waste as low-cost and environmentally friendly adsorbents for pollution mitigation [6], [7], [8].

Water pollution, caused by contaminants such as heavy metals (HMs), microplastics, pharmaceuticals, and agricultural runoff, is a significant cause for alarm [9]. The reason for this concern lies in the lasting consequences these pollutants have on ecosystems and the overall well-being of the public [10]. Among these, the contamination of water by HMs such as chromium (Cr), cadmium (Cd), Copper (Cu), mercury (Hg), nickel (Ni), lead (Pb), and zinc (Zn) poses a serious threat to human health by causing kidney damage, skin damage, liver damage etc. due to their hemotoxicity [11], [12]. Additionally, HMs' contamination can degrade water quality, disrupt aquatic ecosystems, reduce biodiversity, and lead to the bioaccumulation of toxic substances across food chains [9] [10]. Unlike organic pollutants, HMs are not biodegradable and can accumulate in living organisms, exerting toxic or carcinogenic effects [13]. HMs are among the most common causes of diseases in living organisms, leading to increased attention toward their detection and removal from polluted water/wastewater [11].

Several techniques including adsorption [14], microbial remediation [15], coagulation [14], ion-exchange [14], chemical precipitation [16], reverse osmosis [17], membrane filtration [17], electrocoagulation [14], and solvent extraction [14] have been developed for removing HMs from polluted water [18], [19]. Among these methods, adsorption offers several advantages including low cost, high efficiency, ease of operation, and environmental sustainability, when using abundant and biodegradable waste materials [6], [7], [8]. Unlike other conventional techniques, adsorption does not require high maintenance costs, complex implementation [19], or generate toxic sludge, which is a common issue in chemical precipitation and solvent extraction processes [6]. Moreover, adsorption remains effective even at low HM concentrations (less than 50 ppm) [19].

While synthetic adsorbents such as activated carbon, nano-carbon, resins, and alginate nanoparticles have been widely used for adsorption applications, their large-scale feasibility is often restricted by high operational costs and time-consuming recovery processes [20]. To address these challenges, bio-adsorbents derived from natural and waste materials have gained significant attention for HMs removal [18]. Importantly, the use of natural adsorbents also offers a dual benefit—reducing the environmental burden associated with organic waste disposal by repurposing it for water/wastewater treatment applications [21]. Among various bio-based alternatives, seafood waste is a good alternative due to its abundance, cost-effectiveness, and high adsorption capabilities [18].

The production of seafood, and consequently fisheries waste, has been increasing over the last few decades [18], [20]. According to the Food and Agriculture Organization (FAO), global seafood production reached 223.2 million tons in 2022, marking a 4.4% increase from 2020. It is estimated that up to two-thirds of the total fish volume is discarded as waste, which contributes to environmental concerns [22]. Shrimp is one of the popular seafood among all the others and as a result a total of 3.8 million tons of shrimp shell waste (SSW) is produced annually, which accounts for about 50–60% of the total shrimp volume that is generated through shrimp consumption and processing [20][23]. Although a minor fraction of SSW is converted into fertilizers and supplements, such as chitosan-based products, the majority is improperly disposed of through

methods like landfilling and ocean dumping, which will lead to environmental degradation, including soil contamination, water pollution, and harm to marine ecosystems [24], [25]. Additionally, seafood waste (e.g., SSW) often produces obnoxious gases like ammonia and methane, which can be toxic to humans and other ecosystems [24], [25]. Therefore, effective management of this waste stream is crucial due to environmental and economic considerations.

Shrimp shell is a natural source of polymer chitin and chitosan [18], [19], [20]. Chitin is the second most abundant polysaccharide, following cellulose, and can be converted to chitosan, which is its deacetylated form [26]. Shrimp shells contain a significant amount of calcium carbonate, protein, minerals, oxygen, polysaccharides and nitrogen-containing functional groups [18], [19], [20], [26], [27]. The presence of amine ($-NH_2$), hydroxyl (-OH), and carboxyl (-COOH) functional groups in shrimp shells enables them to interact with HM ions through adsorption. The porous structure of shrimp shells also increases their surface area and results in improvement in HMs' adsorption, which could result in an improvement in HMs' adsorption capacity [19]. Moreover, calcium carbonate enhances alkalinity, which facilitates metal precipitation and immobilization[19]. These combined characteristics make shrimp shell capable of removing HMs from aqueous solutions.

1.2 Research Objectives

This study aimed to convert shrimp shell waste (SSW) to chitin using two different methods, the conventional method and the deep eutectic solvents (DES) method, and to optimize its physicochemical properties and its adsorption efficiency in removing Cd(II), Ni(II), and Cu(II) from liquid phase.

The specific objectives of this study are explained below:

- Modification of SSW using two methods (conventional and DES) to convert it to chitin as a potential biosorbent for the removal of the selected heavy metal ions (Cd(II), Cu(II), and Ni(II)).
- Optimization of adsorbents' performance by changing experimental factors, including pH, adsorbent dosage, contact time, initial metals concentration, and temperature.

- Comparison of the adsorption uptake capacity of the synthesized chitin by DES method with that of the conventional method in a competitive environment for selected HMs.
- Evaluation of Langmuir and Freundlich isotherm models to describe the experimental data in order to evaluate interaction mechanisms and to calculate the maximum adsorption capacity of adsorbents used in this study.
- Investigation of two different kinetic models, pseudo-first order and pseudo-second order models, to understand the rate and mechanism of adsorption.
- Conducting a thermodynamic analysis of the adsorption process by performing adsorption tests at different temperatures to determine the adsorption mechanism.

1.3 Thesis Organization and Outline

This thesis is structured into 5 chapters to present the key findings of this research. The content of each chapter is as follows:

• **Chapter 1: Introduction** – Provides a brief overview of SSW and its potential applications in adsorption. This chapter outlines the challenges associated with HM contamination, the limitations of existing removal techniques, and the significance of developing sustainable and low-cost adsorbents. The research objectives and thesis structure are presented as well.

• **Chapter 2: Literature Review** – Provides a literature review about HMs (characteristics, environmental concerns, structure, etc.) and the importance of their removal from liquid phase. The current techniques of HM removal, along with their obstacles, are discussed in detail in this chapter. It also presents a review pf adsorption as an alternative technique to recover HMs. In addition, this chapter covers the chitin synthesis and modification processes, and the impact of key parameters such as pH, adsorbent dosage, contact time, and temperature on adsorption performance.

• **Chapter 3: Materials & Methods** – Describes the materials, reagents, and experimental procedures used in this research. This includes the preparation and characterization of the modified SSW adsorbent or chitin, the setup of adsorption experiments, and the analytical methods employed to assess HM removal efficiency.

The methodologies used for adsorption isotherm, kinetics, and thermodynamics studies are also detailed in this chapter.

- **Chapter 4: Results and Discussion** – Presents and analyzes the experimental results obtained from adsorption studies. The adsorption performance of the modified SSW is evaluated under different conditions, and the findings are compared with existing literature. The adsorption mechanisms and the effects of various process parameters on HMs' removal are discussed. Chapter 4 is formatted as a technical paper.
- **Chapter 5: Conclusion and Future Works** – Summarizes the key findings of the study, highlighting the efficiency and feasibility of using modified SSW for HMs' removal. This chapter also provides recommendations for future research in the field of sustainable adsorption technologies.

1.4 References

The references are merged with the other chapters' references and presented at the end of the thesis.

Chapter 2

Literature Review

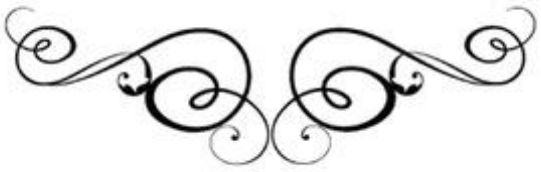

Chapter 2: Literature Review

2.1 Water Resources Pollution

In the 21st century, the protection of WRs is among the most important environmental issues. Different industrial, agricultural and domestic activities could cause pollution of water resources through the discharge of different types of contaminants. It is estimated that more than one-third of the population around the world don't have access to sufficient quantities of safe drinking water [28]. Heavy metals (HMs) are either directly or indirectly released into natural water resources through effluents from industries such as mining, smelters and refineries, battery production, etc. [29]. Commonly observed HMs in wastewater streams are cadmium (Cd), chromium (Cr), copper (Cu), lead (Pb), mercury (Hg), nickel (Ni), and zinc (Zn) [29]. In Canada, cadmium and copper contamination in water is a significant environmental concern. In 2022, Ontario reported the highest cadmium releases into water, accounting for 47% (1,030 kg) of the national total [30]. In 2021, according to the government of Canada, copper contamination in water varied widely, with concentrations ranging from natural background levels of 0.2–30 µg/L to as high as 5,273 µg/L near industrial sites such as in Saskatchewan [31], [32]. Health Canada has established a health-based guideline of 2 mg/L for copper, with an aesthetic objective of 1 mg/L to prevent taste and staining issues and the maximum acceptable concentration for cadmium in drinking water is 0.005 mg/L (5 µg/L) [33]. Moreover, data collected between 1981 and 1992 indicated that most of the industrially impacted rivers and lakes contained nickel concentrations ranging from 50 to 2,000 µg/L [34] while the Canadian Drinking Water Quality Guideline (Health Canada) for nickel proposes a limit of 0.1 mg/L (100 µg/L) [33].

2.2 HMs – Properties and Impact

HMs are defined as metallic elements that have a high density, typically greater than 5 g/cm^3, and an atomic weight between 63.5 to 200.6 [35]. HMs often have negative health impacts due to their non-biodegradable nature and ability to bioaccumulate in living organisms [29]. This makes HMs one group of the most serious environmental contaminants that could cause severe threats to human health and well-being [36], [37]. Even

though HMs have existed naturally in the earth's crust for years (natural sources) [38], [39], human activities (anthropogenic sources) have led to greater releases of these hazardous substances [38], [40]. Table 2-1 summarizes chemical properties and characteristics of common HMs. The main health problems caused by HM toxicity include injury or decline in mental and central nervous system function, increased cancer risk, lower energy levels, and harm to the blood, kidneys, lungs, liver, and other vital organs [38], [40], [41]. Therefore, organizations like WHO and USEPA have set standards for maximum contamination of drinking water with HMs [42]. Some of these data have been presented in Table 2-1.

Table 2-1 Chemical properties and Characteristics common HMs along with maximum contamination in drinking water (mg/L) [38-42].

HMs	Common Sources	Human Health Effects	Maximum Contaminant Level (mg/L)			Molecular Weight (g/mol)	Electronegativity
			WHO*	USEPA*	Canada*		
Arsenic (As)	Naturallry Occuring Electronics Production	Skin damage Circulatory system issues	0.01	0.01	0.01	74.9	2.18
Cadmium (Cd)	Naturallry Occuring Chemical Industries	Kidney damage Carcinogenic	0.003	0.005	0.005	112.4	1.69
Chromium (Cr)	Naturallry Occuring Steel Manufacturng	Allergic dermatitis Diarrhea, Nausea , Vomiting	0.05	0.1	0.05	-	-
Copper (Cu)	Naturallry Occuring Household Plumbing Systems	Gastrointestinal issues Liver or kidney damage	2.0	1.3	1.0	63.5	1.9
Lead (Pb)	Lead-based Products Household Plumbing Systems	Kidney damage Reduced neural development	0.01	0.0	0.005	207.2	2.33
Mercury (Hg)	Fossil Fuel Combustion Electronics Production	Kidney damage Nervous system damage	0.006	0.002	0.001	200.6	2
Nickel (Ni)	Nickel-Cadmium Batteries Electroplating	Carcinogenic Dermatitis, Nausea	-	5.0	0.1	58.7	1.91
Zinc (Zn)	PVC stabilizers Manufacturing Industries	Kidney damage Nervous system damage	0.006	0.002	5.0*	65.4	1.65

* Values established by the World Health Organization (WHO, 2017)

* Values established by the United States Environmental Protection Agency (USEPA, 2019)

* Values established by the Canadian Drinking Water Quality Guidelines (Health Canada)

* Zn is not considered a health concern at levels typically found in drinking water, so only an aesthetic objective is set due to taste and water staining issues.

2.2.1 Cadmium (Cd)

The main anthropogenic sources of Cadmium (Cd) release are mining, electroplating, battery manufacturing, and pigment production. In electroplating, Cd is used to coat metals for corrosion resistance, especially in the aerospace and automotive industries. It is also found in rechargeable batteries. Cd can cause kidney damage, bone demineralization, and cancer in humans (Table 2-1) as well as disrupting aquatic ecosystems and bioaccumulating in fish and other organisms [35]. Moreover, Cd can persist in soils and lead to long-term ecological impacts. Higher Cd levels in soil can inhibit microbial activity, which affects soil health and fertility. Additionally, Cd can be taken up by plants and later enter the food chain and posing risks to herbivores and higher trophic levels [43]. As shown in Table 2-1 and according to USEPA and WHO, the maximum allowable concentration of Cd(II) in drinking water is 0.005 and 0.003 mg/L, respectively.

2.2.2 Copper (Cu)

Copper (Cu) contamination in water bodies arises from both natural processes and human activities. While natural sources include geological deposits and the weathering of rocks and soils, anthropogenic sources significantly elevate Cu levels in aquatic environments [29]. Key contributors include mining operations, agriculture, and sludge from industrial solid waste. Industries such as electronics manufacturing, metal finishing, and plumbing release substantial amounts of copper into wastewater systems [29]. The use of copper in printed circuit board production, roofing materials, and piping systems leads to its eventual leaching into water sources [29]. Even at low concentrations, Cu is toxic to aquatic life, interfering with gill function and enzyme activity in fish and invertebrates [44]. Prolonged exposure can lead to bioaccumulation in aquatic organisms, disrupting ecosystems and food chains. Excessive copper levels degrade water quality by altering clarity and reacting with other pollutants to form harmful compounds [44], [45]. For humans, consuming water contaminated with high levels of copper can cause gastrointestinal distress, liver damage, and kidney dysfunction (Table 2-1) [35][36]. Implementing effective copper removal

strategies is necessary to mitigate its adverse effects and ensure cleaner water resources and sustainable wastewater management practices.

2.2.3 Nickel (Ni)

Nickel (Ni) contamination often results from mining, metal plating, stainless steel production, battery production, and the manufacture of alloys [29][35]. To avoid corrosion and enhance the durability of products like kitchenware, automotive components, and electronics, Ni is extensively used in the electroplating industry. Additionally, Ni is a key material in battery production and serves as a conversion catalyst in petroleum refining. Beyond these industrial uses, Ni is also released into the environment from the combustion of fossil fuels, waste incineration, and sewage sludge disposal [29]. Once introduced into water bodies, Ni can accumulate in sediments and aquatic ecosystems, posing risks to both environmental and human health. High levels of Ni in wastewater can cause adverse health effects, including respiratory issues, dermatitis, and potential carcinogenicity [35][36]. Chronic exposure to Ni has also been linked to gastrointestinal distress, kidney damage, and neurological effects. The persistence of Ni in aquatic environments further contributes to its bioaccumulation in organisms, disrupting ecosystems and food chains.

2.3 Methods of HMs' Removal

The removal methods for HMs from liquid phase include membrane filtration [17], chemical precipitation [16], ion-exchange and adsorption [14]. These removal methods are briefly introduced below.

2.3.1 Membrane Filtration

The basic principle of membrane filtration involves the selective separation of dissolved or suspended particles from a liquid stream by passing it through a semi-permeable membrane. Microfiltration (MF), ultrafiltration (UF), nanofiltration (NF), Forward osmosis, reverse osmosis and electrodialysis are some of

the most commonly used membrane filtration types [17], [46], [47]. Table 2-2 summarizes the results of different types of membrane filtration methods for removal of Cd, Cu and Ni.

Table 2-2 Various types of membrane technologies involved in Cd, Cu and Ni removal.

Membrane Technology	HMs	Type of Membrane	pH	Removal efficiency (%)	References
NF	Cu	polyether-imide based NF membranes	-	67%	[48]
UF	Ni	commercial membrane	3-9	90%	[49]
	Cu	poly(ether sulfone)	1-12	99%	[50]
	Cd	surfactant enhanced UF membrane	1-7	68%	[51]
Forward Osmosis	Cd	thin film nanocomposite	4, 7, 9	98%	[52]
	Cu		7	99%	[53]
Reverse Osmosis	Ni	spiral bound membrane	2-5.5	98.5%	[54]
	Cu			96%	[54]
Electrodialysis	Cd	bipolar membrane	1-3, 7, 11-13	83%	[55]
	Ni			80%	[55]
	Cu			90%	[55]

2.3.1.1 Microfiltration (MF)

MF is a low pressure-driven membrane process which has a microporous membrane to separate micron-sized particles in the range of 0.1–10 μm. Bacteria, viruses, protozoa, contaminants, pollutants, etc. are some of these particles that can be removed from a solution by MF. Because of the low removal ability of HM (Table2-2), the application of MF has not drawn enough attention. However, MF has been used by modifying the membrane or chemical pre-treatment of the feed solution to improve its application in the removal of HMs [56].

2.3.1.2 Ultrafiltration (UF)

UF membranes have pore sizes typically ranging from 0.01 to 0.1 μm, allowing them to effectively remove HM ions and other larger contaminants from water and wastewater. High efficiency, easy operation, and low space requirements make UF an effective method for HMs removal. Controlling factors like membrane material, pore size, operating pressure, pH of the solution, and feed water composition can improve the removal efficiency of HMs to over 90% [17], [46], [47].

2.3.1.3 Nanofiltration (NF)

NF membranes with pore sizes in the range of 0.001 to 0.01 μm have smaller pore sizes compared to UF. This allows NF to effectively remove HMs ions from liquid phase. NF removal efficiency for HMs exceeded 90-95% because of NF's ability to decline both ionic and uncharged HMs through size exclusion and electrostatic interactions. Material selection and surface modifications are considered as factors that can enhance the performance of NF membranes [17], [46], [47].

2.3.1.4 Reverse osmosis

RO membranes have the smallest pore sizes, generally less than 0.001 μm, which allows them to effectively remove a wide range of contaminants, including HM ions, dissolved salts, and organic matter. Size exclusion, Donnan exclusion and other mechanisms support reverse osmosis to exhibit the outstanding removal percentage often in the range of 90-99%. However, reverse osmosis has some drawbacks including high energy consumption and the need for pretreatment to prevent membrane fouling. Therefore, its large-scale application can be limited in some cases [17], [46], [47].

2.3.1.5 Electrodialysis

Electrodialysis is another membrane-based separation technique that utilizes electric potential to move ions across selective membranes, then separating ionic species from solutions. In this process, cation exchange membranes allow only cations to pass, while anion exchange membranes allow only anions to pass. These membranes are alternately arranged between two electrodes in an electrodialysis stack. When a voltage is

applied, cations migrate toward the cathode through cation exchange membranes, and anions travel toward the anode through anion exchange membranes, resulting in the creation of concentrated and diluted streams. Electrodialysis is commonly used for the removal of HMs due to its several advantages including high water recovery rate (80-90%), an effective wide pH range (1-13), and it does not require phase changes like thermal processes do. Nevertheless, its challenges such as membrane fouling (e.g. from particulates and organic matter), and high initial costs (e.g. membrane expenses and energy requirements) limit its application [17], [56].

Drawbacks and Disadvantages

Although membrane filtration methods have shown acceptable results (with removal efficiencies ranging from 67%-99%, presented in Table 2-3) for HMs removal from wastewater, they have some drawbacks which cannot be overlooked. One key issue is membrane fouling, which can reduce permeate flux and separation efficiency over time [17]. Fouling is caused by the buildup of contaminants, scales, and other materials on the membrane surface or within the porous structure [40][41]. Therefore, there is a need for regular cleaning or replacement of the membranes. Thus, the operational and maintenance costs will increase. Another source of high cost will be the requirement of high operating pressures which consume significant energy [49]. This is the case for many membrane processes, such as reverse osmosis. The concentrate or brine waste stream produced also requires further treatment or disposal, which will add to the overall treatment costs [40][41]. Moreover, the limitations of some membrane materials in terms of chemical and thermal stability will restrict their application in treating wastewater with extreme pH or high temperatures [17], [46], [47], [56]. A brief comparison between the performances of the mentioned membrane filtration methods is given in Table 2-3.

Table 2-3 Comparison of the performance of different membrane filtration methods [17][46][47][56].

Methods	Advantages of HMs removal	Disadvantages of HMs removal	Size (nm)	Operation pressure (bar)
UF	Low operational cost and pressure, great performance for HM macro-molecules	Secondary pollutants and requirement of posttreatment	1-100	2-10
NF	Higher HM rejection and more sophisticated separation compared to UF	Higher energy consumption and lower water permeability	< 2	5-30
Reverse Osmosis	Remarkable HM rejection efficiency	Higher energy requirements and lower water permeability	<1	10-100
Electrodialysis	High separation efficiency and metal resource reusability at industrial level	Higher operational cost than UF and NF, but lower than RO	-	-

2.3.2 Chemical Precipitation

Chemical precipitation involves adding chemical substances (e.g., hydroxide, sulfide, and carbonate ions) to the wastewater or aqueous solution to convert dissolved metal ions into insoluble precipitates [14], [16]. These precipitates can then be separated from the liquid through sedimentation or filtration [16]. Chemical precipitation is generally categorized into hydroxide precipitation, sulfide precipitation, carbonate precipitation, and chelating agent precipitation depending on the type of precipitates [16]. The pH, the type of chemicals, the quantity of wastewater, and the pollutant specifications are some of the factors that can influence cost and performance [14].

2.3.2.1 Hydroxide Precipitation

This method involves the addition of alkaline chemicals, such as lime ($Ca(OH)_2$) or sodium hydroxide (NaOH), to increase the pH of the wastewater. The metal ions form insoluble metal hydroxides that can be removed from the solution by increasing pH (see Table 2-5). This process is effective with a removal rate of approximately 76% to 99% for HMs, including copper (Cu), lead (Pb), and zinc (Zn).

2.3.2.2 Sulfide Precipitation

Sulfide precipitation is achieved by adding sulfide compounds (one common chemical used include sodium sulfide (Na_2S)) to the wastewater. HMs can be efficiently removed with the rate of 99% through sulfide precipitation because metal sulfides have very low solubility in water (Ksp values typically range from 10^{-24} to 10^{-36}), causing them to form solid precipitates that can be easily separated from the solution [14]. The sulfide precipitation must be conducted in a basic or neutral pH environment to avoid the formation of toxic hydrogen sulfide gas [14]. Table 2-5 has presented the results of some studies on removal of HMs using sulfide precipitation.

2.3.2.3 Carbonate Precipitation

This method involves the introduction of carbonate salts carbonates such as calcium carbonate ($CaCO_3$) or sodium carbonate (Na_2CO_3) into the contaminated water to precipitate metal ions. When these compounds are added, they react with dissolved metal ions (e.g., Cd(II), Cu(II), Ni(II)) to form insoluble metal carbonates, which precipitate out of the solution. The general reaction can be represented as [16]:

$$M^{2+} + CO_3^{2-} \rightarrow MCO_3(s)$$

where M^{2+} denotes the divalent metal ion and $MCO_3(s)$ is the resulting solid precipitate.

2.3.2.4 Chelating Agent Precipitation

This approach utilizes chelating agents, such as dimethylglyoxime or dithiocarbamate, which form strong complexes with metal ions. These complexes are then precipitated out of the solution. Chelating agent precipitation is effective across a broad pH range and can be used in combination with other methods to improve HM removal [16]. Table 2-5 has presented the results of some studies on removal of HMs using chelating agent precipitation.

2.3.2.5 Disadvantages and Drawbacks

The creation of a large volume of sludge and the cost of chemicals are two of the major disadvantages for chemical precipitation removal of HMs. And it can lead to secondary pollution if not managed properly.

All of these will lead to higher operational costs [16]. Moreover, the presence of complex agents or other ions can affect the efficiency of precipitation methods and may alter the solubility and formation of precipitates [16][50]. Additionally, pH control is necessary in methods such as sulfide precipitation, to prevent the formation of toxic byproducts like hydrogen sulfide gas. Overall, while precipitation methods are effective for HM removal, their operational challenges and environmental impacts need to be addressed through careful process management and potential combination with other treatment technologies to avoid high operational costs [16][57].

Table 2-4 Removal of HMs by different precipitation methods.

Type	Chemical Reagent	pH	HMs	Removal efficiency (%)	References
Hydroxide precipitation	Lime $[Ca(OH)_2]$	11	Cu, Pb, Zn	99.99%, 76.14%, 99.99%	[58]
Hydroxide precipitation	Soda Ash $[Na_2CO_3]$	11	Cu, Pb, Zn	99.99%, 97.78%, 99.99%	[58]
Sulfide precipitation	Sodium Sulfide $[Na_2S]$	9	Cu, Pb, Zn	99.99%, 99.75%, 99.99%	[58]
Chelating agent precipitation	CN-containing HM wastewater	7-11	Cr, Fe, Ni, Zn	-	[59]
Chelating agent precipitation	Dimethylglyoxime	5	Ni	98.7%	[60]
Chelating agent precipitation	Diethyldithiocarbamate	7.3-11	Cd, Cu, Pb, Zn	86.72%, 98.42%, 88.82%, 75.20%	[61]
Chelating agent precipitation	Diphenyldithiocarbamate	7.3-11	Cd, Cu, Pb, Zn	87.97, 99.98%, 93.40%, 95.76%	[61]

* Please note that the results provided on this table are the best indicated removal % of the specific HM with mentioned reagent in the given reference. The optimal pH and other experimental conditions can be found in detail in related paper.

2.3.3 Ion-Exchange

The ion-exchange method is a widely used technology for the removal of HMs from wastewater, primarily due to its high selectivity and efficiency (90-99%) [16]. This process works by exchanging ions present in a solution with ions on the surface of ion exchange resins. These resins, which are highly porous with a large surface area [14], act as a medium for capturing metal ions [16]. Their high porosity allows for increased exchange capacity, as more active sites become available for metal ion binding. Moreover, a larger surface area enhances interaction with contaminants, improving the overall efficiency of the removal process [16]. Depending on the charge of the ions being removed, ion-exchange resins are classified into cationic, anionic, and chelating types [14]. Cationic ion-exchange resins remove positively charged ions (cations) by exchanging them with other cations attached to the resin [14]. Anionic ion-exchange resins, on the other hand, are designed to exchange negatively charged ions (anions) [14]. Chelating resins contain specific functional groups such as iminodiacetic acid ($-N(CH_2COOH)_2$) or thiol (-SH) that form strong bonds with metal ions, making them especially useful for selectively removing toxic metals such as Cu, Cd, Pb and Zn [14][16]. Tavakoli et al. (2017) investigated the removal of Cu^{2+}, Pb^{2+}, Cd^{2+}, and Zn^{2+} from squid oil using chelating ion-exchange resins, including CR11, PEI-chitosan beads, and PEI-chitosan fibers. The CR11 resin demonstrated the highest efficiency toward Cu^{2+} with removal efficiency of 96% at 573 K [62]. Similarly, Bensalah et al. (2022) studied the AmIRC-50 cationic exchange resin for Co^{2+} removal, achieving 100% efficiency under optimal conditions of pH 5, 120 minutes contact time, and a temperature of 30 °C [63].

The results of a few research regarding the removal of HMs using ion-exchange method have gathered and provided in Table 2-5.

Table 2-5 Removal of HMs by ion exchange.

Method	Material	pH	HMs	Removal efficiency (%)	References
Ion-Exchange	MTS9301, MTS9570, MTS9501, TP214, C107E	4-6.5	Cu, Fe, Pb, Zn	Cu>Fe>Pb>Zn	[64]
	Lewatit TP 207 resin/Lewatit MonoPlus MP 64 resin	1-4,7	Cu, Ni, Zn	-	[65]
	Iminodiacetate chelating resin (Suqing D401)	4-7	Cu, Ni, Zn	-	[66]
	Bispicolylamine-based chelating resin (Puromet MTS9600)	2-4	Cu, Ni	97%, 98%	[67]
	Carboxymethyl chitosan-hemicellulose resin	4-6	Ni, Cd, Cu, Hg, Cr, Mn	100%<=	[68]

Moreover, zeolites [64] and clay minerals [65] are used as an ion-exchange material, which will be briefly explained.

Zeolite

Zeolites $(MAl_2)\ (SiO_2)_x\ (H_2O)_y$, where M is usually H^+ and Na^+, are aluminosilicate minerals that contain alkali or alkaline earth metals and crystal water. 20 to 50% of zeolites' structure consist of void spaces [69]. Therefore, zeolites have been widely studied and used for removing HMs from aqueous [70], [71]. The main advantage of using zeolites in HM removal is their high cation exchange capacity which allows them to effectively adsorb and exchange metal ions like lead (Pb), cadmium (Cd), and copper (Cu) [70], [72]. This ion-exchange property is facilitated by the negatively charged framework of zeolites that can attracts and holds positively charged metal ions [70], [72].

However, the use of zeolites also comes with some disadvantages. Zeolites' selectivity is one of its limitations. Zeolites may favorably adsorb certain metal ions over others, which can affect their overall efficiency in treating complex wastewater that contains multiple types of contaminants [71]. The potential need for modification of natural zeolites to enhance their adsorption performance is another challenge. This will add complexity and cost to the treatment process [70], [73].

Clay Minerals

Bentonite, montmorillonite, and kaolinite are some of the clay minerals that are highly effective for removing HMs from contaminated environments. The high efficiency is due to their high cation exchange capacity and large specific surface area [74], [75]. This property enables clay minerals to adsorb HM ions through ion exchange and surface adsorption mechanisms [75]. The abundance of clay minerals makes them a cost-effective adsorbent and furthermore highlights their applications in removing HMs as a suitable choice of an adsorbent [76]. Bentonite and montmorillonite are used for treating wastewater and contaminated soil because they have high adsorption capacity [75], [77]. However, factors such as pH, temperature, and the presence of competing ions can affect the function of CMs and as a result, affect the adsorption process. Although raw clay minerals are effective, to further enhance their adsorption performance, there is often a need for modification process, which naturally can increase the cost and complexity of treatment [75].

Several factors influence the effectiveness of ion-exchange resins. The pH [14] of the wastewater is critical, as resins may perform better within specific pH ranges depending on the metal being removed [33,34]. Other important factors include temperature[14], contact time , resin dosage, and the presence of competing ions in the solution [14][16], [57].

Disadvantages and Drawbacks

Secondary fouling is one of the primary drawbacks for this method [14]. During the regeneration of resins using chemicals such as acids or bases, residual contaminants may build up on the resin and then lower its efficiency over time [14]. Another significant issue is the need for pre-treatment. Wastewater often contains oils, greases, or other organic materials that can clog ion-exchange resins. This will cause the requirement of additional filtration steps before ion exchange can be used [16]. Furthermore, in real industrial wastewater which has the presence of multiple metal ions, resin saturation can occur quickly and thus results in reducing the resins' ability to selectively remove specific metals [57]. Although chelating resins offer better selectivity, they can still suffer from rapid saturation and may require frequent regeneration [57]. The

costs and environmental impacts of resin regeneration, along with operational complexities, present challenges that limit ion exchange's widespread use in large-scale wastewater treatment systems [16], [57].

2.3.4 Adsorption

Compared to other methods discussed above, adsorption offers some benefits including flexibility and ease of operation, possibility in terms of production of high-quality product, economic viability in the context of initial capital cost and chemical requirement, and effectiveness in the purification process [78]. Adsorption is a process in which a compound is transferred and accumulates at the boundary between two phases (e.g. liquid-solid or gas-solid) [49]. The target substance, known as the adsorbate, adheres to the surface of the solid phase, called the adsorbent, through physical or chemical interactions (Figure 2-1) [56]. Various adsorbents have been employed for HMs adsorption, including activated carbons [79], bio-sorbents [80], and nano-adsorbents [81].

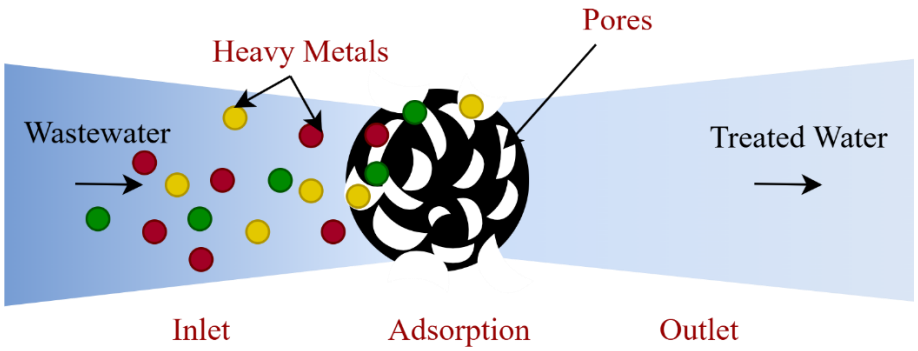

Figure 2-1 Adsorption process used for removing HMs [56]

Activated Carbon

Activated carbon (AC) is a carbon-based material and a highly effective adsorbent known for its extensive surface area, high porosity, broad spectrum of oxygenated functional groups, and adaptable adsorption capabilities [82], [83]. These properties make AC widely used in water treatment and pollution remediation. Despite its effectiveness in adsorption processes, activated carbon has some limitations and disadvantages. One of the primary drawbacks is the high production cost. This can be particularly related to using chemical

and physico-chemical activation methods, which require significant capital investment and operational expenses [84]. In addition, the modification of AC can be problematic. For example, using strong oxidants for modification can damage the porous structure, and reduce adsorption capacity [84]. Another issue is the regeneration of AC, which can be costly and energy-intensive [83], [85]. The disposal of used AC also poses environmental challenges, because it may contain adsorbed toxic substances. All these drawbacks limit activated carbon's application on a large scale.

Bio-Sorbents

The need to remove or recover HMs from water has led some researchers to explore low-cost alternatives. This has drawn attention to natural materials and certain industrial and agricultural waste products for their potential in HMs uptake [86]. The term "low-cost adsorbents" typically refers to materials that are inexpensive and available in large quantities. Biological-origin adsorbents (bio-adsorbents) have advantages over those from chemical sources. Typical bio-adsorbents include non-living biomass such as bark, lignin, shrimp, krill, squid, and crab shells. Other sources of bio-adsorbents include algal biomass and microbial biomass like bacteria, fungi, and yeast [87].

Bio-adsorption of HMs from aquatic environments is a relatively new and promising technique, particularly suitable for treating solutions with low concentrations of HMs (2.5-25 mg/L) [88]. Chitin has gained significant interest as a raw material for metal sorption among various bio-adsorbents due to its abundance of functional groups, including amine and hydroxyl groups, as well as its ease of modification [87]. Additionally, its biodegradability, biocompatibility, and bioactivity contribute to its widespread applicability. Furthermore, chitin can be extracted from SSW which makes it both readily available and cost-effective. Given these advantages, the following sections review the literature on chitin's structure, properties, synthesis, modifications, and diverse applications.

Table 2-6 provides findings of some studies on various bio-sorbents (e.g., lignin, chitosan, flax fiber, etc.) and zeolites and clay minerals as an ion-exchange material.

Table 2-6 Finding on studies of various bio-sorbents, zeolites and clay minerals.

Adsorbents	HMs Removed	pH range	adsorption capacity (mg/g)	Removal (%)	Reference
Carbon-based materials (biochar/AC)	Hg, Cr, Cu, Pb, Cd, Ni, Zn	1-12	2.67-145.74	33.22 – 99.9	[89][90]
DES Modified Oat Straw	Cu, Zn, Se	2-6, 2-9	48.21, 55.06, 87.85	-	[91]
SiO2/lignin	Pb	1-9	89.02	> 90	[92]
Lignin-based composite	Cr	1.5-7	898.2	85%	[93]
Hydrolyzed Corn starch	Zn	2-7	508.85	-	[94]
Flax Fiber	Cr	2-8	97.4	> 90	[95]
Chitosan	Cr	2-8	321.3	-	[96]
Bentonite Clay Mineral	Pb, Cd, Hg, Cr	2-7	10.2 - 11.35	> 90	[89]
Zeolites	Pb, Cd, Cu, Co, Cr, Hg, Ni, Zn	3-8	0.25 – 150	70 – 99.5	[97]

2.4 Shrimp Shell Waste (SSW), Chitin and Chitosan

Marine materials have gained significant attention as bio-adsorbents because they are biocompatible, cost-effective, widely available, and contain chitin that can further convert to chitosan [27]. The processing of crustaceans generates millions of tons of shell waste each year that could lead to environmental pollution [98]. Literature reviews indicate that these marine resources are non-toxic and insoluble in water and have active functional groups like $-NH_2^-$, -CH, $-PO_4^{3-}$and −OH [27]. Global shrimp production exceeded 3.5 million tons in 2008 [27], therefore causing a lot of challenges to use cost-effective and environmentally friendly techniques for their management and disposal [98]. Thailand, Vietnam, China, Ecuador, India, Brazil, Iran, and Saudi Arabia can be named as the main countries in the global production and export of shrimps [27]. Currently, SSW is managed through various valorization pathways such as the extraction of

chitin and chitosan, production of animal feed ingredients, composting, and biogas generation [99]. In many regions, small-scale and industrial setups are increasingly utilizing enzymatic and microbial treatments to convert shrimp shell waste into high-value bioactive compounds [99]. Shrimp shells contain several valuable bioactive compounds, including proteins, and calcium carbonate [98] and it is structurally very similar to the two highly cost-effective biopolymers, chitosan and chitin [27].

Chitin is a high molecular weight, white color, hard, inelastic polysaccharide containing nitrogen. It is a natural biopolymeric substance composed of 2-acetamido 2-deoxy-β-D-glucose linked by a β-(1,4) bond [27][100]. Following cellulose, chitin is the most abundant linear mucopolysaccharide polymer on Earth [101]. As shown in Figure 2-2 [102], chitin can be considered cellulose with the hydroxyl group at position C-2 substituted by an acetamido group [26][102][103].

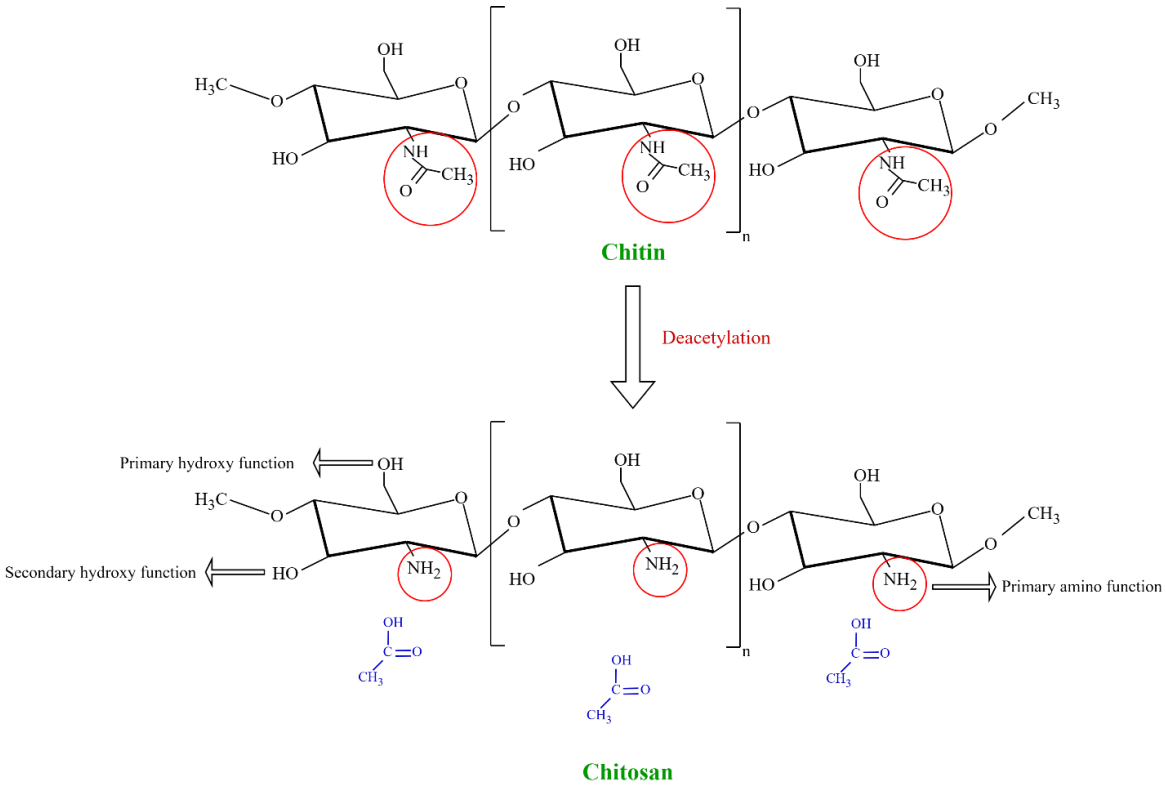

Figure 2-2 Structure of Chitin and Chitosan [26]**[92]**

In 1859, Rouget discovered that chitin could be modified by boiling it in potassium hydroxide solutions. Hoppe-Seiler, in 1894, renamed this "treated chitin" as "chitosan" and pronounced it as “kite-O-san” [104].

Figure 2-2 indicates that chitosan is the N-deacetylated form of chitin [105] and is poly[(1,4)-β-linked 2 amino-2-deoxy-D-glucose]. Also, it has amino groups in its structure (poly-glucosamine). Solid-form chitosan is a semi-crystalline polymer, with lower crystallinity compared to chitin.

Despite having the same chemical structure, chitin and chitosan can be distinguished by their solubility in acidic solutions. Chitosan is identified by its solubility in diluted acidic solutions, such as 1% acetic acid or 1% hydrochloric acid, which is typically associated with a degree of deacetylation (DD) greater than 0.55 [103]. In dilute aqueous acids, chitosan becomes fully soluble below pH=3, as the free amino groups at the C2 position of its backbone (D-glucosamine unit) are protonated [106]. The DD, which is the ratio of 2-acetamido-2-deoxy-D-glucopyranose to 2-amino-2-deoxy-D-glucopyranose units, is crucial in defining chitosan and chitin [107]. This parameter, also referred to as the degree of acetylation (DA), significantly impacts the properties of chitin and chitosan. For chitosan, a typical DD is greater than 65-70% [103]. Table 2-7 [26] has summarized some properties of chitin and chitosan.

Table 2-7 Some physical and chemical properties of chitin and chitosan [26].

Properties	**Chitin**	**Chitosan**
Structure	Poly-(2-acetamido-2-deoxy-D-glucose)	Poly-(2-amino-2-deoxy-D-glucose)
DD (%)	< 50	>65-70
Molecular Weight (kDa)	100-1000	20-750
Reactive groups	Hydroxyl and Carboxyl groups	Amino and Hydroxyl groups

Chitin's unique properties, such as non-toxicity, hydrophilicity, biodegradability, and biocompatibility, make it an effective adsorbent [108]. The active functional groups of carboxyl and hydroxyl in chitin will adsorb the metal ions through either complex formation or chelation, which results in effective adsorption of HMs [27].

2.4.1 Chitin and Chitosan production

Shrimp shells are among the most abundant raw materials for production of chitin [101][109]. Organisms (e.g., marine crustaceans such as shrimp, crabs, and lobsters) that contain chitin in their structure consist of three main components: chitin (20-30%), minerals (30-60%), and proteins (20-40%). Chitin functions as a structural framework, minerals (primarily inorganic carbonate salts) provide necessary strength, and proteins contribute to the formation of living tissue [110]. Hence, there is a need to extract the mineral and protein components from the raw materials to produce chitin. Chitin extraction from SSW typically involves either chemical or biological methods, with chemical approaches being more commonly used due to their greater efficiency and scalability. In the following section, two chemical extraction techniques are discussed in detail for isolating chitin from SSW.

2.4.1.1 Conventional Method

The common chemical extraction process for chitin includes steps such as demineralization (removing calcium carbonate and calcium phosphate), deproteinization (removal of proteins), and sometimes decolorization (removal of pigments), as illustrated in Fig 2-3. The demineralization generally involves acids such as sulphuric acid, nitric acid, formic acid, and acetic acid, with the most commonly used acid being hydrochloric acid (HCl) [111][112]. Then, deproteinization is carried out using alkali to remove protein. Sodium hydroxide (NaOH) is commonly used for this step [111], [112]. The key factor in producing chitin is the quality of the final product, which depends on the molecular weight (MW) and the DD [95].

To convert chitin to chitosan, concentrated sodium hydroxide (NaOH) solution (40-50%) is typically used at temperatures of 100°C or higher to remove some or all acetyl groups [113]. This step is named deacetylation.

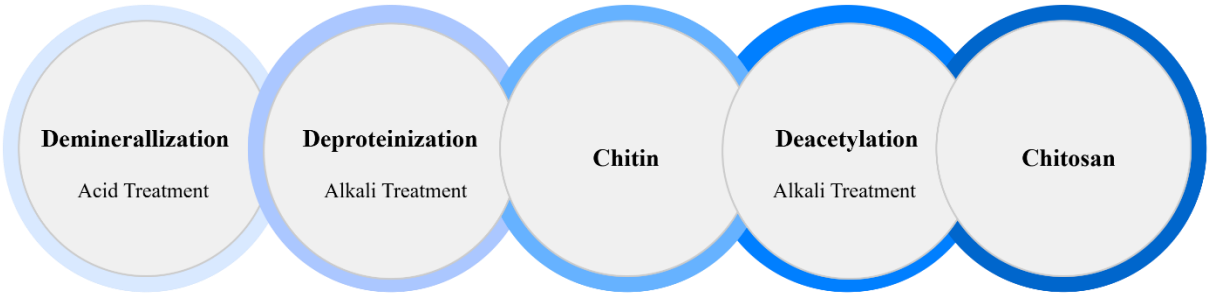

Figure 2-3 Chitin and Chitosan chemical extraction procedure

A few chemical extraction methods are tabulated in Table 2-8. Although chemical processes have some drawbacks, their short extraction time continues to make them the most widely used method in commercial applications [113].

Table 2-8 Chemical extraction methods for recovery of chitin [24].

*DM demineralization, DP deproteination.

Method	Type of Conditions	Properties of recovered chitin
Chemical + enzymatic	DM: 1.5 M HCl, ratio 1:10, at 50˚C for 6 h, DP: A21 pro-tease enzyme/sybstrate 7, 75 U/mg (60 ˚C, 6 h)	88% DP
Chemical + enzymatic	DM: 0.55 M HCl, ratio 1:10 (w/v) at room temperature DP: B. mojavensis A21 crude protease (3 h, 50 ℃, pH 9.0)	DA was 88.5% (shrimp) and 78.6% (crab shell)
Chemical	DM: 1 M HCl, ratio 1:30 75 min at room temperature DP: 3 M NaOH, ratio 1:30 75 min at room temperature	-
Chemical + enzymatic	DM: 1.5 M HCl (50˚C, 2 h) DP: Alcalase (50˚C, 3 h)	80% DP
Chemical	DM: 1.0 M HCl (35˚C, 30 min) DP: 2.0 M NaOH (80˚C, 20 h)	82% DA

Conventional methods for chitin extraction rely on strong acids and alkalis, which can cause environmental concerns and degrade the quality of the final product. As a result, researchers have explored alternative

solvents that offer more sustainable and efficient extraction processes. Among these, Ionic Liquids (ILs) and Deep Eutectic Solvents (DESs) have gained attention for their potential in green chemistry applications.

2.4.1.2 Ionic Liquids (ILs)

Ionic liquids (ILs) are liquid organic salts with promising characteristics and application in various field such as organic synthesis, extraction, electrochemistry, and biochemistry [114] [115]. Unlike conventional salts i.e., sodium chloride, ILs have bulky and asymmetrical ion structures [114]. Non-volatility, low vapor pressure, non-flammability, broad electrochemical windows, excellent thermal stability, and high electrical conductivity are among the other properties that highlight the utilization of ILs in industrial field [116]. Fig 2-4 [114] shows the general properties of ILs. In room temperature, ILs are liquid which typically consist of inorganic anions and organic cations [115]. Ammonium, sulfonium, imidazolium, triazolium, pyridinium, phosphonium, pyrazolium, guanidinium etc. are some of the organic cations that can combine with anions of interest to design ILs [114].

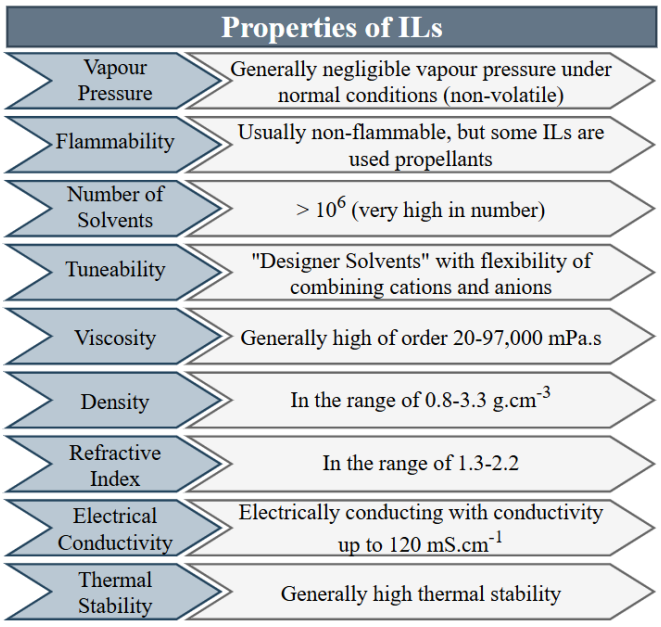

Figure 2-4 General properties of ILs [114].

Due to ILs' properties, it is considered a green solvent, and its application has been widely documented for the removal of dyes, metal ions, organic compounds, and other pollutants from both domestic and industrial

wastewater [117]. Extensive research has highlighted the ability of ILs to effectively extract HMs such as Cu, Cd, Fe, and Ni from aqueous solutions, with the benefit of being recyclable through back-extraction [115]. Furthermore, ILs have been utilized in biomass extraction processes for HM removal. Morias et al. (2020) reviewed several studies on the extraction of different biomass i.e., chitin and chitosan using ILs [118].

Chitin Extraction with ILs

Chitin extraction using ILs typically follows a green, single-pot approach that avoids harsh chemicals. The process begins with dissolving dried crustacean shells (e.g., shrimp or crab) in ILs such as [C2C1im][CH3COO] or [aC1im]Br to remove protein and minerals from chitin [118]. Qin et al. (2010) studied the extraction of chitin from crustacean shells with $[C_2C_1im][CH_3COO]$ which showed a 94 wt% chitin yield [119]. Chitin yield refers to the percentage of chitin extracted from raw shell material, calculated based on the dry weight of the initial biomass. A higher yield indicates a more efficient extraction process. Furthermore, this study carried out a comparison between Cl^- and $[CH_3COO]^-$ anions which revealed higher efficiency of $[CH_3COO]^-$ in chitin extraction due to its higher hydrogen bond basicity [119]. For dissolving chitin from crab shells, Setoguchi et al. (2012) utilized $[aC_1im]Br$ at a temperature ranging from 80°C to 120°C [120]. For precipitation of the polymer and the demineralization process, citric acid was later introduced to the solution as a coagulant and anti-solvent. Although extracted chitin presented a lower molecular weight in higher temperatures, it was concluded that in the higher temperatures the chitin yield is increased to 12.6 wt% [120].

Despite their effectiveness, the application of ILs in chitin extraction presents certain drawbacks. High production costs, complex synthesis processes, and potential environmental toxicity limit their large-scale implementation [121]. Additionally, the viscosity of ILs can hinder efficient mass transfer, which highlights the necessity of further optimization for practical applications [121]. Given these limitations, researchers have explored alternative green solvents such as deep eutectic solvents (DESs) as a more sustainable and cost-effective approach for chitin extraction [121].

2.4.1.3 Deep Eutectic Solvents (DESs)

Deep eutectic solvents (DESs) have emerged as an environmentally friendly and cost-effective alternative to conventional solvents [122]. Due to shared physicochemical and advantages of DESs with ILs, they are often considered analogs to ILs [122]. However, their fundamental formation mechanism is different. Unlike ILs, which are composed primarily of discrete anions and cations (covalent bonds), DESs are formed from a eutectic mixture of hydrogen bond donors (HBDs) and hydrogen bond acceptors (HBAs) [123]. A DES can be generally represented by the formula:

$$Cat^{+}X^{-}zY$$

where Cat^{+} is a quaternary ammonium, phosphonium, or sulfonium cation, X^{-} is a Lewis base, usually halide anion, and Y is a HBD (e.g., urea, carboxylic acids, polyols) [123]. Between X^{-} and either a Lewis or BrØnsted acid Y (which z is referred to number of Y molecules that interact with the anion), the complex anionic species are formed [124].

The term DES refers to liquids formed near the eutectic composition of their components. The eutectic point is the specific molar ratio where the mixture reaches its lowest melting point. As shown in Fig 2-5, DESs follow a typical eutectic phase diagram, where two or more solid components interact through hydrogen bonding and charge delocalization, which will create a stable liquid phase at lower temperatures than their individual melting points [123]. If the composition is not at the eutectic point, it means the mixture has too much HBD or HBA, which will cause partial crystallization. However, when the eutectic composition is achieved, the freezing point drops to its lowest value. This happens because the molecular interactions in the system disrupt the solid structure of the separate components and forms a homogeneous liquid [124].

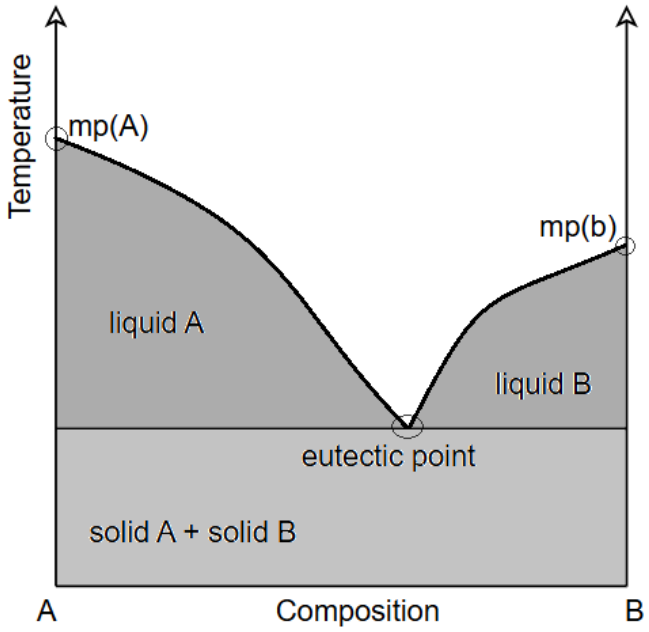

Figure 2-5 Schematic representation of a eutectic point on a two-component.

One of the common characteristics of DESs is their significantly lower melting point compared to each of their compounds [125]. This reduction in melting point arises from strong hydrogen bonding interactions between a HBA, and a HBD, such as glycerol [125]. Choline chloride (ChCl) is the most common HBA which is a non-toxic, low cost and biodegradable salt also known as vitamin B4 and can be combined with HBD such as urea, renewable carboxylic acids (e.g., citric, amino acids, oxalic) or renewable polyols (e.g., glycerol, carbohydrates) [126][111]. DESs are non-toxic, biodegradable, thermally stable, easy to prepare, and usually hydrophilic [122], [125]. However, this can limit their application as their water instability can lead to the separation of components [122]. DESs are categorized into four groups: 1) a mixture of organic salts and metal salts, 2) a mixture of organic salts and metal hydrates, 3) a mixture of organic salts and compound being HBD, 4) a mixture of metal chlorides and compounds being HBD [111]. Among all these types, type 3 is the most employed DESs due to strongest hydrogen bond interaction between HBA and HBD. The structure of some of these DESs is shown in Fig 2-6 [123].

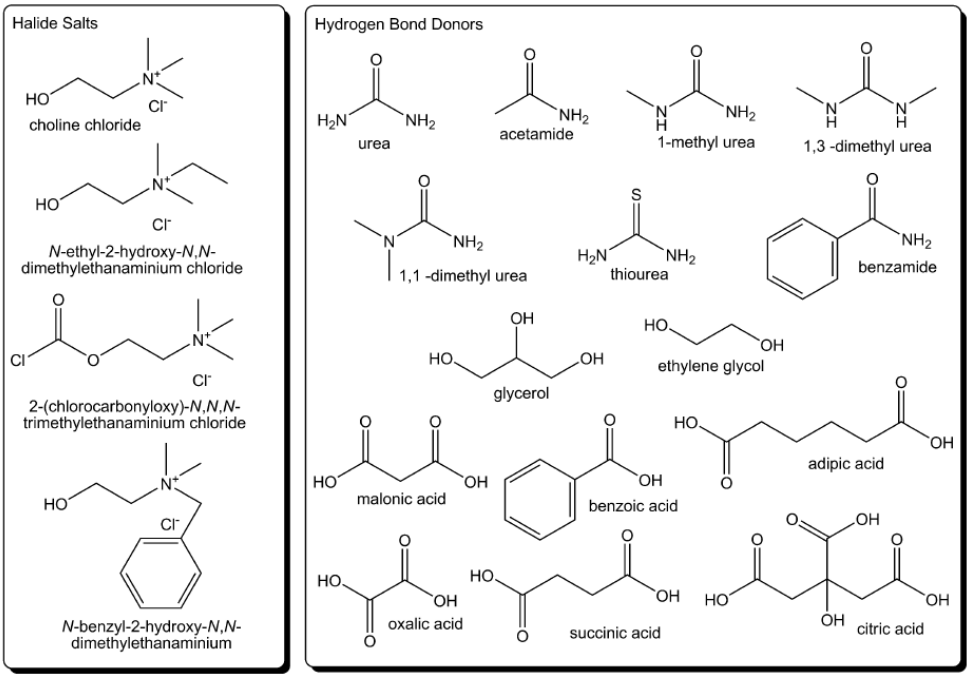

Figure 2-6 Structures of various halide salts and HBDs involved in the synthesis of DESs [123]**.**

The properties of DES can directly be influenced by the hydrogen bonding mechanism, which the greater the hydrogen bonding interaction is, the lower melting point and more viscous the mixture will be.

2.4.1.4 DESs Synthesis

There are different methods for preparing DESs including heating method, freeze-drying method, grinding method, etc. [111]. The heating method is a commonly applied method which consists of a mixing process under a fixed stirring and heating process at approximately 50-100 °C until obtaining a homogeneous solution [111]. The synthesis of DESs was first reported in 2004 by Abbott et al. [127]. The initial studies focused on the combination of a quaternary ammonium salt with a HBD, specifically using (2-hydroxyethyl) trimethylammonium chloride ($C_5H_{14}ClNO$), which is commercially known as choline chloride (ChCl) [127].

Although DESs were applied in detecting HMs in simple matrices like fruit juices, water, and edible oils primarily, their application has expanded to more complex solutions over time [125]. These advancements

demonstrated the potential of DESs as safe, reproducible, and degradable solvents with applications in environmental and agricultural sciences, industrial processes, and HM extraction [125].

2.4.1.5 Chitin Extraction with DES

Nowadays, DESs are also being used for extraction of chitin from biomass which can facilitate the removal of $CaCO_3$ and protein in a single step as illustrated in Fig 2-7.

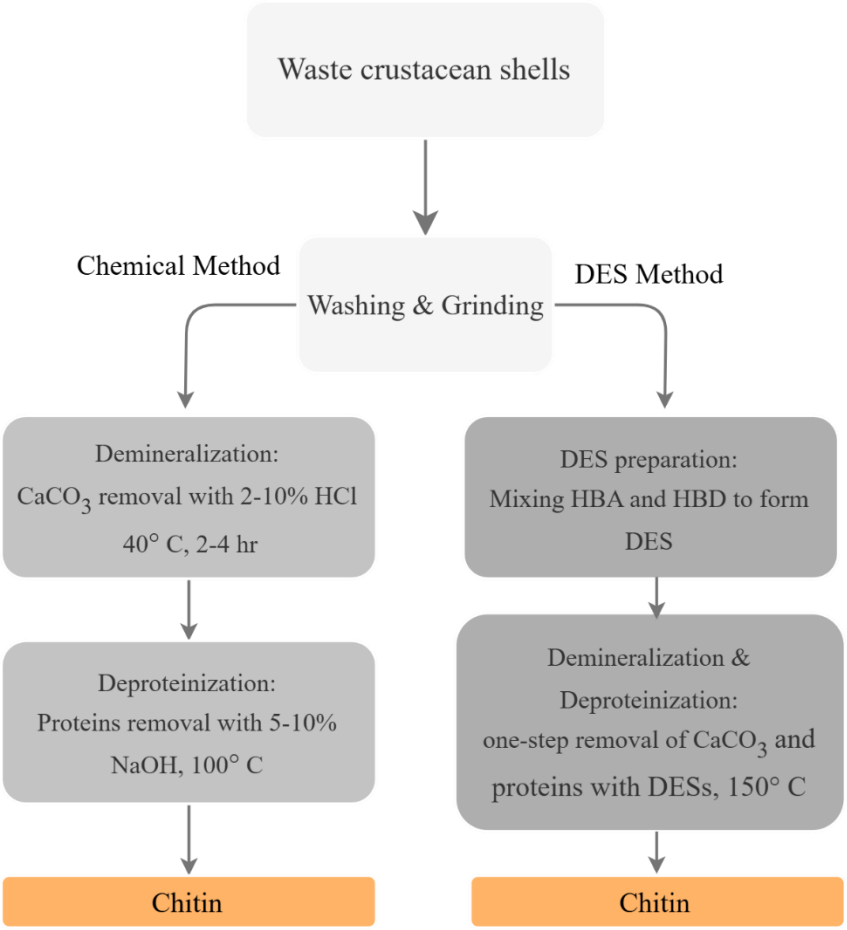

Figure 2-7 Comparing Conventional method and DES method for extracting chitin from crustacean shells (e.g., in this study SSW).

The application of [Ch]Cl:thiourea, [Ch]Cl:glycerol and [Ch]Cl:malonic acid was studied by Zhu et al. (2017) on the extraction of chitin from lobster shells [128]. The process was conducted under 50 -110 °C, 2 to 6 h, and the mass ratios of lobster shells/DES between 5 and 20 wt%. The conditions were varied based

on the examined DESs. The [Ch]Cl:malonic acid showed best results among the studied DESs, with the best chitin extraction yield at 50 °C, 2 h duration, and 7 wt% ratio of lobster shells/DES [128]. More recently, a complete chitin extraction was developed by Bradic et al. (2020) based on [Ch]Cl as the HBA and lactic acid, malonic acid, urea or citric acid as the HBDs. The best chitin extraction of 85% and purity grade of 98% was for [Ch]Cl:LA (1:1) which removed minerals and protein in a one-step process [129]. More research data [130], [131], [132] has been gathered and is presented in Table 2-9.

Table 2-9 Conditions applied in research on chitin extraction by DES and conditions for DES synthesis.

Raw Source	DESs Synthesis			Chitin Extraction Conditions				Reference
	DES Type (HBA:HBD)	Molar ratio	Temperature ℃	Material/Liquid ratio	Temperature ℃	Time h	Chitin Extraction Yield (%)	
Lobster Shells	ChCl:Glycerol	1:2	100	1:20	90	4	–	[128]
	ChCl:Malonic acid	1:2	100	1:7	50	2	20.63 ± 3.30	
	ChCl:Urea	1:2	90	1:10	100	6	–	
Shrimp Shells	ChCl:Urea	1:2	80	1:25	60-90	3-6	17.69 ± 5.15	[129]
	ChCl:Citric acid	1:1					18.04 ± 4.70	
	ChCl:Malonic acid	1:1					16.88 ± 3.50	
	ChCl:Lactic acid	1:1					14 ± 3.50	
Crab Shells	ChCl:Lactic acid	1:2	80	1:20	80	2	33.97 ± 4.91	[130]
	ChCl:Lactic acid+Glycerol	1:1.5:0.5	80				36.75 ± 0.51	
	ChCl:Lactic acid+Glycerol	1:1:1	80				34.27 ± 4.04	
	ChCl:Malic acid	1:1	90				33.95 ± 0.88	
	ChCl:Malic acid+Glycerol	2:1.5:0.5	90				32.15±0.75	
	ChCl:Malic acid+Glycerol	2:1:1	90				34.38 ± 0.10	
Shrimp Shells	ChCl:Lactic acid	1:3	80	1:20	80	2	54.00	[131]
	ChCl:Malic acid	1:2					53.15	
	ChCl:Citric acid	1:2					51.70	
	ChCl:Tartaric acid	1:3					48.85	
	ChCl:Oxalic acid	1:1					63.20	
Shrimp Shells	ChCl:Glycerol	1:2	80	1:25	80	2	51.63 ± 3.02	[132]
	ChCl:Lactic acid	1:2					29.20 ± 1.97	
	ChCl:Malic acid	1:2					25.00 ± 0.60	
	ChCl:Citric acid	1:2					25.18 ± 0.38	
	ChCl:Malonic acid	1:2					23.86 ± 0.07	
	ChCl:Oxalic acid	1:2					75.92 ± 1.02	
	ChCl:Urea	1:2					50.54 ± 1.07	
	ChCl:Ethylene glycol	1:2					52.45 ± 2.01	

2.5 SSW, Chitin, and Chitosan adsorption uptake

Various researchers have implemented chitin to remove HMs (e.g., Cu(II), Cd(II), and Ni(II)) from aqueous media, and since chitin and chitosan are both derived from SSW and exhibit many similar properties, their adsorption capacities are reported in Table 2-10 as well. It should be noted that comparing the adsorption capacities of the adsorbents reported in literature is impossible unless the experimental conditions are the same.

Table 2-10 Cd, Cu and Ni adsorption on chitin, chitosan and SSW.

Adsorbent	Adsorbate	Adsorption Uptake (mg/g)	References
Chitosan from SSW	Cd	19.8	[133]
MnFe2O4/chitosan prepared by SSW	Cd	60.6	[20]
Modified SSW Chitosan	Cd	15	[105]
Phosphorylated Chitin	Cd	62.71	[134]
Chitosan Nanoparticles	Cd	12	[108]
MnFe2O4/chitosan prepared by SSW	Cu	62.3	[20]
Treated Shrimp Shells	Cu	22.67	[19]
Chitin	Cu	52.74 - 54.01	[135]
Raw SSW, Cooked SSW, Chitosan	Cu	184, 170, 129	[136]
Chitosan	Cu	20.3	[105]
Chitosan Nanoparticles	Ni	7	[108]
Chitosan from SSW	Ni	4.51	[133]
Chitosan Beads	Ni	108.7	[137]

2.6 Adsorption mechanisms and influencing parameters

Adsorption isotherms illustrate the relationship between the amount of adsorbate that can be adsorbed by the adsorbent (q_e) and the equilibrium concentration of the adsorbate in the fluid phase (C_e) [138]. Various adsorption isotherm models are available to analyze experimental data and describe the equilibrium of the adsorption process and some of these models are given in Table 2-11 [89]. These models, through their different parameters and underlying thermodynamic assumptions, offer insights into the adsorption mechanism, surface properties, and the affinity of the adsorbent [139]. Therefore, selecting the most appropriate isotherm model is essential for optimizing adsorption system design. Among these isotherm models, Freundlich and Langmuir models have been used more frequently due to better fitting for HMs. The Langmuir isotherm model assumes that adsorption occurs on distinct, uniform active sites without interactions between adsorbed molecules. It represents monolayer adsorption, where q_{max} denotes the maximum adsorption capacity. In contrast, the Freundlich model describes non-ideal, reversible adsorption, allowing for multilayer adsorption and variations in adsorption heat and affinity across the surface. It suggests that stronger binding sites are occupied first, with adsorption energy decreasing exponentially. The parameter $\frac{1}{n}$ reflects surface heterogeneity and energy distribution, where adsorption is favorable if $0 < \frac{1}{n} < 1$ and unfavorable if $\frac{1}{\mathrm{n}} > 1$ [140].

Table 2-11 Frequently used adsorption isotherms models for single-component system.

Isotherm Models	Equations	Parameters	Reference
BET model (multilayer sorption)	$q_e = \frac{K_B Q_{MAX} C_e}{(C_s - C_e)\left[1 + \frac{(B-1)C_e}{C_s}\right]}$	q_e : The equilibrium solid phase concentration (uptake, mg/g) C_e : The equilibrium solute concentration in solution (mg/L) C_s : The saturation concentration of the adsorbed component (mg/l) K_B : Constant indicating the energy of interaction between the solute and the adsorbent surface B : Constant indicating the amount of solute adsorbed forming a complete monolayer Q_{max} : Langmuir constants related to maximum sorption capacity	[141]
Redlich- Peterson	$q_e = \frac{K_{RP} C_e}{1 + (a_{RP} C_e)^{\beta}}$	q_e : The equilibrium concentration of the solid phase (mg/g) C_e : The equilibrium concentration of liquid phase (mg/L) a_{RP}, K_{RP}, β : Redlich-Peterson parameters	[142]
Freundlich	$Q_e = K_f C_e^{\frac{1}{n}}$	Q_e : The equilibrium metal sorption capacity (mg/g) C_e : The equilibrium solute concentration in solution (mg/L) K_f : Biosorption equilibrium constant representative of the sorption capacity n : Constant indicative of biosorption intensity	[143]
Langmuir	$Q_e = \frac{q_{max} b C_e}{1 + b C_e}$	Q_e : The equilibrium solid phase concentration (uptake, mg/g) C_e : The equilibrium solute concentration in solution (mg/L) Q_{max} : Langmuir constants related to maximum sorption capacity b : Bonding energy of adsorption (or affinity)	[144]

It can be difficult to find consistent information about the adsorption capacities of HMs on SSW (chitin and chitosan are derived from shrimp) because many factors affect how well adsorption works. Experimental conditions should be the same for comparing two adsorbent materials. Typically, batch adsorption tests are used to study how different factors influence adsorption by adding a known amount of adsorbent to a fixed volume of liquid with a set initial concentration (of pollutant, here is HMs) and then changing the key conditions. Some of the main factors that greatly impact the adsorption process include (1) the pH of the solution, (2) contact time, (3) the initial concentration of the pollutant (e.g., HMs), (4) temperature, (5) agitation speed, (6) the volume of the adsorbate (e.g., SSW), (7) the ionic strength of the solution, (8) the dosage of the adsorbent, (9) the surface area of the adsorbent, and (10) other components present in the system [140], [145]. Therefore, meaningful comparisons can only be made within the same study using the same adsorbent and adsorbate systems.

2.6.1 Solution pH

The metal's speciation, the level of ionization, and the surface properties of the adsorbent during the adsorption process can be influenced by pH of the solution [146]. Research has shown that the optimum pH mainly depends on the target HMs and the type of adsorbent. Thus, each metal ion can be adsorbed on a particular adsorbent within a specific pH range [147]. Literature shows that at low pH values, an abundance of H+ ions in the solution leads to strong competition between these protons and metal ions for the limited binding sites on the adsorbent. This competition, combined with the electrostatic repulsion between the positively charged metal ions and the adsorbent's surface, results in a decreased adsorption efficiency [148], [149], [150]. As the pH increases, the adsorption rate improves due to weakened competition by protons and a decrease in repulsion force [151]. However, beyond a certain pH level, the efficiency drops again due to the formation of metal hydroxide complexes, which can precipitate out of solution rather than being adsorbed [152]. This pattern is generally observed for most metal ions. Although there are a few exceptions, and hexavalent chromium is one of them since it has opposite behavior due to its negative charge in solution [153].

2.6.2 Adsorbent Dosage

Generally, as the adsorbent dosage in the batch adsorption test increases, the adsorption efficiency also increases due to the availability of more active sites [154], [155]. However, while more adsorbent means more available adsorption sites, it also leads to an increase in unoccupied sites. As a result, the apparent adsorption uptake of the adsorbent decreases because most of the HM ions in the solution have already been adsorbed and equilibrium concentration is decreased [156]. Therefore, although increasing the adsorbent dosage improves efficiency, it can also lead to a reduction in the per-unit adsorption uptake as the dosage continues to rise [156]. For determining the optimum dosage of adsorbent in batch adsorption test, both adsorption efficiency and uptake should be considered.

2.6.3 Metal Initial Concentration

The initial concentration of metals significantly influences the adsorption uptake of the chosen adsorbent. The adsorption uptake rises accordingly by the increase in the initial concentration of metal ions. This increase occurs because the higher initial concentration provides a stronger driving force to overcome the mass transfer resistance of HMs between the aqueous solution and the solid adsorbent. Adsorption isotherms are used to understand how adsorbates interact with adsorbent. This is critical for optimizing the use of adsorbents [147].

2.6.4 Temperature

Temperature plays an important role in the adsorption of metal ions onto adsorbents. This is primarily due to the influence that temperature has on the solid/liquid interfaces, the swelling behavior of the adsorbents, and the mobility of metal ions. Typically, the adsorption of HMs onto SSW (chitosan and chitin has derived from shrimp shells and show the same behavior) improves with rising temperatures, as higher temperatures enhance the diffusion rate of metal ions from the solution to the adsorbent [157]. Despite this, adsorption processes are not conducted at high temperatures because it would lead to higher operational costs on the industrial scale [151].

The impact of temperature on adsorption could be used to evaluate the thermodynamic parameters of an adsorption process. The evaluation of thermodynamic parameters provides valuable insights into the possible mechanisms of adsorption, helping to determine whether the process is spontaneous, random, endothermic, or exothermic [138]. These parameters, including Gibbs free energy change (ΔG), enthalpy change (ΔH), and entropy change (ΔS), can be calculated using the thermodynamic equilibrium coefficient obtained at different temperatures [138].

At a constant temperature and pressure, the ΔG value serves as the primary criterion for spontaneity, where a negative ΔG indicates a spontaneous adsorption process [151]. ΔG is determined by using the equilibrium constant at each temperature, as described by the Gibbs free energy equation which is provide in Table 2-15. This calculation assumes that adsorption is reversible and that equilibrium conditions are established in a batch system. Additionally, the changes in enthalpy (ΔH) and entropy (ΔS) can be derived using the Van't Hoff equation, given in Table 2-15, by assuming these parameters remain independent of temperature [151] [138]. A positive ΔS value suggests an increase in randomness during adsorption, often attributed to the exchange of metal ions with more mobile ions. A negative ΔG value, along with a decrease in entropy (negative ΔS), corresponds to a negative ΔH, confirming that the adsorption process is exothermic. In contrast, endothermic adsorption is associated with a positive ΔH value [151] [158]. The ΔH parameter is particularly useful for evaluating the interaction forces between adsorbate and adsorbent, which reflects the bonding strength [151] [138] [158]. Adsorption on solid surfaces can be categorized as either physical or chemical. Typically, the ΔH values for physical adsorption range from 4 to 40 kJ/mol, while chemical adsorption exhibits a broader range, spanning from 40 to 800 kJ/mol [138] [158].

Table 2-12 Thermodynamic equations and their parameters.

Expression	Linear Equations	Parameters
Sorption equilibrium constant	$K_L = \frac{C_{ad}}{C_e}$	C_{ad}: The adsorbed amount at equilibrium (mg/L) C_e: The equilibrium concentration in solution (mg/L)
Gibbs		R: The universal gas constant (8.314 J/(mol.K))

	ΔG°=-RT lnK_L	T: The absolute temperature (K) K_L: The equilibrium constant
Van't Hoff	$\ln K_L = \frac{\Delta S^{\circ}}{R} - \frac{\Delta G^{\circ}}{RT}$	R: The universal gas constant (8.314 J/(mol.K)) T: The absolute temperature (K) K_L: The equilibrium constant

2.6.5 Contact Time

Contact time directly impacts the economic efficiency of the operation, which is closely linked to adsorption kinetics [89][156]. In order to select an adsorbent in terms of economic feasibility an industrial application, a high affinity for adsorbates (adsorption capacity) and a rapid adsorption rate is needed. The most commonly used kinetic models in the literature for adsorption processes include: (i) the Elovich [159], (ii) the intraparticle diffusion model [160], (iii) the pseudo-first-order kinetic model [161], and (iv) the pseudo-second-order kinetic model [162], as presented in Table 2-13 [89]. These models are also employed to analyze the mechanisms that control the adsorption process, however among these, pseudo-first-order and pseudo-second-order are the most commonly used. The pseudo-first-order model, initially proposed by Lagergren (1898) [163], assumes that the rate of adsorption is directly proportional to the number of available (unoccupied) adsorption sites. It is typically associated with physisorption, where weak van der Waals forces dominate the interaction between the adsorbate and the adsorbent surface [161], [163]. In contrast, the pseudo-second-order model, developed by Ho and McKay (1999) [162], assumes that adsorption follows chemisorption mechanisms, involving stronger valence forces such as covalent bonding or electron exchange between the adsorbent and adsorbate [162]. This model presumes that the rate-limiting step may be related to the square of the number of unoccupied sites and generally fits well when the adsorption process involves active functional groups such as amine and hydroxyl groups found in chitin-based materials [162].

Table 2-13 The kinetic models used for HM adsorption.

Kinetic Models	Equations	Parameters	Reference
Elovich	$q_t = \frac{1}{\beta}\ln(\alpha\beta) + \frac{1}{\beta}\ln t$	q_t : The amount of adsorbed on the adsorbent (mg/g) at time t (min) α : The initial sorption rate of Elovich kinetic model ((mg/g)/min) β : Related to the extent of surface coverage (g/mg)	[159]
Intraparticle Diffusion	$q_t = K_m t^{1/2} + C$	q_t : The amount of adsorbed on the adsorbent (mg/g) at time t (min) K_m : the intraparticle diffusion constant (mg/g/min^(1/2))	[160]
Pseudo-first-order	$\log(q_e - q_t) = \log q_e - \frac{K_1}{2.303}$t	q_t : The amount of adsorbed on the adsorbent (mg/g) at time t (min) q_e : The amount of adsorbed on the adsorbent at equilibrium (mg/g) k_1 : The rate constant of first-order adsorption (1/min)	[161]
Pseudo-second-order	$\frac{t}{q_t} = \frac{1}{k_2 {q_e}^2} + \frac{1}{q_e}t$	q_t : The amount of adsorbed on the adsorbent (mg/g) at time t (min) q_e : The amount of adsorbed on the adsorbent at equilibrium (mg/g) k_2 : The rate constant of second-order adsorption ((g/mg)/min)	[162]

2.7 Summary and Research gap

The accumulation of SSW presents both an environmental challenge and an untapped opportunity for resource recovery. While chitosan, a derivative of chitin, has been extensively studied and applied as an effective adsorbent for the removal of HMs from aqueous solutions, the adsorption potential of chitin itself has not been thoroughly explored. Most existing studies have focused on chitosan due to its solubility and functional versatility, often overlooking the fact that chitin, when properly extracted and processed, can serve as a sustainable and efficient alternative.

This study aims to fill that gap by utilizing SSW to develop two chitin-based adsorbents through green chemical method and conventional method, employing non-toxic and cost-effective reagents under mild chemical conditions. The synthesized materials were tested for their capacity to remove Cd(II), Cu(II), and Ni(II) from aqueous media. A comparative evaluation was conducted to assess the adsorption performance of the two chitin types. Moreover, unlike conventional studies that examine single-metal systems, this research also evaluates the adsorbents in competitive multi-metal environments to more accurately simulate real-world wastewater. This integrated approach highlights chitin's overlooked potential and demonstrates a novel pathway for turning seafood biowaste into value-added materials for water purification.

2.8 References

The references are merged with the other chapters' references and presented at the end of the thesis.

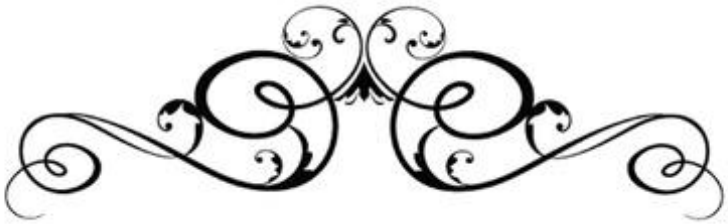

Chapter 3

Materials & Methods

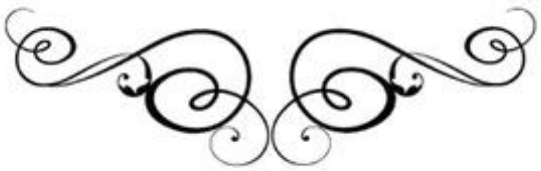

Chapter 3: Materials & Methods

3.1 Reagents and Chemicals

The wastewater samples were simulated in the laboratory by diluting heavy metals (HMs) standard solutions (Cd standard for AAS 1,000 ppm in 2% HCl, Cu standard 10,000 ppm, and Ni standard for ICP 10,000 ppm in 3% (v/v) HNO_3). The HMs' standard solutions were purchased from VWR Chemicals (BDH Chemicals). For each metal, a calibration curve was prepared using standard solutions (1.5, 4.5 and 9 mg/L). Furthermore, Glycerol and choline chloride were purchased from Sigma Aldrich. Shrimp shells were collected from a local Japanese restaurant, Ottawa, ON, Canada, in June 2024. Sodium hydroxide (NaOH) and hydrogen peroxide (H_2O_2) were purchased from Sigma Chemical Co. (Canada). All the chemicals utilized in this study were of analytical grade.

3.2 Preparation of Shrimp Shells

Shrimp shells (without head) were cleaned using tap water to eliminate unwanted material. Then, the shrimp shells were washed with distilled water several times. As shown in Fig 3-1, shrimp shells were air-dried for 24 h and were subsequently ground mechanically using a grinder to fine particles and sieved (#100, with an opening size of 150 μm).

Air-Dried and Clean SSW | Grinding Mechanically | Shrimp Shells Power

Figure 3-1 The process of preparing Shrimp Shells Powder.

3.3 DES Synthesis

Deep Eutectic Solvents (DES) was prepared by mixing choline chloride as hydrogen bond acceptor (HBA) and glycerol as hydrogen bond donor (HBD) at different specific molar ratios (Table 3-1). In this study, several molar ratios (HBA:HBD) were examined to determine the eutectic point of the chosen DES. After mixing HBA and HBD, the mixture was stirred continuously at a temperature of 80 ℃ until a clear homogenous liquid was formed.

Table 3-1 The different molar ratios that were examined in this study for DES.

Synthesis of DES			
Abbreviation	HBA	HBD	HBA:HBD
DES-1	Choline Chloride	Glycerol	1:1
DES-2	Choline Chloride	Glycerol	1:2
DES-2.5	Choline Chloride	Glycerol	1:2.5
DES-3	Choline Chloride	Glycerol	1:3

3.4 Chitin Extraction using Conventional Method

To eradicate biological pigment and protein, the shrimp shell powder was added to a solution mixture of 5 wt.% NaOH and 1 wt.% H_2O_2, L/S = 20, and stirred (180 rpm) for 72 h at 30 ℃. The remaining solids were cleaned with distilled water until the solution became neutral ($\sim 6.5 - 7$). Then, it was filtered with EZFlow

Membrane filter paper (47 mm diameter and 0.45 μm pore size). Finally, the treated shrimp shells or chitin was dried in an oven at 50℃ overnight [19] and then stored in an airtight container and named Ch-C for further application. Fig 3-2a shows the process of chitin extraction using the conventional method.

3.5 Chitin Extraction using DES Method

The shrimp shells powder and DESs were mixed at a molar ratio of 1:20 (g/mL) and heated at 80 ℃ while mixing using magnetic stirring (300 rpm) for 2 h. Then, the obtained extract was cooled down to room temperature. In the next step, the mixture was centrifuged at 4000 rpm for 20 min and the precipitate was recovered. The residue was washed several times until the pH of the wash water was neutralized ($\sim 6.5 - 7$). Finally, the recovered residue or chitin was dried in an oven at 50℃ overnight. The chitin was then stored in an airtight container and named Ch-DES for further application. Fig 3-2b illustrates the process of extracting chitin from SSW using the DES method.

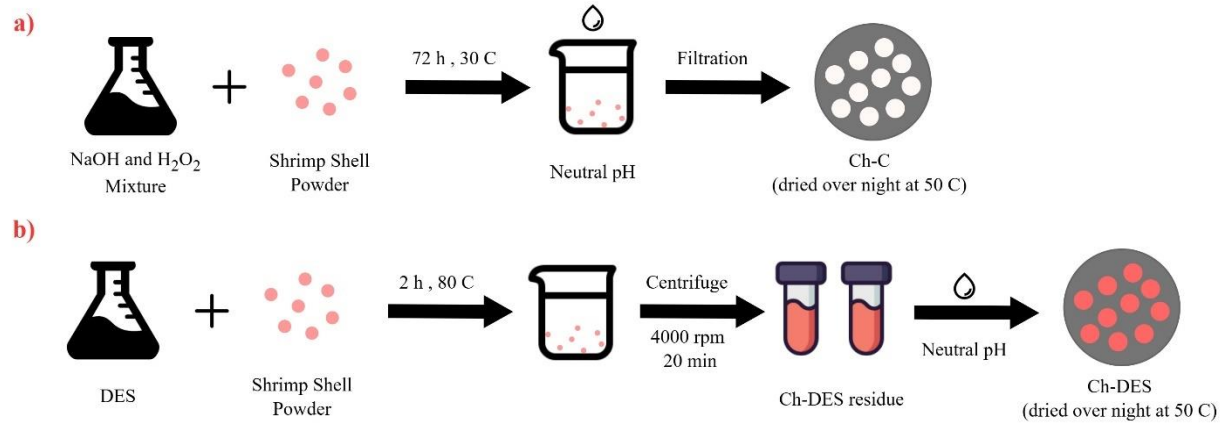

Figure 3-2 Schematic representation of chitin extraction by; (a) Conventional method (Ch-C), (b) DES method (Ch-DES).

To determine the optimal HBA:HBD ratio, the chitin yield (%), representing the proportion of the extracted substance relative to the original material, was calculated using Eq. (1);

$$Chitin\ Yield\ (\%) = \frac{Weight\ of\ extracted\ material\ (g)}{Initial\ material\ weight\ (g)} \times 100 \quad (1)$$

3.6 Ch-C and Ch-DES Characterization

The existing Functional groups on Ch-C and Ch-DES (before and after adsorption) were analyzed through Fourier Transform Infrared Spectroscopy (FT-IR) using an attenuated total reflectance (ATR) sampling method within 400–4000 cm^{-1} range (Thermo Fischer, Nicolet 6700). To identify the surface topography and surface elemental composition of Ch-C (before and after adsorption in a single-HM solution), Scanning Electron Microscopy (SEM) (JEOL JSM-7500F equipped with Oxford EDS INCA 350) was used at 3.0 kV acceleration voltage. The specific surface area and total pore volume of SSW, Ch-C and Ch-DES were measured by N_2 adsorption isotherms at 77 K using Micromeritics 3Flex adsorption analyzer and computed using Brunauer–Emmett–Teller (BET) method by the Micromeritics Software. Before measurements, all samples were activated using a Micromeritics Smart VacPrep under a high vacuum at 50 °C for 7 hours and finally at 140 °C for 12 hours.

3.7 Batch adsorption isotherm tests

A series of preliminary batch adsorption tests using Ch-C as an adsorbent in a single-component system for the removal of Cd(II), Cu(II), and Ni(II) was conducted to optimize the key experimental factors. Adsorption of Cd(II), Cu(II) and Ni (II) using Ch-C in batch mode were examined at variable experimental parameters such as pH (4,5,6,7 and 8), contact period (5, 10, 15, 20, 30, 45 min, 1, 3, 6, 16 and 24 h), initial concentration of HMs (2.5, 10, 25, 50 and 100 $mg.L^{-1}$), and biosorbent dosage (0.1, 0.2, 0.3, 0.4 and 0.5 gr in 100 mL) at 180 rpm. The initial concentration was fixed at 25 mgL^{-1} for examination of the effect of experimental factors. Samples with 25 ppm concentration were prepared by diluting the stock solutions in distilled water. The initial pH of the solution was adjusted to the appropriate value using 0.1 M HCl and 0.1 M NaOH, and was measured using a HACH (HQ40D) Instrument. After completion of each adsorption experiment, biosorbents loaded with HMs were separated from the aqueous phase using vacuum filtration (refer to Fig AP-1). All experimental runs were triplicated to estimate error and ensure reliable results. Equilibrium concentrations of HMs were measured using Atomic Absorption Spectroscopy (AAS) (PinAAcle 500, Perkin Elmer, Canada) and the average values were reported here. The employed

wavelength was 228.8 nm for Cd(II), 324.75 nm for Cu(II), and 232 nm for Ni(II). Initial and equilibrium concentrations of Cd(II), Cu(II) and Ni(II) in the solution were identified as C_i and C_e respectively. The efficiency of adsorption (removal %) was calculated using Eq. (2);

$$Adsorption\ Removal\ (\%) = \frac{C_i - C_e}{C_i} \times 100 \quad (2)$$

The adsorption capacity of chitin (q_e) was evaluated from the Eq. (3);

$$Adsorption\ Capacity\ (mg/L) = \frac{(C_i - C_e)\,V}{chitin\ dosage} \quad (3)$$

V in this equation is the volume of the solution (L), C_i and C_e are initial and equilibrium concentration of HMs (mg. L^{-1}), and chitin dosage (gr).

Furthermore, the adsorption isotherm tests were conducted at room temperature, initial concentrations ranging from 2.5 to 100 mg/L, adsorbent dosage of 2.5 g/mL, over a 24-hour to compare the performance of Ch-C and Ch-DES in both single-component and competitive environments. The pH was adjusted to 5.5 for three-HMs solution, 5 for both Ni and Cu solutions, and 6 for the Cd solution.

To analyze the adsorption isotherm results, two of the most frequently used models, Langmuir and Freundlich, were applied, as summarized in Table 2-11. The isotherm models' fitness was evaluated using the coefficient of determination (R^2) and root mean square error (RMSE) based on the average experimental equilibrium data.

Following the adsorption of metal ions (Cu(II), Cd(II), and Ni(II)) onto Ch-C and Ch-DES, the chitin was separated by filtration and rinsed with de-ionized water and air-dried. The dried Ch-C and Ch-DES were then subjected to desorption in 50 mL of various solutions, including DI water, sodium chloride (NaCl, 1 M), and sulfuric acid (H_2SO_4, 0.1 M) for 24 h. AAS was utilized to quantify the amount of desorbed metal ions. The percentage of desorption was determined using the following equation:

$$\text{Desorption}\ (\%) = \frac{\text{Amount of metal ions desorbed (mg/L)}}{\text{Amount of metal ions adsorbed (mg/L)}} \times 100 \quad (4)$$

3.8 Kinetic Study

A kinetic study, pseudo first order and pseudo second order, was conducted to illustrate adsorption behavior of Ch-C and Ch-DES at optimal initial concentrations (2.5 mg L^{-1}) at optimum pH and 20 ℃. The efficiency of adsorption was estimated at different time intervals (5, 10, 15, 20, 30 min, 1, 3, 6, 16 and 24 h). The pseudo-first-order and pseudo-second-order were calculated using equations presented in Table 2-13.

3.9 Thermodynamic Study

A series of flasks containing 50 mL of HMs' solution (2.5mg/L for single-component solution, 100 mg/L for three-components solution) at pH 5 (single Cu and Ni solution), 5.5 (HMs' combination) and 6 (single Cd solution) were prepared. Ch-C and Ch-DES powder weighing 125 mg (equivalent to 2.5 g/L) were added to each flask and agitated in an incubator shaker at 180 rpm for 24 hours at varying temperatures (5, 20, and 40°C). This experiment was conducted to assess the effect of temperature on adsorption and to determine the thermodynamic parameters.

3.10 References

The references are merged with the other chapters' references and presented at the end of the thesis.

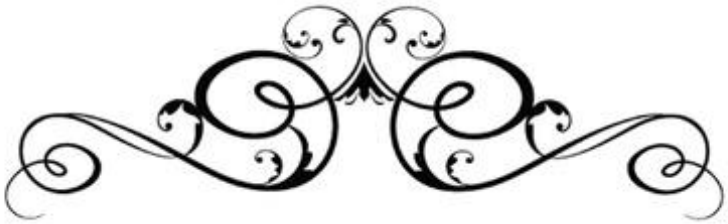

Chapter 4

Results & Discussion

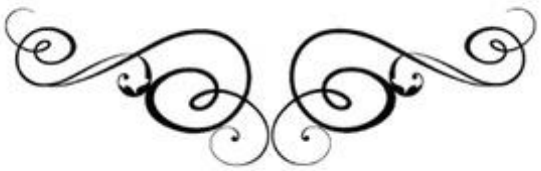

Chapter 4: Technical Paper

Application of Deep Eutectic Solvent (DES) Extracted Chitin from Shrimp Waste Biomass as a Biosorbent for Removal of Heavy Metals from Aqueous Solution: Cu(II), Cd(II), Ni(II)

4.1 Abstract

Contamination of water resources by heavy metals (HMs) is a serious environmental issue that affects both human and living organisms' health. This study aimed to evaluate the efficiency of removing Cd(II), Cu(II), and Ni(II) from aqueous solutions through batch adsorption using chitin in both single-component component and multi-component systems. Chitin was extracted from shrimp shell waste (SSW) through the conventional and deep eutectic solvent (DES) extraction methods. Scanning Electron Microscopy (SEM) and Fourier Transform Infrared Spectroscopy (FT-IR) analyses were conducted to characterize the adsorbent's surface morphology and functional groups, and proved that the treatment in SSW was effective. Brunauer-Emmett-Teller (BET) study also showed an increase in surface area of synthesis chitin (almost 9 times larger). Furthermore, experimental factors were examined to find the optimal values for each HMs in a single-component system, these factors consisted of pH, adsorbent dosage, contact time, and temperature on the adsorption efficiency. The Langmuir isotherm model was found to best describe the adsorption of Cd(II), Cu(II), and Ni(II), with maximum adsorption capacities of 38.25 mg/g, 42.20 mg/g, and 23.48 mg/g, respectively, in a competitive environment using chitin extracted by DES method, which showed approximately 28% increase compared to conventional method. The computed thermodynamic parameters (4, 20, 40 °C) showed the spontaneity and exothermic nature of HMs adsorption on the synthesized bio-sorbents. The pseudo-second-order kinetic model fitted Cd(II) and Ni(II), and Cu(II). This study demonstrated that chitin is an effective, cost-efficient biosorbent for the removal of HMs from wastewater.

Keywords: Shrimp shell waste, Chitin extraction, Heavy metals (HMs), Biosorption, Deep eutectic solvent (DES).

4.2 Introduction

Over the last few decades, growing population and industrialization have resulted in the release of various pollutants, including heavy metals (HMs), into water bodies, which could have significant adverse effects on both public health and the environment [10]. In addition, the generation rates of solid waste have been increasing. Addressing these challenges requires a shift towards sustainable development and circular economy principles, which focus on minimizing and recovery of waste and optimizing resource usage to promote the reuse and recycling of materials. One promising approach involves the application of solid waste as low-cost and environmentally friendly adsorbents for pollution mitigation [6], [7], [8].

The contamination of water and wastewater by HMs such as cadmium (Cd), Copper (Cu), and nickel (Ni) poses a serious threat to human health such as kidney damage, respiratory issues, and potential carcinogenic effects due to their hemotoxicity [11], [12], [33], [35]. Additionally, HMs' contamination can degrade water quality, disrupt aquatic ecosystems, reduce biodiversity, and lead to the bioaccumulation of toxic substances across food chains [9] [10]. Cd(II), Cu(II), and Ni(II) are all commonly found in electroplating, metal plating industries, battery manufacturing, electronics production, pigment and dye manufacturing, plumbing and piping systems, petroleum refining, and waste incineration processes. WHO have set a limit of 0.003, 0.005 and 2 mg/L for Cd(II), Cu(II), and Ni(II) in drinking water, while USEPA's limitation are 1.3 ,0.005 and 5 mg/L, respectively [29]. Moreover, Canadian Drinking Water Quality Guidelines specify maximum concentrations of 0.005 mg/L for Cd(II), 1 mg/L for Cu(II), and 0.1 mg/L for Ni(II).

Several techniques including adsorption [14], microbial remediation [15], coagulation and chemical precipitation [14], [16], ion-exchange [14], reverse osmosis [17], membrane filtration [17], electrocoagulation [14], and solvent extraction [14] have been developed for removing HMs from polluted water. Among these methods, adsorption offers several advantages including low cost, high efficiency, ease of operation, and environmental sustainability when using abundant and biodegradable organic waste materials [6], [7], [8]. A variety of adsorbents have been explored for HMs adsorption, including activated carbon [83], [85], [164], clay minerals [75], [77], carbon nanotubes [165], and bio-adsorbents [166]. Among

these, the use of bio-adsorbents derived from organic waste material has gained increasing attention due to their cost-effectiveness, biodegradability, non-toxic nature, and recycling of organic waste to promote circular economy and sustainability [18], [167], [168].

The production of seafood, and consequently fisheries waste, has been increasing over the last few decades [18], [20]. According to the Food and Agriculture Organization (FAO), global seafood production reached 223.2 million tons in 2022, marking a 4.4% increase from 2020 [22]. Shrimp is one of the popular seafood among all the others. A result a total of 3.8 million tons of shrimp shell waste (SSW) is produced annually, which is about 50–60% of the total weight of shrimp through processing and consumption [20][23]. Although a minor fraction of SSW is converted into fertilizers and dietary supplements, such as chitosan-based products, the majority is improperly disposed through methods like landfilling and ocean dumping, which will lead to environmental degradation, including soil contamination, water pollution, and harm to marine ecosystems [24], [25]. Additionally, seafood waste (e.g., SSW) often produces obnoxious gases like ammonia and methane, which can be toxic to living organisms such as fish [24], [25]. Therefore, proper management of this waste stream is crucial due to environmental and economic considerations.

Shrimp shell contains chitin, a natural biopolymer, along with calcium carbonate and proteins, which can naturally attract HMs [19], making SSW a low-cost and sustainable alternative biosorbent for the removal of HMs from aqueous phase. Moreover, the conversion of SSW to biosorbent offers a sustainable management option for this solid waste stream and alleviates the subsequent environmental impacts. Chitin is primarily found in the exoskeletons of shellfish, such as shrimp, crab, and lobster, and is composed of β-(1→4)-2-acetamido-2-deoxy-d-glucopyranose units [169], [170]. Chitin is a versatile biopolymer with distinctive properties, including high porosity, low density, and biodegradability [171]. It is a natural, cationic, hydrophilic, non-toxic, and biocompatible polysaccharide that is suitable for various applications, including adsorption of HMs [169]. The presence of functional groups, such as amino and hydroxyl groups, enhances its adsorption abilities and allows chitin to bond with different organic and inorganic compounds [171], [172], [12]. The lone pairs of electrons on the nitrogen in the acetamido group and the oxygen in the

hydroxyl group act as chelating sites to adsorb HMs and allows chitin to form coordination complexes with metal ions [169], [170]. Although there are still limitations including undesirable thermal and mechanical properties, it is still an viable biosorbent for HMs' removal due to the biodegradability of chitin [26], [171]. To convert SSW to an efficient biosorbent, chitin needs to be extracted first. The conventional extraction method involves a chemical process that includes demineralization, deproteinization, and, in some cases, decolorization. Demineralization is typically performed using strong acids such as HCl, which removes inorganic components like $CaCO_3$ [111], [112]. This is followed by deproteinization, in which NaOH is used to solubilize and remove protein from SSW [111], [112]. It is possible to further modify chitin to chitosan, using a deacetylation step by treating chitin with concentrated NaOH (40–50%) at elevated temperatures (above 100 °C) [113]. Chitosan has applications in pharmaceuticals, food packaging, agriculture, biomedicine, and is also an effective biosorbent for HMs due to its high affinity for metal ions through chelation and ion exchange mechanisms [6], [8], [101].

Although the conventional extraction methods are effective, they pose significant environmental and safety concerns due to the extensive use of harsh chemicals. In response to these drawbacks, researchers have explored greener alternatives such as ionic liquids (ILs) and deep eutectic solvents (DESs) [115]. ILs are room-temperature molten salts that offer remarkable solvent properties, including non-volatility, thermal stability, and the ability to dissolve biopolymers like chitin [114], [116]. However, their widespread application is limited by high production costs and complex synthesis procedures [121]. In contrast, DESs have emerged as a more sustainable and cost-effective alternative solvent [121]. DESs are formed by mixing hydrogen bond acceptors (HBAs), such as choline chloride, with hydrogen bond donors (HBDs) like urea, glycerol, organic acids, or polyols, which results in a eutectic mixture with a significantly lower melting point than the individual components [122-126]. These solvents are biodegradable, non-toxic, and easy to prepare, which often require only mild heating and stirring to form a homogeneous liquid [122], [125]. Compared with ILs, DESs are derived from low-cost, renewable materials and can efficiently extract chitin in a single step by simultaneously removing proteins and minerals [111], [127]. Their ability to

simplify the extraction process while reducing chemical usage and environmental burden makes them a promising green alternative for chitin extraction from biomass sources such as SSW [125].

The primary objective of this study was to convert SSW into chitin using DES extraction and evaluate and optimize its performance in removing Cd(II), Ni(II), and Cu(II) from the liquid phase. The performance of the DES extracted chitin was compared with chitin extracted by the conventional method using NaOH and H_2O_2. The performance of the synthesized chitin was evaluated under different experimental conditions including pH, adsorbent dosage, contact time, initial metal concentration, and temperature to determine the optimal parameter ranges for efficient metal removal. The adsorption uptake was evaluated for the single-component system and multiple-component system. The SEM and SEM-EDS analyses were conducted to characterize the surface topography and porosity of chitin and SSW before and after loading with HMs. FT-IR analysis was also used to determine the functional groups of chitins and compare them with those of SSW. In addition, BET analysis was conducted to estimate the surface area and total pore volume of SSW and chitin. Furthermore, Langmuir and Freundlich isotherm models were applied to batch adsorption experimental data to determine which model best describes the adsorption isotherm data, and if possible to determine the maximum adsorption capacity of the chitin both in a multi-component and single-component systems. Using batch adsorption tests at different temperatures and thermodynamic study, ΔG^o, ΔH^o, and ΔS^o were calculated to draw some conclusions about the adsorption process. Lastly, the adsorption rate and mechanism were investigated using pseudo-first-order and pseudo-second-order kinetic models to better understand the adsorption behavior.

4.3 Materials & Methods

4.3.1 Reagents and Chemicals

The wastewater samples were simulated in the laboratory by diluting heavy metals (HMs) standard solutions (Cd standard for AAS 1000 ppm in 2% HCl, Cu standard 10000 ppm, and Ni standard for ICP 10000 ppm in 3% (v/v) HNO_3). The HMs' standard solutions were purchased from VWR Chemicals (BDH Chemicals). For each metal, a calibration curve was prepared using standard solutions (1.5, 4.5 and 9 mg/L).

Furthermore, Glycerol and choline chloride were purchased from Sigma Aldrich. Shrimp shells were collected from a local Japanese restaurant, Ottawa, ON, Canada, in June 2024. Sodium hydroxide (NaOH) and hydrogen peroxide (H_2O_2) were purchased from Sigma Chemical Co. (Canada). All the chemicals utilized in this study were of analytical grade.

4.3.2 Preparation of Shrimp Shells

Shrimp shells (without head) were gathered and cleaned by using tap water to eliminate unwanted material. After that, the shrimp shells were washed with distilled water several times. The shrimp shells were air dried for 24 h. Then the shrimp shells were grounded mechanically using a grinder to fine particles and sieved (#100, with an opening size of 150 μm).

4.3.3 DES Synthesis

DES was prepared by mixing choline chloride as HBA and glycerol as HBD at different molar ratios (Table 4-1), to determine the optimal ratio for chitin extraction. After mixing HBA and HBD, the mixture was stirred continuously at a temperature of 80 ℃ until a clear homogenous liquid was formed.

Table 4-1 The different molar ratio that were examined in this study for DES.

Synthesis of DES			
Abbreviation	HBA	HBD	HBA:HBD
DES-1	Choline Chloride	Glycerol	1:1
DES-2	Choline Chloride	Glycerol	1:2
DES-2.5	Choline Chloride	Glycerol	1:2.5
DES-3	Choline Chloride	Glycerol	1:3

4.3.4 Chitin Extraction using Conventional Method

To eradicate biological pigment and protein, the powder of shrimp shells was added to the solution mixture (5 wt.% NaOH and 1 wt.% H_2O_2, liquid/solid (L/S) = 20) and stirred (180 rpm) for 72 h at 30 ℃. The residue obtained after 72 h was washed with distilled water until the solution became neutral ($\sim 6.5 - 7$). Then it was filtered with EZFlow Membrane filter paper (47 mm diameter and 0.45 μm pore size). Finally,

the treated shrimp shells or chitin was dried in an oven at 50℃ overnight [19]. Then, the chitin was stored in an airtight container and named Ch-C for further application. Fig 4-1a shows the process of chitin extraction using the conventional method.

4.3.5 Chitin Extraction using DES Method

As illustrated in Fig 4-1b, the shrimp shells powder and DESs were mixed at a molar ratio of 1:20 (g/mL) and heated at 80 ℃ under magnetic stirring (300 ppm) for 2 h. After the heating process, the obtained extract was cooled down to room temperature, then it was centrifuged at 4000 rpm for 20 min, and the precipitation was recovered. The residue was washed several times until the washed water pH was neutralized ($\sim 6.5 - 7$). Finally, the recovered residue or chitin was dried in oven at 50℃ overnight. After completely dried, the chitin was stored in an airtight container and named Ch-DES for further application.

To determine the optimal HBA:HBD ratio, the chitin yield (%), representing the proportion of the extracted substance relative to the original material, was calculated using Eq. (4-1);

$$Chitin\ Yield\ (\%) = \frac{Weight\ of\ extracted\ material\ (g)}{Initial\ material\ weight\ (g)} \times 100 \qquad (4\text{-}1)$$

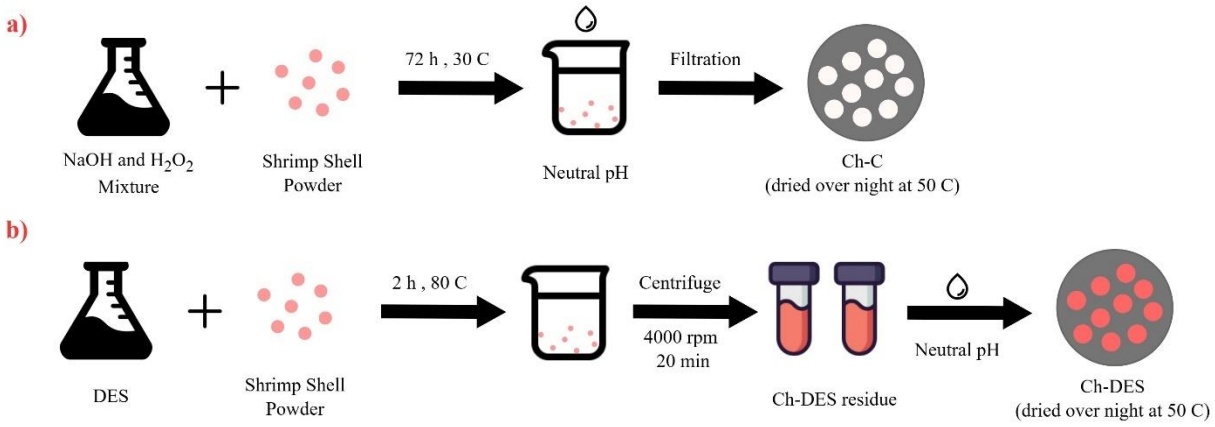

Figure 4-1 Schematic representation of chitin extraction by; (a) Conventional method (Ch-C), (b) DES method (Ch-DES).

4.3.6 Ch-C and Ch-DES Characterization

The existing functional groups on Ch-C and Ch-DES (before and after adsorption) were analyzed with Fourier Transform Infrared Spectroscopy (FT-IR) using an attenuated total reflectance (ATR) sampling method within 400–4000 cm^{-1} range (Thermo Fischer, Nicolet 6700). To identify the surface topography and surface elemental composition of Ch-C (before and after adsorption in a single-HM solution), Scanning Electron Microscopy (SEM) (JEOL JSM-7500F) was used at 3.0 kV acceleration voltage. The SEM equipped with Oxford EDS INCA 350 spectrometer for Energy Dispersive Spectroscopy (EDS) characterization was further used to identify the surface topography and surface elemental composition of Ch-DES and Ch-C (before and after adsorption in a competitive environment). The samples were coated with gold-palladium. The specific surface area and total pore volume of SSW, Ch-C and Ch-DES were measured by N_2 adsorption isotherms at 77 K using Micromeritics 3Flex adsorption analyzer and computed using Brunauer–Emmett–Teller (BET) method by the Micromeritics Software. Prior to measurements, all samples were activated using a Micromeritics Smart VacPrep under a high vacuum at 50 °C for 7 hours and finally at 140 °C for 12 hours.

4.3.7 Batch adsorption isotherm

This study examined the removal of Cd(II), Cu(II), and Ni(II), initially using Ch-C as an adsorbent in a single-component system to optimize key experimental factors such as pH and adsorbent dosage. Once the optimal conditions were established, the performance of Ch-C was assessed in a competitive environment. Additionally, to compare the adsorption uptakes of Ch-C and Ch-DES, the removal of HMs in a competitive solution was evaluated using Ch-DES under the same conditions. Adsorption uptake of Cd(II), Cu(II) and Ni (II) using Ch-C in batch mode were examined at variable experimental parameters such as pH (4,5,6,7 and 8), contact time (5, 10, 15, 20, 30, 45 min, 1, 3, 6, 16 and 24 h), and biosorbent dosage (0.1, 0.2, 0.3, 0.4 and 0.5 gr in 100 mL). The batch adsorption isotherm experiments were performed in 125 mL Erlenmeyer flasks with 50 mL of HMs solutions at 180 rpm for 24 h to ensure equilibrium was achieved. The initial pH of the solution was adjusted to the appropriate value with 0.1 M HCl and 0.1 M NaOH, which

was measured using a HACH (HQ40D) Instrument. After completion of each experiment, biosorbent loaded with HMs were separated from aqueous phase by filtration using a EZFlow Membrane filter paper with 47 mm diameter and 0.45 μm pore size. All experimental runs were triplicated to estimate experimental error and ensure reliable results. Equilibrium concentrations of HMs were measured using Atomic Absorption Spectroscopy (AAS) (PinAAcle 500, Perkin Elmer, Canada). The wavelength was 228.8 nm for Cd(II), 324.75 nm for Cu(II), and 232 nm for Ni(II). Concentrations of Cd(II), Cu(II) and Ni(II) in synthetic phase before and after were labelled as C_i and C_e respectively. The removal efficiency (%) was calculated using Eq. (4-2);

$$Adsorption\ Removal\ (\%) = \frac{C_i - C_e}{C_i} \times 100 \quad (4\text{-}2)$$

The adsorption uptake of chitin (q_e) was determined using Eq. (4-3);

$$Adsorption\ Capacity\ (mg/L) = \frac{(C_i - C_e)\,V}{chitin\ dosage} \quad (4\text{-}3)$$

V in this equation is the volume of the solution (L), C_i and C_e are initial and equilibrium concentrations of HMs (mg. L^{-1}), and chitin dosage (gr).

Following the adsorption of metal ions (Cu(II), Cd(II), and Ni(II)) onto Ch-C and Ch-DES, the chitin was separated by filtration and rinsed with de-ionized water and air-dried. The dried Ch-C and Ch-DES were then subjected to desorption in 50 mL of various solutions, including DI water, sodium chloride (NaCl, 1 M), and sulfuric acid (H2SO4, 0.1 M) for 24 h. AAS was utilized to quantify the amount of desorbed metal ions. Each experiment was replicated three times. The percentage of desorption was determined using the following equation:

$$\text{Desorption}\ (\%) = \frac{\text{Amount of metal ions desorbed (mg/L)}}{\text{Amount of metal ions adsorbed (mg/L)}} \times 100 \quad (4\text{-}4)$$

4.3.8 Adsorption isotherm models

Batch adsorption experiments were conducted at room temperature using 50 mL HMs' solutions with initial concentrations ranging from 2.5 to 100 mg/L over a 24-hour period. Ch-C and Ch-DES powder, at a dosage of 2.5 g/L, were introduced into the solutions, and the pH was adjusted to 5.5 for the multi-component HMs solution, 5 for Ni and Cu solution, and 6 for a solution with only Cd as a HM. These pH levels were determined as the optimal pH for each component. To analyze the adsorption isotherms, two of the most frequently used models, Langmuir [143] and Freundlich [144] , were applied, as presented by Eq. (4-5) and Eq. (4-6), respectively. The isotherm models' fitness was evaluated using the coefficient of determination (R^2) and root mean square error (RMSE) based on the experimental equilibrium data.

Langmuir isotherm model:

$$Q_e = \frac{q_{max} b C_e}{1 + b C_e} \tag{4-5}$$

Freundlich isotherm model:

$$Q_e = K_f C_e^{\frac{1}{n}} \tag{4-6}$$

Where Q_e is the equilibrium metal adsorption uptake (mg/g), C_e is the equilibrium metal concentration (mg/L) and q_{max} is the maximum adsorption capacity (mg/g). The K_f is the Freundlich adsorption equilibrium constant, n is constant indicative of adsorption intensity, and b is bonding energy of adsorption that represents affinity.

4.3.9 Thermodynamic Study

A series of flasks containing 50 mL of HMs' solution (2.5mg/L for single-component solution, 100 mg/L for three-components solution) at pH 5 (single Cu and Ni solution), 5.5 (HMs' combination) and 6 (single Cd solution) were prepared. Ch-C and Ch-DES powder weighing 125 mg (equivalent to 2.5 g/L) were added to each flask and agitated in an incubator shaker at 180 rpm for 24 hours at varying temperatures (5, 20, and 40°C). This experiment was conducted to assess the effect of temperature on adsorption and to determine the thermodynamic parameters.

4.3.10 Kinetic Study

A kinetic study, Pseudo first order (PFO) [161] and Pseudo second order (PSO) [173], [174], was conducted to illustrate adsorption behavior of Ch-C and Ch-DES at optimal initial concentrations (2.5 mg L^{-1}) at optimum pH and 20 ℃. The adsorption uptake was estimated at different time intervals (5, 10, 15, 20, 30 min, 1, 3, 6, 16 and 24 h). The equations for PFO and PSO are outlined as follows [175]:

Pseudo-first-order equation:

$$q_t = q_e(1 - (\exp(-\mathrm{kt})) \quad (4\text{-}7)$$

Pseudo-second-order equation:

$$q_t = k_2 q_e^2 t(1 + k_2 q_e t)^{-1} \quad (4\text{-}8)$$

Where q_t and q_e (mg/g) represent the amounts of adsorbate on the adsorbents at time t and at equilibrium, respectively. k_1 (1/min) and k_2 (g/mg/min) denote the rate constants of PFO and PSO kinetic models.

4.4 Results & Discussion

4.4.1 Chitin Yield%

Chitin yield was determined by comparing the mass of the extracted chitin to the original weight of the SSW, which is calculated using Eq. (4-1). As shown in Table 4-2, chitin extracted by DES with a ratio of 1:2.5 (HBA:HBD) had the highest chitin yield of approximately 56.94 ± 1.63. A higher yield is desirable, as it indicates that a larger fraction of shrimp shell weight is converted to the biosorbent [128], [129]. Moreover, the DES synthesized at molar ratio of 1:1 showed recrystallization at room temperature.

Table 4-2 Chitin yield (%) using different DESs synthesized under given conditions.

Raw Source	DESs Synthesis			Chitin Extraction Conditions		
	DES	Temperature ℃	Solid/Liquid	Temperature ℃	Time h	Chitin Yield (%)
SSW	DES-1	80	1:20	80	2	46.75 ± 0.51
	DES-2	80	1:20	80	2	48.54 ± 1.07
	DES-2.5	80	1:20	80	2	56.94 ± 1.63
	DES-3	80	1:20	80	2	50.63 ± 1.15

Furthermore, the adsorption uptake of each extracted chitin was evaluated using 2.5 g/L of adsorbent for 100 mg/L initial concentration of HMs in a multi-component system, at the optimal pH of 5.5. The contact time and temperature were 24 h and 20 °C, respectively. As shown in Fig 4-2, the highest adsorption uptake is related to the chitin extracted with DES-2.5, which also has the highest chitin yield compared to other synthesized DES. Therefore, the HBA:HBD ratio of 1:2.5 or DES-2.5 was chosen for the chitin extraction.

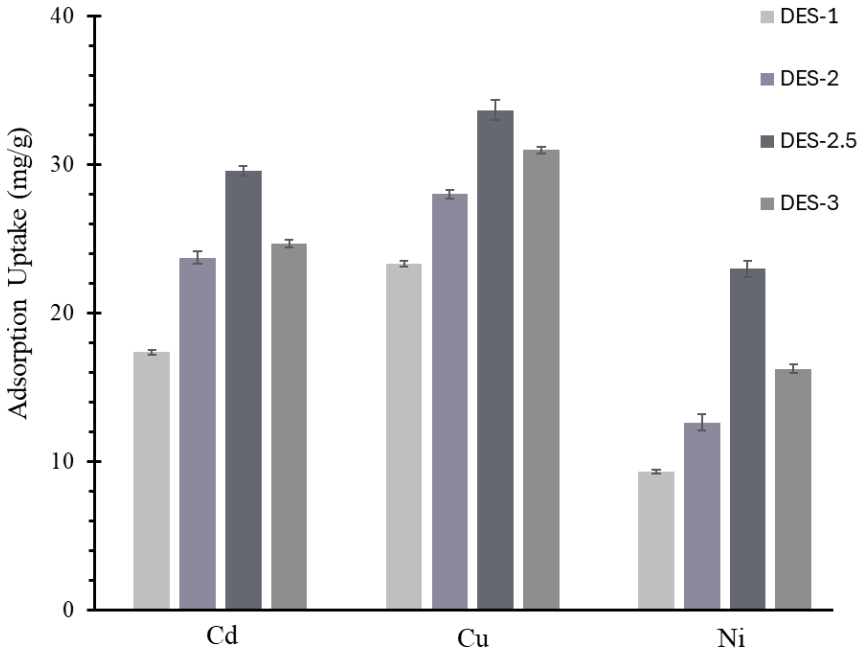

Figure 4-2 Adsorption uptake (mg/g) of chitin for Cd, Cu, and Ni using different synthesized DESs.

4.4.2 Effect of Experimental factors on Adsorption in Single Component System

The optimization of experimental parameters was initially performed using a single component solution with Ch-C as the adsorbent. After determining the optimal conditions, the same parameters were applied to both Ch-C and Ch-DES in a competitive environment (multi-component system) for performance comparison. The optimization of experimental factors were not conducted for Ch-DES for three main reasons: (i) the optimization using Ch-C provided a reliable baseline for adsorption conditions, (ii) FT-IR characterization, presented in the following section, confirmed that Ch-C and Ch-DES exhibit similar functional group behavior and (iii) to ensure a meaningful comparison between the two adsorbents, it was essential to maintain identical experimental conditions. Therefore, applying the same optimized parameters to both adsorbents avoids unnecessary experimental variation and ensures that differences in performance are attributable to material properties rather than differing test conditions.

4.4.2.1 Ch-C dosage

Finding the optimum adsorbent dosage is important because it increases the interactions between HM ions and adsorption sites of the adsorbent in the solution while maintaining high removal efficiency. The impact of different Ch-C dosage on adsorption of Cd(II), Cu(II) and Ni(II) were studied using 0.1 - 0. 5 g L^{-1} while the HMs' concentration was 25 mg L^{-1}, the initial solution pH was 4 which is the natural pH of the solution, and the samples were at 20 ℃ for a contact period of 24 h. Fig 4-3 illustrates the variation of adsorption uptake and removal percentage of HMs as a function of adsorbent dosage (Ch-C). For Cd(II), the results showed a sharp increase in removal percentage from 54.36 to 99.83 %, and then reaching a plateau by changing Ch-C dosage from 1 to 5 mg/L, which is in agreement with a previous study [135], [176]. However, adsorption uptake witnessed a reverse trend [177], [178], declining from 13.59 to 4.99 mg/g with an increase in the adsorbent dosage. The trend was the same for Cu and Ni as shown in Fig 4-3. By increasing the Ch-C dosage from 1 to 5 g/L, removal percentage increased from 63.85 to 98.79 % for Cu(II) and 77.80 to 97.91 % for Ni(II), while the adsorption uptake gradually dropped from 15.96 to 4.94 mg/g for Cu(II) and 19.45 to 4.89 mg/g for Ni(II). In general, as shown in Fig 4-3, by increasing chitin loading,

the adsorption efficiency improved due to the greater number of available binding sites in the solution. However, the adsorption uptake (mg/g) for all metals declined, which can be a result of the incomplete saturation of these binding sites during the adsorption process. Within the range studied in this experiment, the removal efficiency and adsorption uptake for HM ions were at their optimum level when the Ch-C dosage was 0.25 g (in 100 mL). Therefore, this dosage was chosen as the optimal dosage for following experiments.

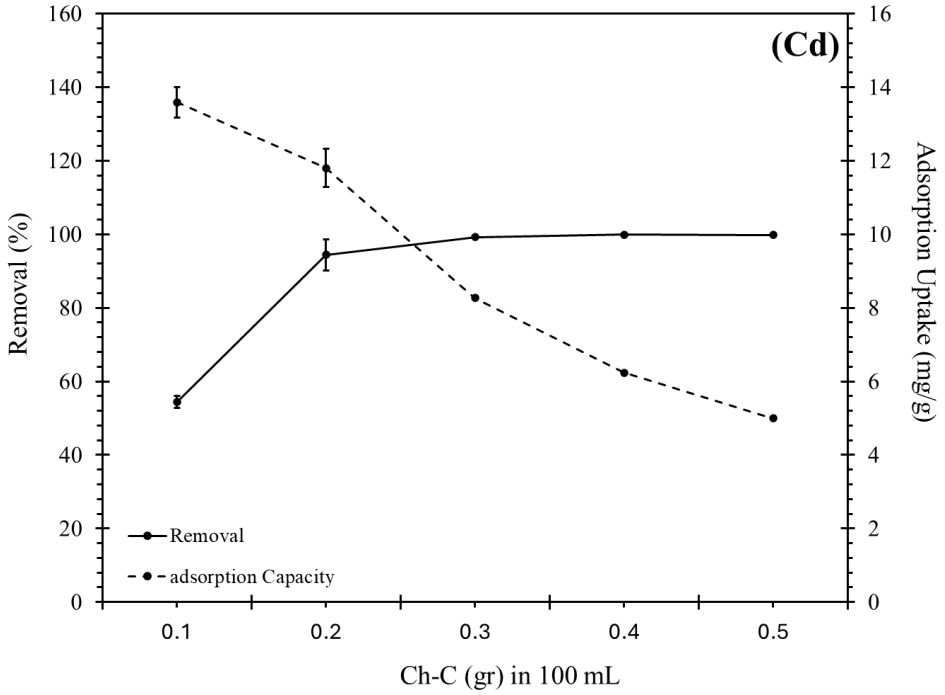

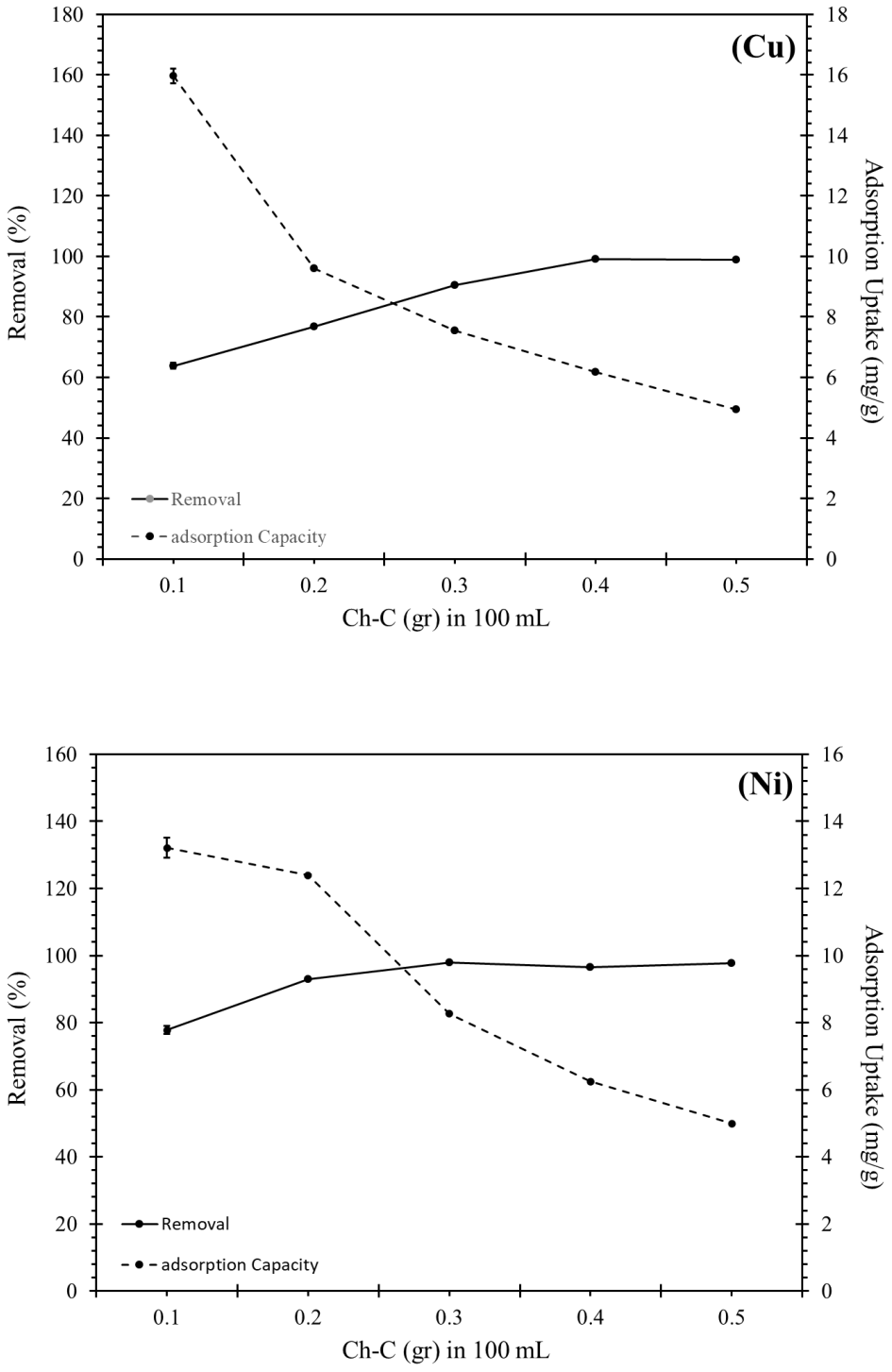

Figure 4-3 Effect of Ch-C dosage on removal efficiency (%) and adsorption uptake (mg/g) of Cd(II), Cu(II), and Ni(II).

4.4.2.2 pH

The pH of the solution is another important parameter that influences adsorption efficiency by shifting the adsorbent-adsorbate interactions. The effect of initial pH is more significant than the final pH, as it affects the degree of ionization and protonation or deprotonation of active sites on adsorbent, surface properties of adsorbent, speciation of metal ions and surface functional groups [179]. Previous literature indicates that Cu(II), Cd(II), and Ni(II) tend to precipitate as hydroxides at pH levels above 8 [180][181]. Accordingly, pH ranges up to 8 were chosen for this investigation. Fig 4-4 illustrates the effect of initial pH within the range of 4.0 to 8.0 on the adsorption efficiency of Ch-C toward Cd (II), Cu(II) and Ni(II) when the adsorbent dosage was 2.5 mg/L, at room temperature with a duration of 24 h. The results revealed an increase in removal percentage from 84.79% to 87.99% for Cu(II) and 94.29% to 99.67% for Ni(II) while pH increased from 4 to 5. This is due to the existence of amino groups in Ch-C. After pH 5, the removal efficiency of Cu and Ni gradually dwindled. Moreover, according to the experiments conducted, the Cu(II) and Ni(II) start to precipitate after pH 5 and at pH 5.5. For Cd(II), the removal percentages under the influence of pH, remains almost constant although with slight difference, the maximum efficiency was in pH 6 with removal efficiency of 99.75%. Similar patterns were observed by previous study [19][182], [183], [184], [185], [186].

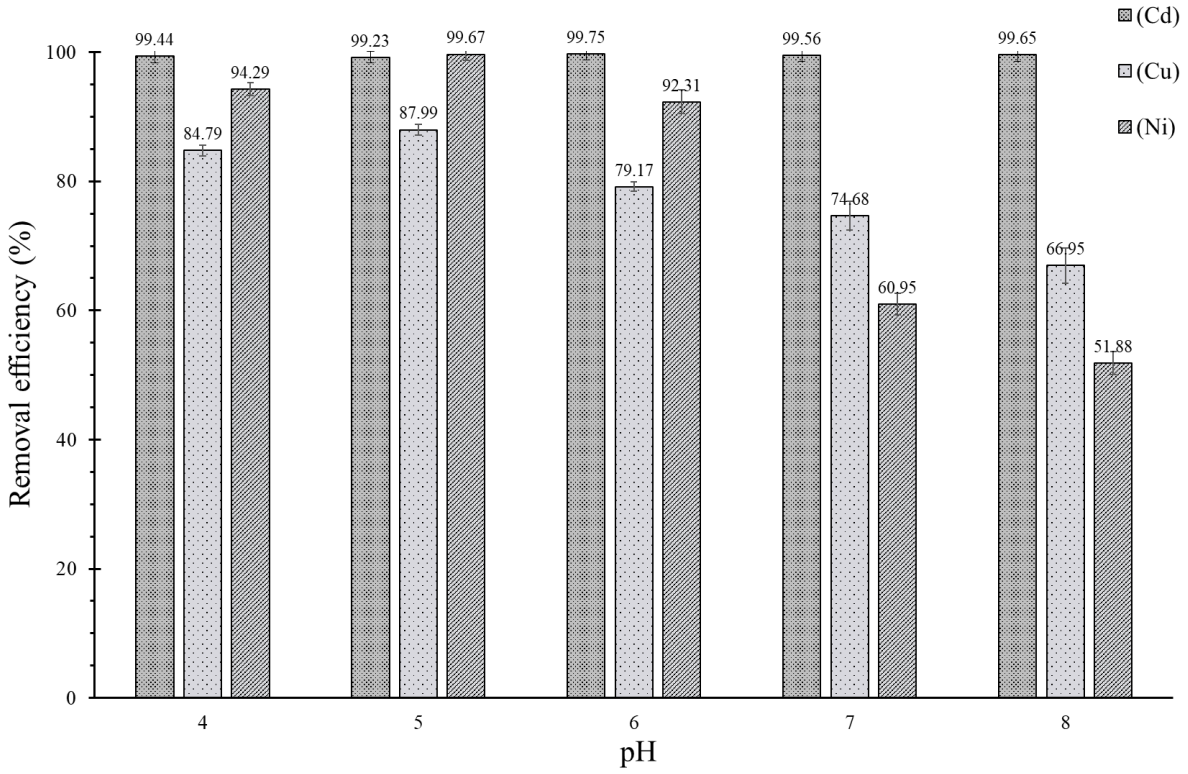

Figure 4-4 Effect of pH on removal efficiency (%) of Cd(II), Cu(II) and Ni(II), onto Ch-C.

Furthermore, the addition of Ch-C to solution results in a noticeable increase in pH, as shown in Table 4-3. This change is important because it reduces the chance of the nitrogen atoms in chitin's acetamido groups becoming protonated. When these groups are not occupied by hydrogen ions (H^+), they are more available to bind with metal ions like Cd(II), Cu(II), and Ni(II) [6][7]. At lower pH values, the high number of H^+ ions compete with metal ions for the same binding sites, which makes it harder for the metals to attach to the Ch-C surface. This competition reduces the overall adsorption uptake [187], [188]. For initial pH values of 4, 5, 6, 7 and 8, the final pH measurements for Cd(II) were 6.9, 7.1, 7.4, 8.4 and 8.9, respectively – for Cu(II) were 6.4, 7.1, 7.7, 8.2 and 8.9, respectively – and for Ni(II) were 6.4, 7.3, 7.9, 8.5 and 9.0, respectively.

Table 4-3 Initial pH (before adsorption) and final pH (after adsorption).

pH						
Theoretical	Cd (II)		Cu (II)		Ni (II)	
	Initial	Final	Initial	Final	Initial	Final
4	4.01	6.87	4	6.41	3.96	6.39
5	5.02	7.09	4.79	7.08	5.01	7.31
6	6.13	7.41	6.14	7.68	5.93	7.92
7	7.07	8.36	6.89	8.17	6.78	8.47
8	8.13	8.93	7.86	8.85	7.89	8.98

Correspondingly, as illustrated in Fig 4-5, the adsorption uptake (mg/g) was from 9.94 ± 0.1 mg/g – 9.97 ± 0.11 mg/g for Cd(II), from 8.5 ± 0.2 mg/g – 0.5 ± 0.02 mg/g for Cu(II), and from 9.43 ± 0.1 mg/g – 0.11 ± 0.01 mg/g for Ni(II). Considering the increases in adsorption uptake beyond an initial pH of 4 (with the final pH of 6.41 and 6.39) and significant decrease in adsorption uptake beyond pH 5 for Cu(II) and Ni(II) and the importance of maintaining the final pH below 7.5 during adsorption tests (because of precipitation), with taking note that the maximum efficiency of adsorption of these HMs (87.99%, and 99.67%, respectively) was observed in weak acidic medium at pH 5. Thus, pH 5 was selected as the optimal initial pH for Cu and Ni. For Cd(II), these increases in pH doesn't have a significant effect on either adsorption uptake (mg/g) nor removal efficiency (%). Therefore, the pH 6 was chosen as initial pH for this HM, which results in slightly highest removal efficiency (99.75 %) and adsorption uptake (9.97 ± 0.10 mg/g) while maintaining the final pH below 7.5 (7.41). Moreover, the pH was set to 5.5 for the multi-component system, and preliminary tests confirmed that no precipitation of Cu(II) or Ni(II) occurred at this pH.

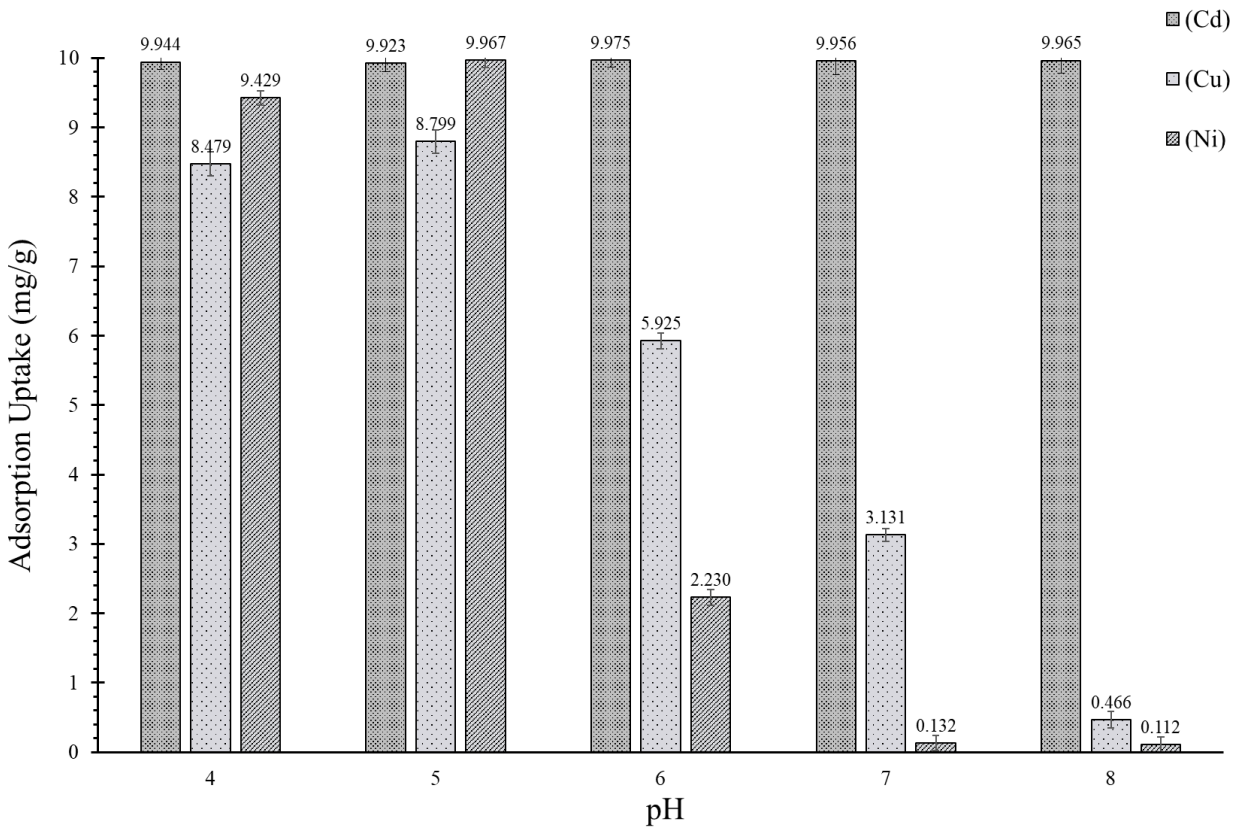

Figure 4-5 Effect of pH on adsorption uptake (mg/g) of Cd(II), Cu(II) and Ni(II), onto Ch-C.

4.4.3 Adsorption isotherm models in single component system (Ch-C)

Adsorption isotherm is based on the relation between the adsorption uptake which is the amount of adsorbate that adsorbent can adsorb, and the adsorbate's concentration in the solution at constant temperature [160]. Isotherm models provide valuable insights into the distribution of adsorption sites on the adsorbent surface and reveal key characteristics such as surface properties and capacities of the adsorbents[172]. This study analyzed the Langmuir, Freundlich isotherm models for the removal of selected HMs (Cd, Cu, Ni) from the media. The two isotherm models are drawn by using experimental data and shown in Fig 4-6. The Freundlich isotherm model is based on the premise of a heterogeneous surface, where active adsorption sites are unevenly distributed. In contrast, the Langmuir isotherm assumes monolayer adsorption on a homogeneous surface, where adsorption occurs only at a specific, fixed number of

equivalent and identical sites without any lateral interaction or steric hindrance among the adsorbed molecules [189].

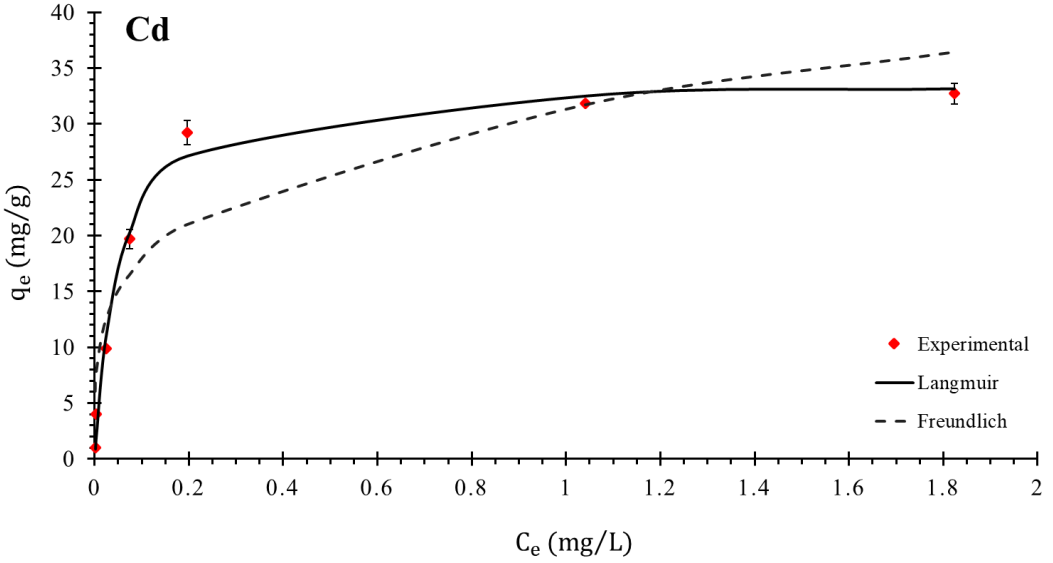

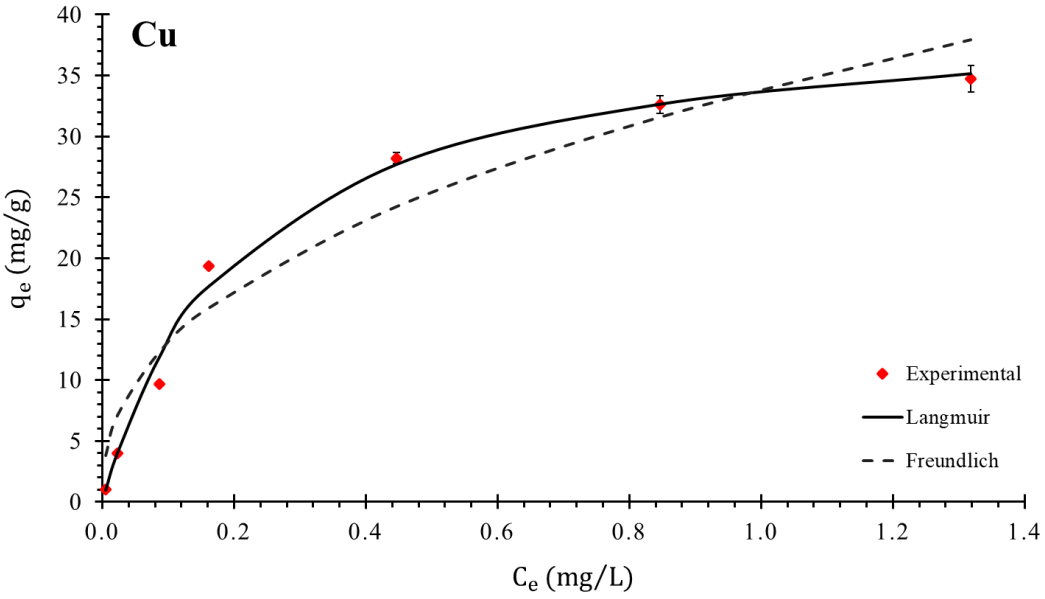

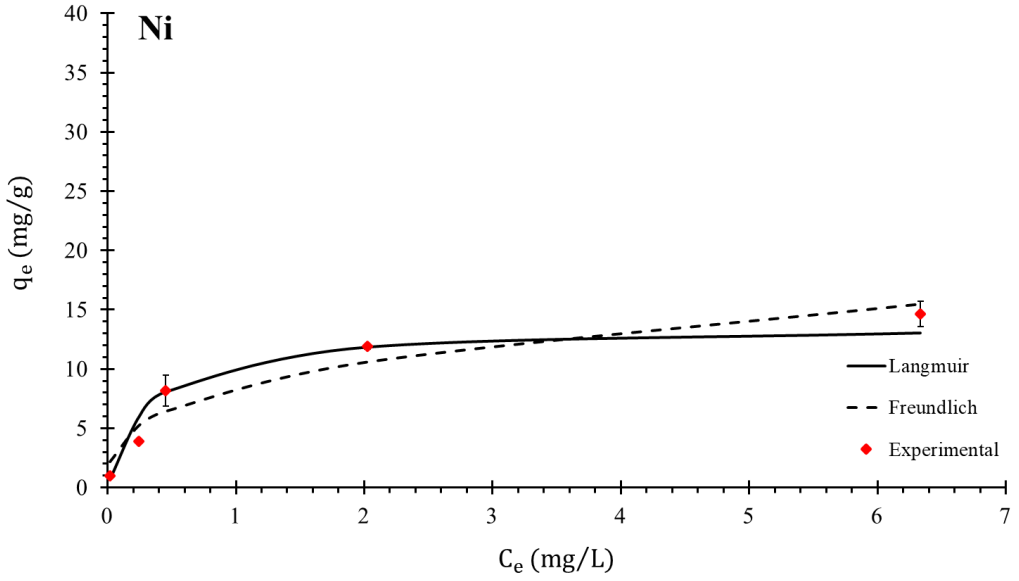

Figure 4-6 Langmuir and Freundlich isotherm models of the adsorption of Cd(II), Cu(II) and Ni(II) on a single-component solution by Ch-C.

The adsorption isotherm parameters, coefficient of determination (R^2) and RSME were determined after fitting the isotherm models to the experimental data, with the results presented in Table 4-4. Based on the R^2 values and RMSE, the Langmuir model showed the best performance. This suggests that the chitin adsorbent surfaces were homogeneous, featuring uniformly distributed sites with equivalent energy levels. According to the Langmuir model, the maximum adsorption capacities for Cd(II) at 20˚C and a pH of 6 using 2.5 g/L Ch-C was determined to be 33.62 mg/g (0.299 mmol/g), and for Cu(II) and Ni(II) at same condition with a pH of 5 was 40.80 mg/g (0.642 mmol/g) and 13.70 mg/g (0.233 mmol/g), respectively. The Langmuir constant, b, has the highest value for Cd(II). This indicates that Ch-C has the highest affinity with Cd(II) ions and more tendency to adsorb more Cd(II) at higher concentration [7]. As indicated in Table 4-4, the RMSE of Langmuir model for Cu, Cd and Ni was calculated as 2.83, 3.11, 2.93 respectively, which is less than RMSE of Freundlich model for each metal.

Table 4-4 Langmuir and Freundlich results for adsorption of Cd(II), Cu(II), and Ni(II) on a single-component solution by Ch-C.

Model	Constants	Cu	Cd	Ni
Langmuir	q_{max} (mg/g)	40.79	33.62	13.70
	b (L/mg)	4.74	18.85	3.18
	RMSE	2.83	3.11	2.93
	R^2	0.997	0.996	0.975
Freundlich	K_f (mg/g)$(L/mg)^{1/n}$	33.81	28.77	8.36
	$1/n$	2.41	3.70	3.00
	RMSE	7.97	11.80	2.63
	R^2	0.959	0.938	0.965

Considering the costs associated with production, stabilization, and disposal, and to evaluate the potential leaching of the adsorbed HMs, it is necessary to assess the desorption of HMs and the regeneration and reuse of adsorbents. As shown in Table 4-5, desorption using DI water and NaCl solution was not effective. However, H_2SO_4 solution exhibited the effective performance, with all the HMs being effectively separated by more than 90% from Ch-DES. The desorption rate in the case of Ch-C using H_2SO_4 solution was also effective and in the range of 87% to 97%.

Table 4-5 The studied desorption media for Cu(II), Cd(II) and Ni(II) onto Ch-C and Ch-DES in a single-component system.

Desorption percentage (%)	Ch-C			Ch-DES		
	Cd(II)	Cu(II)	Ni(II)	Cd(II)	Cu(II)	Ni(II)
DI Water	26.71 ± 0.94	38.32 ± 1.06	22.54 ± 0.97	42.32 ± 1.15	55.29 ± 1.41	23.70 ± 0.81
NaCl (1 M)	37.36 ± 1.21	70.61 ± 0.85	50.93 ± 1.08	50.93 ± 1.31	62.79 ± 1.47	37.36 ± 1.63
H_2SO_4 (0.1 M)	87.27 ± 0.98	96.83 ± 1.17	92.88 ± 1.36	90.63 ± 0.79	97.78 ± 1.82	93.84 ± 1.57

4.4.4 Thermodynamic analysis

Temperature has been recognized as an effective factor for the HMs' adsorption, primarily because on the solid/liquid interfaces, the mobility of metal ions, and the swelling property of adsorbents. To examine the effect of temperature and better understand the nature of an absorption reaction it is critical to know the thermodynamic parameters. The spontaneousness, randomness and endothermic or exothermic nature of the adsorption can be determined by analyzing the thermodynamic parameters such as Gibbs Free Energy (ΔG°), Enthalpy (ΔH°), and Entropy (ΔS). In this study, thermodynamic analysis performed under two different temperatures, 20 and 40 ℃, on adsorption of Cd(II), Cu(II) and Ni(II) in a single component solution when the chitin (Ch-C and Ch-DES) dosage, pH, and initial concentration were 2.5 g/L, 6 for Cd and 5 for both Cu and Ni, and 2.5 mg/L, respectively. The relationship between Gibbs Free Energy and the sorption equilibrium constant for the adsorption process can be expressed as:

$$\Delta G^{\circ} = -RT\ lnk_c \tag{4-9}$$

Where, ΔG° represents the Gibbs Free Energy (J/mol), k_c represents the sorption equilibrium constant, T is the temperature (K), and R is the universal gas constant (8.314 J/(mol·K)). The sorption equilibrium constant (k_c) for the adsorption process is determined using Eq. (4-10) [190] at temperatures of 298.15 K, 313.15 K:

$$k_c = \frac{C_{ad}}{C_e} \tag{4-10}$$

At equilibrium, C_{ad} represents the concentration of solute adsorbed (HMs) on the adsorbent (mg/L), while C_e refers to the equilibrium concentration of HM ions in the solution (mg/L). Using the equilibrium constant calculated for each temperature, ΔG° can be determined using Eq. (4-9). It is important to note that the calculated ΔG° assumes that the adsorption of HM ions is reversible, and that the system reaches equilibrium at all temperatures.

The standard enthalpy change (ΔH°) and entropy change (ΔS°) of an adsorption system can be determined using the Van't Hoff equation (Eq. (4-11)) at various temperatures, assuming these parameters remain

constant with temperature. By plotting ΔG° vs. T, and analyzing the linear behavior of the plot, ΔH° can be calculated from the slope, and ΔS° can be derived from the intercept:

$$\ln k_c = \frac{\Delta S^\circ}{R} - \frac{\Delta H^\circ}{RT} \quad (4\text{-}11)$$

The thermodynamic parameters for the adsorption of Cd(II), Cu(II), and Ni(II) onto Ch-C are summarized in Table 4-6. The negative ΔG° values at both temperatures studied (293.15 K and 313.15 K) for all three HMs, is evidence of spontaneous adsorption [191]. With increasing temperature, the ΔG° values for the adsorption process became less negative that suggests a reduction in adsorption favorability and driving force at higher temperatures [192]. The sign and magnitude of ΔH° suggests the nature of interactions between the adsorbent (Ch-C) and the adsorbates (HMs). Unlike typical endothermic processes, the negative ΔH° values for all three HMs indicate that the adsorption reactions were exothermic [19], [193], signifying that the adsorption process releases energy. Among the three metals, Ni(II) demonstrated the most exothermic behavior with a ΔH° of −115.74 kJ/mol, followed by Cd(II) (−79.33 kJ/mol) and Cu(II) (−4.52 kJ/mol). The differences in adsorption mechanisms and the degree of randomness at the solid/solution interface can be understood by analyzing the entropy changes (ΔS°) [193], [194]. The positive ΔS° value for Cu(II) (+7.97 J/mol·K) suggests increased randomness during adsorption [19], while the highly negative ΔS° for Cd(II) (−215.67 J/mol·K) and Ni(II) (−353.41 J/mol·K) indicates a decrease in randomness. This is possibly due to stronger interactions or structural changes in the adsorbent [192], [193], [194].

Table 4-6 Thermodynamic parameters for HMs adsorption onto Ch-C at pH 6 for Cd(II) and 5 for Cu(II) and Ni(II), dosage 2.5 g/L and HM concentration 2.5 mg/L.

	Equilibrium Constant		ΔG° (kJ mol^{-1})		ΔH° (kJ mol^{-1})	ΔS° (kJ mol^{-1})
Temperature (K)	293.15	313.15	293.15	313.15		
Ch-C + Cd(II)	741.57	92.75	-16.11	-11.79	-79.33	-215.67
Ch-C + Cu(II)	16.69	14.82	-6.86	-7.02	-4.52	7.97
Ch-C + Ni(II)	145.20	7.00	-12.13	-5.06	-115.74	-353.41

Furthermore, the removal efficiency for all three HMs at 20 ℃ was higher than the removal percentage at 40 ℃ , which is in agreement with other studies [7][19][186], [195], [196]. The removal efficiency slightly decreases from 99.87 to 99.73 % for Cd(II), 99.81 to 93.68 % for Cu(II), and 99.32 to 96.87 % for Ni(II). Therefore, by raising the temperature, the attractive forces between active sites on Ch-C surface and metal ions present in solution will be weakened and the optimal efficiency can be achieved at 20 ℃.

The thermodynamic parameters for the adsorption of Cu(II), Cd(II), and Ni(II) onto Ch-DES are summarized in Table 4-7 The negative ΔG° values at both temperatures studied (293.15 K and 313.15 K) for all three HMs, is evidence of spontaneous adsorption. With increasing temperature, the ΔG° values for the adsorption process became less negative that suggests a reduction in adsorption favorability and driving force at higher temperatures. The sign and magnitude of ΔH° suggests the nature of interactions between the adsorbent (Ch-DES) and the adsorbates (HMs). Unlike typical endothermic processes, the negative ΔH° values for all three HMs indicate that the adsorption reactions were exothermic , signifying that the adsorption process releases energy. Among the three metals, Cu(II) demonstrated the most exothermic behavior with a ΔH° of −106.08 kJ/mol, followed by Cd(II) (−18.29 kJ/mol) and Ni(II) (−12.23 kJ/mol). The differences in adsorption mechanisms and the degree of randomness at the solid/solution interface can be understood by analyzing the entropy changes (ΔS°). The negative ΔS° value for HMs indicates a decrease in randomness.

Table 4-7 Thermodynamic parameters for HMs adsorption onto Ch-DES at pH 6 for Cd(II) and 5 for Cu(II) and Ni(II), dosage 2.5 g/L and HM concentration 100 mg/L.

Temperature (K)	Equilibrium Constant		ΔG° (kJ mol^{-1})		ΔH° (kJ mol^{-1})	ΔS° (kJ mol^{-1})
	293.15	313.15	293.15	313.15		
Ch-DES + Cu(II)	11.72	0.73	-6.00	0.83	-106.08	-341.39
Ch-DES + Cd(II)	4.77	2.95	-3.81	-2.82	-18.29	-49.39
Ch-DES + Ni(II)	3.03	2.20	-2.70	-2.05	-12.23	-32.48

4.4.5 Kinetics Study

Various kinetic models have been applied to analyze the experimental data and examine the rate-limiting step in the adsorption process for scaling-up in industries. Additionally, reaction kinetics provides insight into the progression of the reaction, the reaction mechanism, interfacial resistance through mass transfer, and the diffusion coefficient. The pseudo-first-order (PFO) [197] and pseudo-second-order (PSO) [173], [174] equations were chosen for kinetic modeling, and the kinetic study was carried out with 2.5 mg/L concentration of HMs at optimal pH and 20℃. The PFO and PSO were modeled using Eq. (4-7) and Eq. (4-8), respectively.

As shown in Fig A1-1 (Appendix A), the adsorption reactions reached equilibrium after 3 h for Cd(II), 6 h for Cu(II), and 45 min for Ni(II), indicating that Cu(II) required a longer time to achieve equilibrium. This fast initial adsorption is due to the large number of available adsorption sites, which progressively diminished as they were occupied over time [187]. It should be noted that the kinetics of Cd(II) and Ni(II) were notably rapid, with approximately 70% and 78% of Cd(II) and Ni(II) being adsorbed within the first 5 min of the process. As indicated in Table 4-8, the R^2 values for Cu(II) and Cd(II) obtained from PSO kinetic model is 0.98, which exceeds the results from PFO for these HMs, 0.97 and 0.89 respectively. Moreover, the experimental data of Ni(II) adsorbed on Ch-C showed better fitting to PSO with R^2 of 0.99 rather than PFO (R^2=0.93). Therefore, the calculated q_e using PSO with values of 0.965, 1.011 and 0.998 mg/g for Cu(II), Cd(II) and Ni(II) is closer to experimental q_e. This suggests that the adsorption process for these HMs is controlled by surface reaction dynamics [137][198][187].

Table 4-8 Results of kinetic study after fitting the models to equilibrium curve.

Model	Constants	Cu	Cd	Ni
PFO	q_e (mg/g)	0.912	0.971	0.977
	$K_{1\ (1/min)}$	0.036	0.204	0.297
	R^2	0.97	0.89	0.93
PSO	q_e (mg/g)	0.965	1.011	0.998
	$K_{1\ (g/mg/min)}$	0.056	0.414	0.744
	R^2	0.98	0.98	0.99

4.4.6 Multi-Component adsorption mechanisms

Thermodynamic, Isotherm and Kinetic studies have been conducted on removing HMs from solutions in a competitive environment using both Ch-C and Ch-DES to compare the performance of these adsorbents for the removal application of HMs.

4.4.6.1 Isotherm Study

In a solution with multiple HMs (Cd(II), Cu(II), and Ni(II)), due to competition of HMs for the same available sites on the adsorbent, the apparent adsorption uptake compared to single-component systems will decline. The competition will lead to a lower adsorption uptake for each of these metals and it depends on each metal's individual properties and interactions with the adsorbent [199]. The Langmuir and Freundlich isotherm models were selected to investigate the adsorption behavior, and the results are given in Table 4-9.

Table 4-9 Isotherm parameters for adsorption of HMs onto Ch-C and Ch-DES in a multi-component system.

Model	Constants	Ch-C			Ch-DES		
		Cu	Cd	Ni	Cu	Cd	Ni
Langmuir	q_{max} (mg/g)	32.88	29.85	19.71	42.20	38.25	23.48
	b (L/mg)	0.53	0.32	0.11	2.19	1.12	1.09
	RMS	13.32	8.81	3.62	6.03	2.19	2.93
	R^2	0.964	0.998	0.998	0.984	0.968	0.993
Freundlich	K_f (mg/g)$(L/mg)^{1/n}$	5.10	8.18	2.24	26.70	14.50	11.24
	$1/n$	0.93	0.50	0.70	0.46	0.66	0.56
	RMS	24.68	9.19	6.62	19.97	7.80	4.63
	R^2	0.879	0.970	0.995	0.966	0.918	0.978

Table 4-9 presents the estimated model parameters, R^2 values, and RMSE values. The R^2 coefficient measures the degree of fitness between the isotherm models and the experimental data and indicates how well the models represent the observed results. Higher R^2 values (≤ 1.00) suggest a strong correlation between the predicted models and the experimental data.

According to Tables 4-9, the Langmuir model showed the best fit with the experimental data, exhibiting a higher R^2 value (> 0.96) and lower values for RMSE for adsorption of Ni(II), Cd(II), and Cu(II), respectively. This suggests that adsorption of these HMs on Ch-C follows a linear pattern and is heterogeneous. The affinity constant (b) for Ni(II) (0.11 L/mg) is less than the b for Cu(II) and Cd(II), respectively. This shows that Ni is outcompeted and in a competitive solution, Cu(II) and Cd(II) have higher maximum adsorption uptake. As illustrated in Figure 4-8, the Langmuir model shows higher adsorption capacity for adsorption of along Cu (II), Cd (II), and Ni (II) on Ch-DES. The Freundlich model is fitted to experimental data and the graphs are presented in Fig A2-1 (Appendix A).

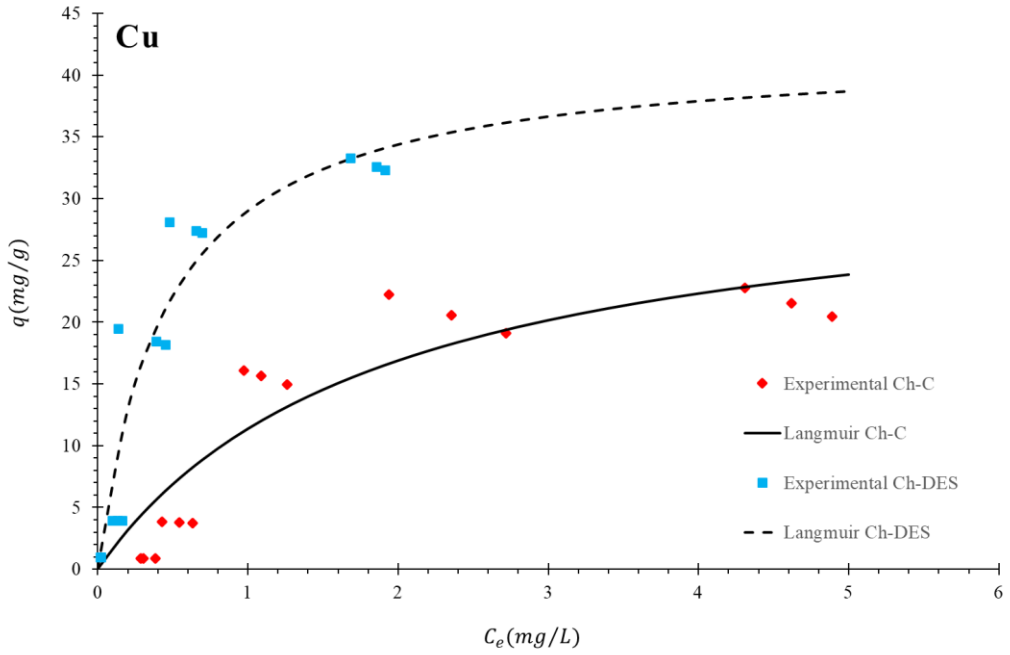

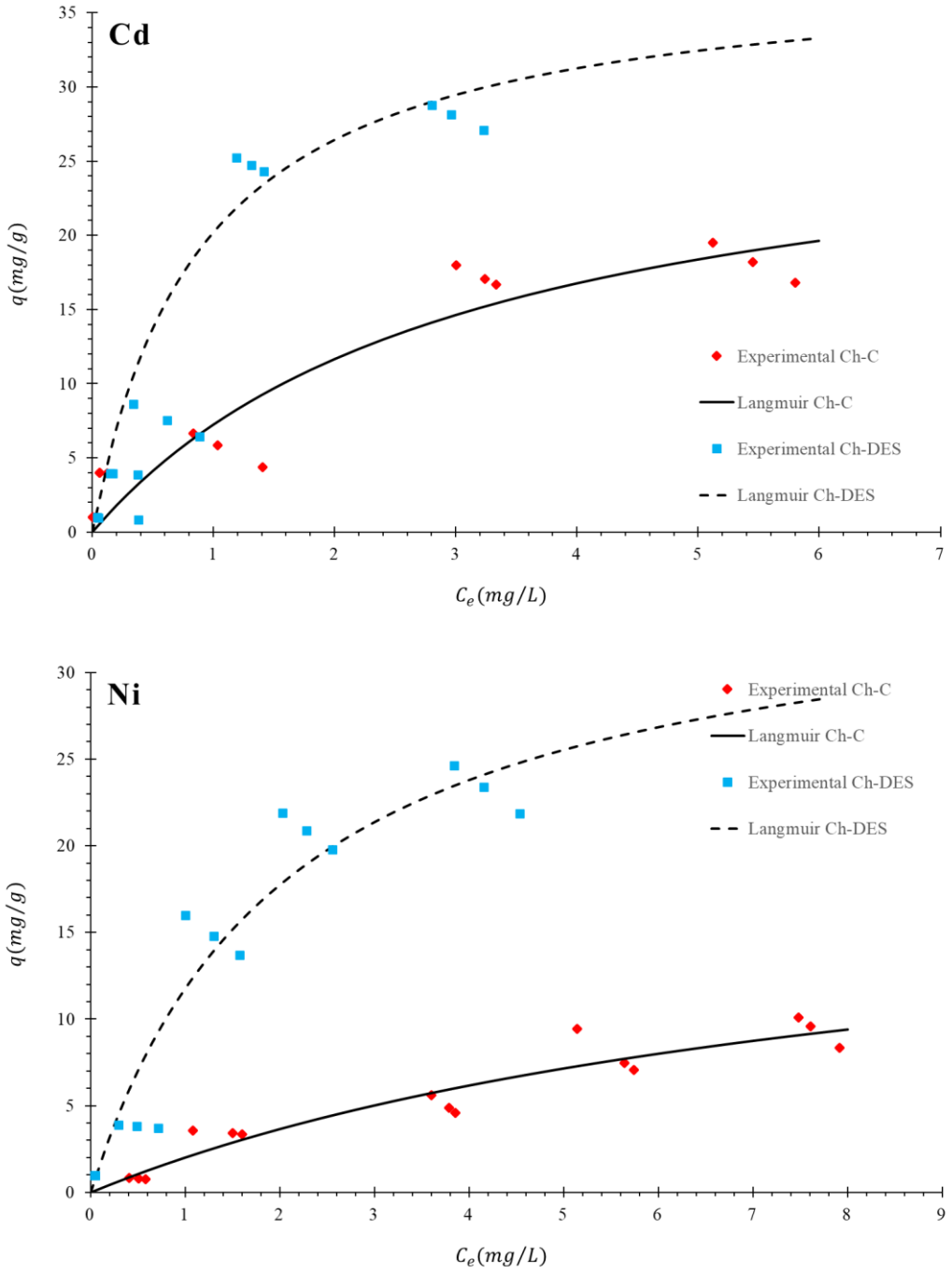

Figure 4-7 Experimental data and Langmuir model for initial concentration 2.5, 10, 50, 75 and 100 ppm of Cu(II), Cd(II) and Ni(II) on Ch-C and Ch-DES with dosage 2.5 g/L at 20 ℃ in a competitive environment.

According to Fig 4-7 and Tables 4-9, Langmuir model showed the best fit with the experimental data, exhibiting a higher R^2 value (0.984, 0.968 and 0.993) and lower values for RMSE (6.03, 2.19, and 2.93) for adsorption of Cu(II),Cd(II) and Ni(II), respectively. Based on the Langmuir model, the calculated

$q_{max}\left(\frac{mg}{g}\right)$ presented in Table 4-8 for Cu(II) and Cd(II) is determined to be 42.20 (0.664 mmol/g) and 38.25 mg/g (0.340 mmol/g) respectively which is higher than the values reported in literature [200][105][108][19]. The affinity constant (b) for Cu(II) (2.19 L/mg) is more than the b of 1.12 and 1.09 for Cd(II) and Ni(II) respectively. This shows that Cu has higher affinity with Ch-DES and in a competitive solution and therefore has higher maximum adsorption capacity. Furthermore, the 1/n value less than 1 indicates that the adsorption is favorable [140].

Following the adsorption, the desorption rates of HMs in various solutions onto Ch-DES in a multi-component system were also investigated and the results are presented in Table 4-10. When comparing the results of single-component to multi-component system onto Ch-DES, the decreased in desorption rate is noticed. This behavior is attributed to the competitive adsorption of metal ions, where ions with higher affinity (Cu) to the adsorbent surface form more stable complexes that are less susceptible to desorption. More than 89% , 63% and 52 of Cu(II), Cd(II) and Ni(II) was desorbed by H_2SO_4 onto Ch-DES in a multi-component system. Following is the NaCl with approximately 61%, 38% and 27% desorption of Cu, Cd and Ni. Given the values, the metal ions can be effectively adsorbed in a H_2SO_4 media when Ch-DES is used as an adsorbent and in a multi-component system and also for both Ch-C and Ch-DES in a single-component system.

Table 4-10 The studied desorption media for Cu(II), Cd(II) and Ni(II) onto Ch-DES in a multi-component system.

Desorption percentage (%)	Cd(II)	Cu(II)	Ni(II)
DI Water	19.25 ± 2.16	22.6 ± 1.54	17.37 ± 1.93
NaCl (1 M)	27.39 ± 1.82	61.41 ± 1.39	37.93 ± 1.66
H_2SO_4 (0.1 M)	63.8 ± 0.91	89.86 ± 1.09	52.23 ± 2.38

4.4.6.2 Thermodynamic Study

The thermodynamic parameters for the adsorption of Cd(II), Cu(II), and Ni(II) onto Ch-C and Ch-DES were calculated using Eq. (4-9) to (4-11) and the results are presented in Tables 4-11 and 4-12, respectively. As shown in Table 4-11, except for Cd at room temperature and Ni at both temperatures, the other samples

for adsorption of Cu experienced negative ΔG° at both temperatures. The data indicates that the adsorption of Cu(II) onto Ch-C occurs spontaneously [192], requiring no external energy input.

Table 4-11 Thermodynamic parameters for HMs adsorption onto Ch-C at pH 5.5, dosage 2.5 g/L and HMs' concentration 100 mg/L in a multi-component system.

	Equilibrium Constant		ΔG° (kJ mol^{-1})		ΔH° (kJ mol^{-1})	ΔS° (kJ mol^{-1})
Temperature (K)	293.15	277.15	293.15	277.15		
Ch-C + Cd(II)	0.83	1.73	0.45	-1.27	-30.94	-107.07
Ch-C + Cu(II)	1.17	3.74	-0.38	-3.04	-48.98	165.77
Ch-C + Ni(II)	0.30	0.96	2.74	0.10	-48.36	-174.85

According to Table 4-12, all the samples experienced negative ΔG° values at both temperatures, which indicates that the adsorption of Cu(II), Cd(II) and Ni(II) onto Ch-DES occurs spontaneously [192]. With increasing temperature from 4 ℃ to 20 ℃, the ΔG° values for the adsorption process became less negative onto both Ch-C and Ch-DES that suggests a reduction in adsorption favorability and driving force at higher temperatures [192]. The ΔH° values were negative for all metal-adsorbent combinations, confirming the exothermic nature of the adsorption reactions [193]. Notably, the magnitude of ΔH° was greater in Ch-DES for Cd(II) and Cu(II), with values of −40.74 and −42.83 kJ/mol, respectively, compared to −30.94 and −48.98 kJ/mol for Ch-C. This suggests that stronger interactions may occur between the DES-modified adsorbent and the metal ions [201]. However, for Ni(II), Ch-C exhibited a slightly more exothermic profile (−48.36 kJ/mol) than Ch-DES (−32.62 kJ/mol), indicating a more favorable interaction in the former [202]. Entropy changes (ΔS°) further reveal the nature of the adsorption mechanism and interfacial organization. The ΔS° values were negative for all HMs on both adsorbents, with the exception of Cu(II) on Ch-C (+165.77 J/mol·K), indicating increased randomness [19] [203]. This positive ΔS° suggests possible desolvation effects or structural rearrangements that enhance disorder. In contrast, the consistently negative ΔS° values for Ch-DES imply that adsorption resulted in a more ordered system, likely due to strong metal-ligand binding or confinement effects within the DES matrix [192], [193], [194]. The strongest entropy

reduction was observed for Cu(II) and Ni(II) on Ch-DES (−133.58 and −108.51 J/mol·K), indicating a more structured interface during adsorption.

Table 4-12 Thermodynamic parameters for HMs adsorption onto Ch-DES at pH 5.5, dosage 2.5 g/L and HMs' concentration 100 mg/L in a multi-component system.

	Equilibrium Constant		ΔG° (kJ mol^{-1})		ΔH° (kJ mol^{-1})	ΔS° (kJ mol^{-1})
Temperature (K)	293.15	277.15	293.15	277.15		
Ch-DES + Cd(II)	2.33	6.13	-2.07	-4.18	-40.74	-131.93
Ch-DES + Cu(II)	4.50	12.42	-3.67	-5.81	-42.83	-133.58
Ch-DES + Ni(II)	1.39	3.02	-0.81	-2.55	-32.62	-108.51

While most of the research conducted by other scientists regarding Cu (II), Cd(II) and Ni(II) adsorption on chitin or chitosan or SSW derivatives show spontaneous adsorption, a variety of ΔS◦ and ΔH◦ has been reported [6][7], [8][204].

4.4.6.3 Kinetic Study

Various kinetic models have been applied to analyze the experimental data and examine the rate-limiting step in the adsorption process for scaling-up in industries. In this study, the PFO [161] and PSO [173], [174] were chosen for kinetic modeling and have been calculated using Eq. 4-7 and Eq. 4-8, respectively. The kinetic study was carried out with 2.5 mg/L concentration of HMs at optimal pH = 5.5 and room temperature (20℃) onto both Ch-C and Ch-DES and the kinetic parameters are represented on Table 4-13.

Table 4-13 Results of kinetic study after fitting the models to equilibrium curve.

Model	Constants	Ch-C			Ch-DES		
		Cu(II)	Cd(II)	Ni(II)	Cu(II)	Cd(II)	Ni(II)
Pseudo-First-Order (PFO)	q_e (mg/g)	0.834	0.797	0.788	0.869	0.830	0.569
	$K_{1\ (1/min)}$	0.046	0.034	0.030	0.059	0.042	2.996
	R^2	0.96	0.97	0.97	0.95	0.97	0.51
Pseudo-Second-Order (PSO)	q_e (mg/g)	0.891	0.860	0.858	0.092	0.064	0.043
	$K_{2\ (g/mg/min)}$	0.069	0.049	0.041	0.922	0.886	0.912
	R^2	0.98	0.98	0.98	0.99	0.98	0.99

As shown in Fig 4-8, metal ions were quickly adsorbed onto both Ch-C and Ch-DES initially, but the rate gradually slowed down until equilibrium was achieved. This fast initial adsorption is due to the large number of available adsorption sites, which progressively diminished as they were occupied over time [187]. The adsorption reactions reached equilibrium after 6 h for Cd(II), Cu(II), and Ni(II), while it only took 3 h for HMs to reach equilibrium when using Ch-DES. It should be noted that the kinetics of these HMs were rapid, with approximately 46%, 54% and 39% of Cd(II), Cu(II) and Ni(II) being adsorbed onto Ch-C and 48%, 60% and 39% of Cd(II), Cu(II) and Ni(II) onto Ch-DES, within the first 20 min of the process. As indicated on Table 4-13, the R^2 values for Cu(II), Cd(II) and Ni(II) obtained from PSO kinetic model are more 0.98 for both adsorbent, which exceeds the results from PFO for these HMs. While Ni(II) adsorption onto Ch-DES shows a low R^2 value of 0.51 when modeling with PFO, the other samples have acceptable R^2. Therefore, the calculated q_e using PSO for Cu(II), Cd(II) and Ni(II) with values of 0.891, 0.860 and 0.858 mg/g onto Ch-C and 0.092, 0.064 and 0.043 mg/g onto Ch-DES, is closer to experimental q_e. This suggests that the adsorption process for these HMs is controlled by surface reaction dynamics [137][198] and it can be concluded that the adsorption of Cu (II), Cd(II) and Ni(II) onto both adsorbents is achieved through a covalent bond formation, representing chemical adsorption [187]. The PFO graphs for each HM onto Ch-C and Ch-DES are presented in Fig A1-2 and Fig A1-3, respectively.

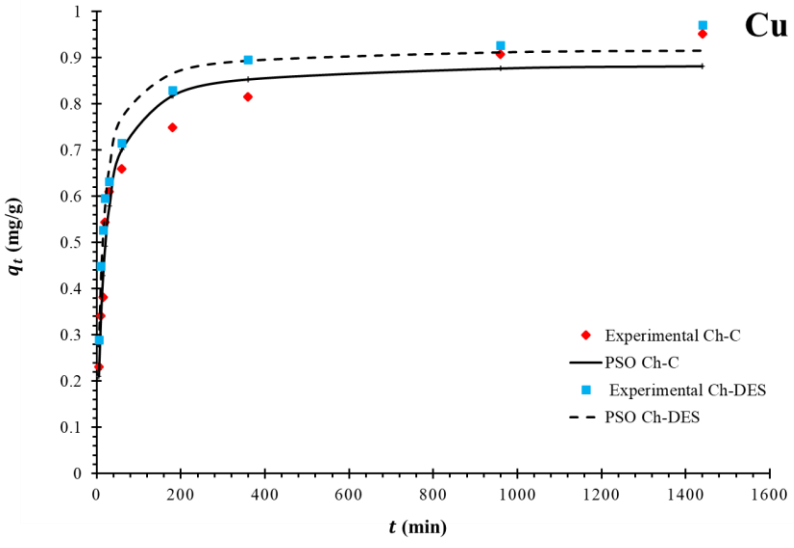

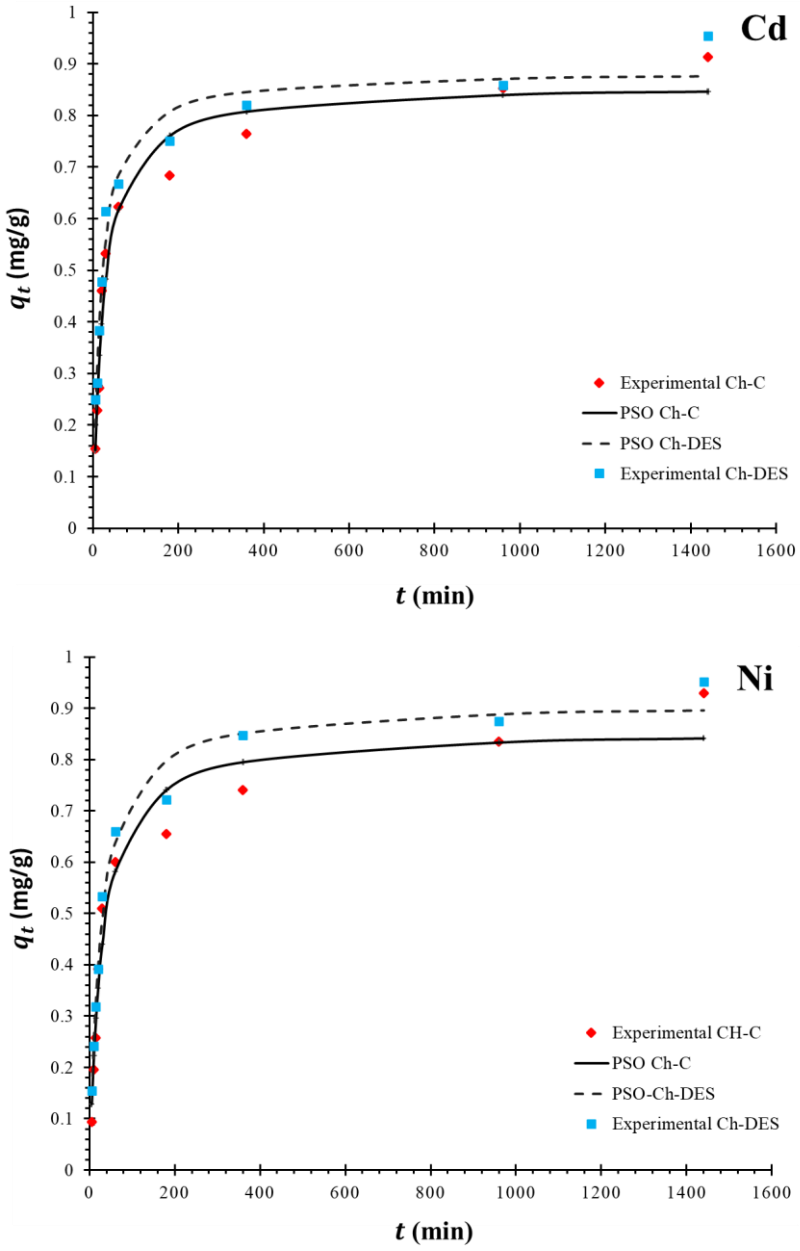

Figure 4-8 PSO kinetics of the adsorption of Cu(II), Cd(II), and Ni(II) in a multi-component system by Ch-C and Ch-DES.

4.5 Chitin Characterization

4.5.1 BET Analysis – Surface Area and Total pore volume

Table 4-14 summarizes the BET surface area and total pore volume of SSW, Ch-C and Ch-DES. As shown, Ch-C with 60.85 m^2/g exhibits a significantly larger BET surface area compared to SSW (6.99 m^2/g) and

Ch-DES (14.62 m²/g), providing almost 9 and 4 times larger surface area compared to SSW and Ch-DES, respectively. Moreover, the total pore volume of Ch-DES (1.346×10^{-1} cm³/g) was 16% higher than Ch-C's (1.156×10^{-1} cm³/g). This observation highlights the superior structural properties of Ch-DES, which offers more active sites and a greater pore network for adsorption processes.

Table 4-14 BET surface area and total pore volume of SSW, Ch-C and Ch-DES.

Adsorbent	BET surface area (m^2/g)	DFT cumulative pore volume (cm^3/g)
SSW	6.99	4.515E-02
Ch-C	6.085E+01	1.156E-01
Ch-DES	1.462E+01	1.346E-01

4.5.2 SEM Analysis

SEM analyses were conducted for the morphology of Ch-C in a single-component solution. The samples' condition for SEM were, initial concentration of 25 ppm, 24 hours, room temperature, pH=6 for Cd and 5 for both Cu and Ni. The Ch-C dosage was considered the optimal amount of 0.25 gr (in 100 ml). All the samples, before and after adsorption, were oven-dried at 50 ℃ overnight and kept in sealed containers until SEM was conducted. The findings obtained are shown in Fig 4-9. The SEM-EDS analysis was conducted on Ch-DES after HMs adsorption in a single-component system and the results are presented in Fig A4-1 (Appendix A). The SEM micrograph exposed that the Ch-C is extremely diverse in nature, porous and rough surface morphology. When comparing unloaded Ch-C and SSW, as shown in Fig. 4-9, SSW has a rougher surface than Ch-C, which is probably due to the natural structural complexity of SSW, including the presence of minerals and proteins. In contrast, Ch-C exhibits smoother and softer surface morphology, likely due to the partial removal of proteins, calcium carbonate, and other impurities during deproteinization and demineralization, which will result in a more purified and uniform chitin structure. SEM investigation of Ch-C was also conducted after Ni(II), Cd (II), and Cu(II) adsorption and provided in Fig 4-9. After

adsorption, the porous of Ch-C surface was covered by Ni(II), Cd (II), and Cu(II) ions, as shown in Fig 4-9 respectively, which support the high removal efficiency of Ch-C.

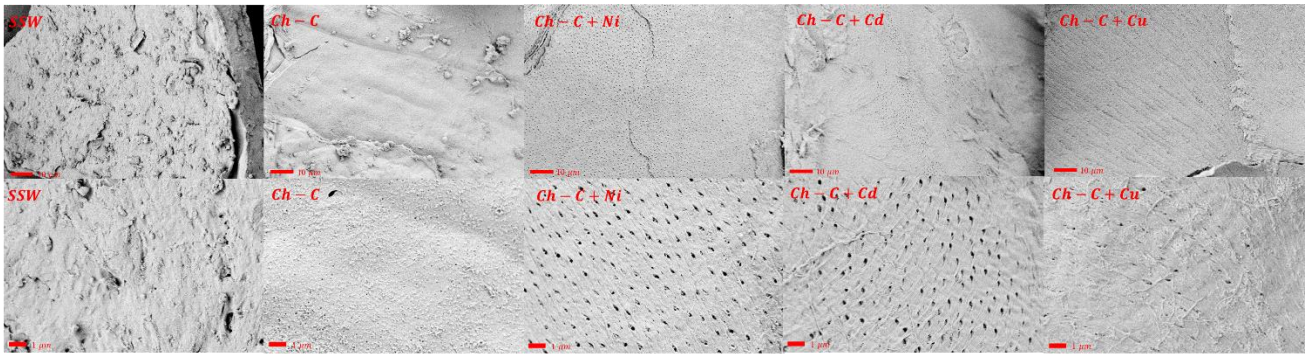

Figure 4-9 Plots of SEM analysis Virgin SSW; Virgin Ch-C; Ch-C loaded with Ni(II), Cd(II) and Cu(II).

4.5.3 SEM-EDS Analysis

The SEM-EDS analysis of Ch-C and Ch-DES after HMs' adsorption are shown in Fig. 4-10 (a) and (b), respectively. The EDS analysis showed the presence of carbon and oxygen, both of which are components of the chitin structure; plus, the Au and Pd peaks in the obtained spectra were caused by the samples being coated with gold-palladium. During the chitin extraction process, calcium carbonate ($CaCO_3$) should be removed. A comparison of the calcium (Ca) peaks in the SEM-EDS analysis reveals that the Ca signal is more prominent in Ch-C (Fig. 4-10 (a)) than in Ch-DES as shown in Fig. 4-10 (b), indicating that the DES method is more effective in removing calcium and, thus, in purifying chitin. The EDS data also confirmed the presence of Cu(II), Cd(II) and Ni(II) signals on both adsorbents. Overall, the EDS analysis of Ch-DES displayed higher peak intensities for HMs compared to Ch-C, indicating a potentially stronger affinity of Ch-DES for HM adsorption. As illustrated in Fig. 4-10 (b), Cu(II) exhibited the most prominent peak among the selected metals, suggesting that Ch-DES has a higher binding affinity for Cu(II) than for Ni(II) or Cd(II).

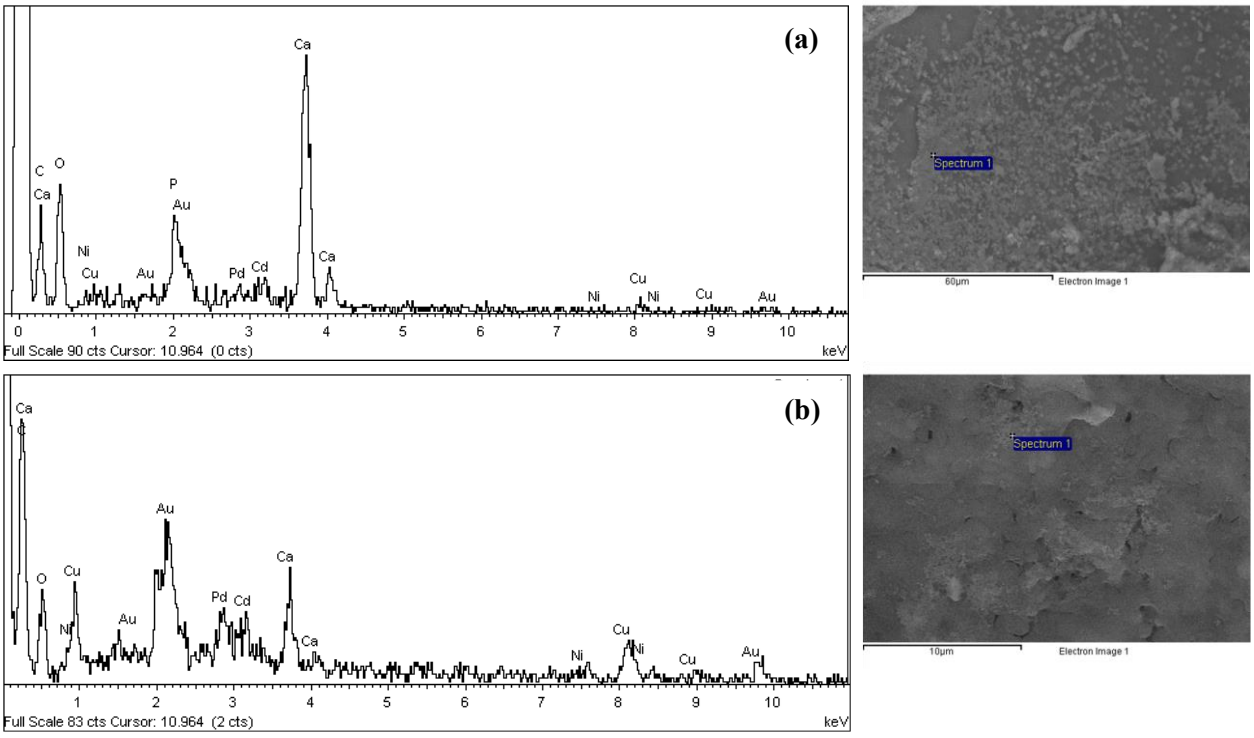

Figure 4-10 SEM-EDS analysis of (a) Ch-C and (b) Ch-DES after adsorption of Cu(II), Cd(II), and Ni(II).

4.5.4 FT-IR Analysis

As shown in Fig 4-11, FT-IR analysis was conducted on unloaded SSW, Ch-C and Ch-DES to compare the functional groups of these adsorbents. To better examine the binding of HMs, the functional groups of Ch-C and Ch-DES was studied after adsorption process when the surface of these adsorbents is loaded with Cd(II), Cu(II) and Ni(II). Additionally, the results of FT-IR analysis for Ch-C and Ch-DES in a single-component system are provided in Appendix A, Fig A3-1 and Fig A3-2 respectively. The samples' condition for FT-IR analysis were, initial concentration of 100 ppm, 24 hours, 20 ℃, pH=5.5 for removal of HMs separately using Ch-C and Ch-DES. The spectrum of SSW, chitin treated using both methods before and after adsorption shows the broad bands in the region of 3400 cm-1 that are attributed to the stretching vibrations of O-H and N-H groups from chitin and proteins [205]. The peak broadening/ shifts in the 3400 cm^{-1} region are for spectrums after metal adsorption (Cu(II), Cd(II), Ni(II)) , suggesting interaction of metal ions with hydroxyl or amino groups. Clearly the bands observed around 3243 cm^{-1}

corresponded to the vibrational stretching of hydroxyl group. The peak at 2910 cm^{-1} and 2850 cm^{-1} are corresponding to C–H symmetric and asymmetric stretching, and the intensification of bands around 2920–2850 cm^{-1}, (Ch-DES) possibly due to better-defined $–CH_2/–CH_3$ groups, suggesting increased chitin purity and ordering [204]. In general, the adsorption band located at 1627cm^{-1} and 1500 cm^{-1} are assigned to C=O group of amide I and N-H bending in amide II structure, respectively, indicating the presence of protein and chitin [135][100]. After metal adsorption (Cu(II), Cd(II), Ni(II)), the FTIR spectra of metal-loaded samples (both Ch-C and Ch-DES) showed shifts or intensity reductions in the amide I and II bands, indicating coordination of metal ions with –NH and C=O groups. The enhanced peaks at ~1620 and 1500 cm^{-1} in Fig 4-11, confirms the exposure of chitin's amide bonds after removal (partial removal) of proteins and minerals. The sharp peaks near 1400-1380 cm^{-1} and at 860 cm^{-1} are associated with calcium carbonate (carbonate group) in SSW structure [205]. The diminished peaks for carbonate groups (~1400 and 860 cm^{-1}), indicating effective demineralization, is stronger for DES treated chitin compared to conventional treatment. The sharp peaks at ~1000–1020 cm^{-1} are associated with C–O stretching in polysaccharides and shift or enhancement in this region shows rearrangement or improved crystallinity of polysaccharide backbones in both methods (the shift/enhancement is clear in DES treatment). The bands seen between 400–550 cm^{-1}, may attributed to M–O or M–N bonds (e.g., Cu–O or Cd–N) [176], [206], [207].

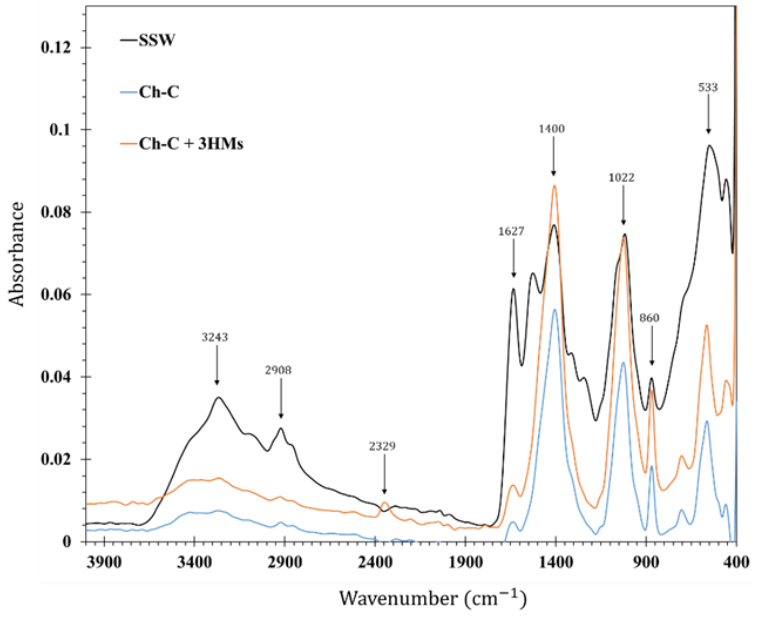

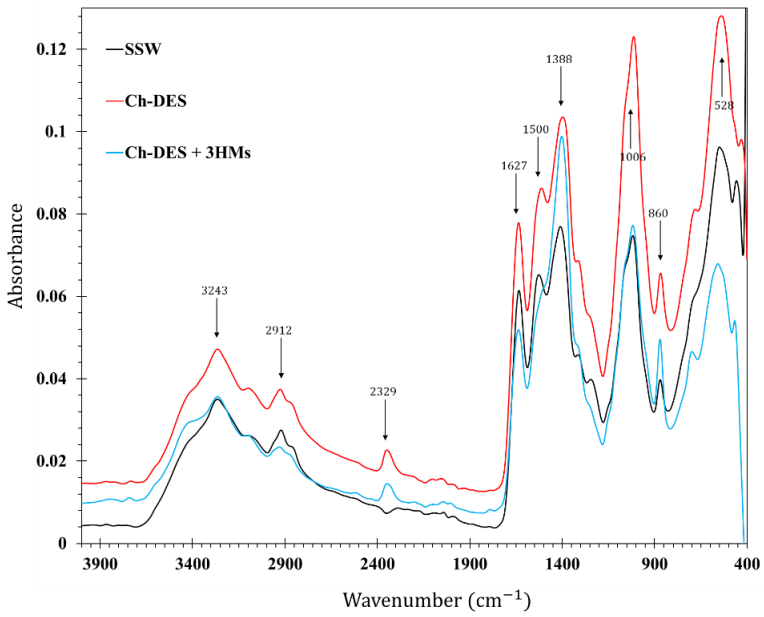

Figure 4-11 FT-IR analysis for SSW, Ch-C and Ch-DES before and after adsorption of HMs.

4.6 Comparison with other adsorbents derived from SSW

A comparison of chitin with various adsorbents is presented in Table 4-15. Based on the Langmuir model, the calculated $q_{max}\left(\frac{mg}{g}\right)$ for Cu(II), Cd(II), and Ni(II) is determined to be 42.20, 38.25 and 23.48 mg/g (onto Ch-DES), respectively which is higher than the values reported in literature, such as 19.8 mg/g for Cd(II) and 4.51 mg/g for Ni(II) adsorption using chitosan [200], 15 mg/g for Cd(II) and 20.3 mg/g for Cu(II) adsorption using chitosan [105], 12 mg/g for Cd(II) and 7 mg/g for Ni(II) adsorption using chitosan nanoparticles [108], and 22.67 mg/g for Cu(II) adsorption using treated shrimp shell waste [19]. Therefore, both Ch-C and Ch-DES proved to be effective adsorbent for the removal of selected HMs (Cu(II), Cd(II), and Ni(II)), however Ch-DES showed improvement in results with approximately +10 mg/g for maximum adsorption capacity and +30 % for removal efficiency of the selected HMs compared to Ch-C in multi-component system. Moreover, Ch-C exhibited a reduced adsorption capacity for Cu(II) and Cd(II) in the multi-component system, with a decrease of approximately −8 mg/g and −4 mg/g respectively, compared to single-component system.

Table 4-15 Comparison of Ch-C and Ch-DES with different adsorbents derived from SSW in a single-component and multi-component system.

Adsorbent	Adsorbate	System	q_{max} (mg/g)	q_{max} (mmol/g)	pH	Isotherm	References
MnFe2O4/chitosan prepared by SSW	Cd, Cu	Multi-Component	60.6, 62.3	0.539, 0.980	6	Langmuir	[20]
Modified SSW Chitosan	Cd, Cu	Multi-Component	15, 20.3	0.133, 0.319	7	Langmuir	[105]
Chitosan Nanoparticles	Cd, Ni	Multi-Component	12, 7	0.107, 0.119	6	Langmuir	[108]
Chitosan cross-linked	Cd, Ni	Multi-Component	68.57, 52.24	0.610, 0.891	6.5	Langmuir	[180]
Chitin hydrogels & $CaCO_3$/Chitin hydrogels	Cd, Cu	Multi-Component	79.18, 89.92 140.52, 151.08	0.704, 1.415 1.250, 2.377	5	Langmuir	[204]
Ch-C	**Cu, Cd, Ni**	**Multi-Component**	**32.88, 29.85, 19.71**	**0.52, 0.27, 0.34**	**5.5**	**Langmuir**	**This Study**
Ch-DES	**Cu, Cd, Ni**	**Multi-Component**	**42.20, 38.25, 23.48**	**0.66, 0.34, 0.40**	**5.5**	**Langmuir**	**This Study**
Treated Shrimp Shells	Cu	Single-Component	22.67	0.357	5	Langmuir	[19]
Phosphorylated Chitin	Cd	Single-Component	62.71	0.558	8	Langmuir	[134]
Modified Shrimp Shell Waste	Cu	Single-Component	54.01	0.850	5	Langmuir	[135]

Raw SSW, Cooked SSW, Chitosan	Cu	Single-Component	184, 170, 129	2.895, 2.675, 2.030	5.8	Freundlich	[136]
Chitosan Beads	Ni	Single-Component	108.7	1.852	6	Langmuir	[137]
Ch-C	**Cu, Cd, Ni**	**Single-Component**	**40.79, 33.62, 13.7**	**0.64, 0.3, 0.23**	**5, 6, 5**	**Langmuir**	**This Study**

* q_{max}(mg/g) : Maximum Adsorption Capacity (mg/g) calculated from Langmuir

4.7 Conclusion

Chitin, a low-cost adsorbent derived from seafood industry waste (e.g., shrimp shells), was selected to promote sustainable waste management and it was modified by two methods and used in batch adsorption of Cd(II), Cu(II) and Ni(II) in both single-component and multi-component systems. Chitin extracted conventionally using NaOH and H_2O_2 (Ch-C) was compared with chitin extracted using a green method involving DES (ChCl:Glycerol), referred to as Ch-DES. FT-IR, SEM, and BET characterization were conducted to compare Ch-C, Ch-DES and SSW functional groups and surface area. In the multi-component system, Ch-DES outperformed Ch-C in adsorption capacity for all three metals. The Langmuir maximum adsorption capacities (q_{max}) of Cu(II), Cd(II), and Ni(II) onto Ch-DES were 42.20, 38.25, and 23.48 mg/g, showing an improvement of 28.3%, 28.1%, and 19.1% over Ch-C, respectively. Langmuir fitting showed q_{max} values of 40.795, 33.616, 13.7 mg/g onto Ch-C in a single-component system. All studies followed PSO kinetics, indicating surface-controlled adsorption. Thermodynamic analysis confirmed that adsorption onto both Ch-C and Ch-DES is exothermic, spontaneous, and mainly physical in nature.

4.8 References

The references are merged with the other chapters' references and presented at the end of the thesis.

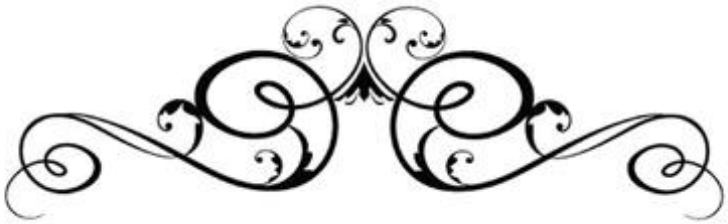

Chapter 5

Conclusion & Future Works

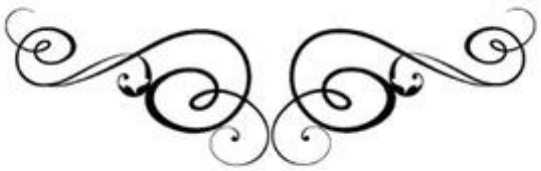

Chapter 5: Conclusion & Future Works

5.1 Conclusion

Chitin extracted from SSW by the conventional method (Ch-C) through demineralizing and deproteinizing by NaOH and H_2O_2 and extracted by a green chemical method using DES (Ch-DES) were compared in terms of the performance for the removal of Cd(II), Ni(II) and Cu(II) from aqueous solution. Furthermore, the optimization study on pH and adsorbent dosage were also conducted. The optimal pH was introduced to be 5 for Cu and Ni while 6 for Cd. Additionally, the optimal adsorbent dosage was determined to be 2.5 g/L. Characterization studies using FT-IR, SEM, and BET confirmed that Ch-DES is more purified and possesses a higher BET surface area compared to Ch-C, resulting in improved removal efficiency. The isotherm study in single-and multi-component adsorption systems showed that Cu(II), Cd(II) and Ni(II) uptake decreased after introducing Ch-C in a competitive environment. For both studies, Langmuir model showed the better fitting to experimental data rather than Freundlich model with q_{max}(mg/g) of 40.8, 33.62, 13.7 (mg/g) in single-component system and 33.73, 19.12, 16.6 (mg/g) in a multi-component system for Cu(II), Cd(II) and Ni(II), respectively. However, when using Ch-DES in a competitive environment, the Langmuir maximum adsorption capacity (mg/g), 43.76, 38.25, 22.99 for Cu(II), Cd(II) and Ni(II) respectively, were higher than the results of Ch-C. Moreover, all studies followed pseudo-second-order which explains that adsorption process for these HMs onto Ch-C and Ch-DES is controlled by surface reaction dynamics. The thermodynamic study revealed that the adsorption process onto both Ch-C and Ch-DES, in single- and multi-component systems, is exothermic, occurs spontaneously, and is primarily governed by physical rather than chemical interactions.

5.2 Recommendations for future work

- **Desorption and Regeneration Studies:** Investigation of reusability of Ch-C and Ch-DES through multiple adsorption-desorption cycles to assess their long-term applicability and economic viability.
- **Application in Real Wastewater:** Evaluation of the performance of Ch-C and Ch-DES in real industrial wastewater samples.
- **Structural Modification of Chitin into Beads:** The synthesis of chitin-based beads (from both Ch-C and Ch-DES) to increase surface area and enhance the removal efficiency, and its performance assessment.
- **Life Cycle Assessment:** Perform an environmental and economic life cycle assessment to compare the sustainability of Ch-DES with other commercial adsorbents.

References

[1] S. E. Vollset *et al.*, "Fertility, mortality, migration, and population scenarios for 195 countries and territories from 2017 to 2100: a forecasting analysis for the Global Burden of Disease Study," *The Lancet*, vol. 396, no. 10258, pp. 1285–1306, Oct. 2020, doi: 10.1016/S0140-6736(20)30677-2.

[2] F. Ahmed, I. Ali, S. Kousar, and S. Ahmed, "The environmental impact of industrialization and foreign direct investment: empirical evidence from Asia-Pacific region," *Environmental Science and Pollution Research*, vol. 29, no. 20, pp. 29778–29792, Apr. 2022, doi: 10.1007/s11356-021-17560-w.

[3] A. Majeed, C. Ye, Y. Chenyun, X. Wei, and Muniba, "Roles of natural resources, globalization, and technological innovations in mitigation of environmental degradation in BRI economies," *PLoS One*, vol. 17, no. 6, p. e0265755, Jun. 2022, doi: 10.1371/journal.pone.0265755.

[4] A. Faizi, M. Z. AK, M. R. Shahzad, S. Yüksel, and R. Toffanin, "Environmental Impacts of Natural Resources, Renewable Energy, Technological Innovation, and Globalization: Evidence from the Organization of Turkic States," *Sustainability*, vol. 16, no. 22, p. 9705, Nov. 2024, doi: 10.3390/su16229705.

[5] R. Arabgol, M. Sartaj, and K. Asghari, "Predicting Nitrate Concentration and Its Spatial Distribution in Groundwater Resources Using Support Vector Machines (SVMs) Model," *Environmental Modeling & Assessment*, vol. 21, no. 1, pp. 71–82, Jan. 2016, doi: 10.1007/s10666-015-9468-0.

[6] M. Roshanfar, M. Sartaj, and S. Kazemeini, "Sustainable recovery of critical metals from spent lithium-ion batteries using chitosan as biosorbent in citrate-sulfate media: A comprehensive isotherm, kinetic, and thermodynamic analysis," *J Environ Manage*, vol. 375, p. 124400, Feb. 2025, doi: 10.1016/j.jenvman.2025.124400.

[7] A. Babakhani and M. Sartaj, "Synthesis, characterization, and performance evaluation of ion-imprinted crosslinked chitosan (with sodium tripolyphosphate) for cadmium biosorption," *J Environ Chem Eng*, vol. 10, no. 2, p. 107147, Apr. 2022, doi: 10.1016/j.jece.2022.107147.

[8] A. Babakhani and M. Sartaj, "Removal of Cadmium (II) from aqueous solution using tripolyphosphate cross-linked chitosan," *J Environ Chem Eng*, vol. 8, no. 4, p. 103842, Aug. 2020, doi: 10.1016/j.jece.2020.103842.

[9] P. Babuji, S. Thirumalaisamy, K. Duraisamy, and G. Periyasamy, "Human Health Risks due to Exposure to Water Pollution: A Review," *Water (Basel)*, vol. 15, no. 14, p. 2532, Jul. 2023, doi: 10.3390/w15142532.

[10] M. Vescovi *et al.*, “Industrial lignins as efficient biosorbents for Cr(<scp>vi</scp>) water remediation: transforming a waste into an added value material,” *RSC Sustainability*, vol. 1, no. 6, pp. 1423–1435, 2023, doi: 10.1039/D3SU00081H.

[11] V. Krstić, T. Urošević, and B. Pešovski, “A review on adsorbents for treatment of water and wastewaters containing copper ions,” *Chem Eng Sci*, vol. 192, pp. 273–287, Dec. 2018, doi: 10.1016/j.ces.2018.07.022.

[12] W. Boulaiche, B. Hamdi, and M. Trari, “Removal of heavy metals by chitin: equilibrium, kinetic and thermodynamic studies,” *Appl Water Sci*, vol. 9, no. 2, p. 39, Mar. 2019, doi: 10.1007/s13201-019-0926-8.

[13] A. B. Albadarin, A. H. Al-Muhtaseb, N. A. Al-laqtah, G. M. Walker, S. J. Allen, and M. N. M. Ahmad, “Biosorption of toxic chromium from aqueous phase by lignin: mechanism, effect of other metal ions and salts,” *Chemical Engineering Journal*, vol. 169, no. 1–3, pp. 20–30, May 2011, doi: 10.1016/j.cej.2011.02.044.

[14] F. C. C, T. Kamalesh, P. S. Kumar, and G. Rangasamy, “A Critical Review on the Sustainable Approaches for the Removal of Toxic Heavy Metals from Water Systems,” *Ind Eng Chem Res*, vol. 62, no. 22, pp. 8575–8601, Jun. 2023, doi: 10.1021/acs.iecr.3c00709.

[15] K. L. Njoku, O. R. Akinyede, and O. F. Obidi, “Microbial Remediation of Heavy Metals Contaminated Media by Bacillus megaterium and Rhizopus stolonifer,” *Sci Afr*, vol. 10, p. e00545, Nov. 2020, doi: 10.1016/j.sciaf.2020.e00545.

[16] Y. Fei and Y. H. Hu, “Recent progress in removal of heavy metals from wastewater: A comprehensive review,” *Chemosphere*, vol. 335, p. 139077, Sep. 2023, doi: 10.1016/j.chemosphere.2023.139077.

[17] B. M. W. P. K. Amarasinghe and R. A. Williams, “Tea waste as a low cost adsorbent for the removal of Cu and Pb from wastewater,” *Chemical Engineering Journal*, vol. 132, no. 1–3, pp. 299–309, Aug. 2007, doi: 10.1016/j.cej.2007.01.016.

[18] A. Rahman, M. A. Haque, S. Ghosh, P. Shinu, M. Attimarad, and G. Kobayashi, “Modified Shrimp-Based Chitosan as an Emerging Adsorbent Removing Heavy Metals (Chromium, Nickel, Arsenic, and Cobalt) from Polluted Water,” *Sustainability*, vol. 15, no. 3, p. 2431, Jan. 2023, doi: 10.3390/su15032431.

[19] S. Boddu, A. Chandra, and A. Ali Khan, “Biosorption of Cu(II), Pb(II) from electroplating industry effluents by treated shrimp shell,” *Mater Today Proc*, vol. 57, pp. 1520–1527, 2022, doi: 10.1016/j.matpr.2021.12.052.

[20] Y. Zhang, Y. Wang, Z. Zhang, W. Cui, X. Zhang, and S. Wang, “Removing copper and cadmium from water and sediment by magnetic microspheres - MnFe2O4/chitosan prepared by waste

shrimp shells," *J Environ Chem Eng*, vol. 9, no. 1, p. 104647, Feb. 2021, doi: 10.1016/j.jece.2020.104647.

[21] G. Crini and E. Lichtfouse, "Advantages and disadvantages of techniques used for wastewater treatment," *Environ Chem Lett*, vol. 17, no. 1, pp. 145–155, Mar. 2019, doi: 10.1007/s10311-018-0785-9.

[22] E. Gilman *et al.*, "Benchmarking global fisheries discards," *Sci Rep*, vol. 10, no. 1, p. 14017, Aug. 2020, doi: 10.1038/s41598-020-71021-x.

[23] N. Rossi, C. Grosso, and C. Delerue-Matos, "Shrimp Waste Upcycling: Unveiling the Potential of Polysaccharides, Proteins, Carotenoids, and Fatty Acids with Emphasis on Extraction Techniques and Bioactive Properties," *Mar Drugs*, vol. 22, no. 4, p. 153, Mar. 2024, doi: 10.3390/md22040153.

[24] A. K. Wani *et al.*, "Eco-friendly and safe alternatives for the valorization of shrimp farming waste," *Environmental Science and Pollution Research*, vol. 31, no. 27, pp. 38960–38989, May 2023, doi: 10.1007/s11356-023-27819-z.

[25] N. Rossi, C. Grosso, and C. Delerue-Matos, "Shrimp Waste Upcycling: Unveiling the Potential of Polysaccharides, Proteins, Carotenoids, and Fatty Acids with Emphasis on Extraction Techniques and Bioactive Properties," *Mar Drugs*, vol. 22, no. 4, p. 153, Mar. 2024, doi: 10.3390/md22040153.

[26] M. Yadav, P. Goswami, K. Paritosh, M. Kumar, N. Pareek, and V. Vivekanand, "Seafood waste: a source for preparation of commercially employable chitin/chitosan materials," *Bioresour Bioprocess*, vol. 6, no. 1, p. 8, Dec. 2019, doi: 10.1186/s40643-019-0243-y.

[27] S. Tamjidi and A. Ameri, "A review of the application of sea material shells as low cost and effective bio-adsorbent for removal of heavy metals from wastewater," *Environmental Science and Pollution Research*, vol. 27, no. 25, pp. 31105–31119, Sep. 2020, doi: 10.1007/s11356-020-09655-7.

[28] R. P. Schwarzenbach, T. Egli, T. B. Hofstetter, U. von Gunten, and B. Wehrli, "Global Water Pollution and Human Health," *Annu Rev Environ Resour*, vol. 35, no. 1, pp. 109–136, Nov. 2010, doi: 10.1146/annurev-environ-100809-125342.

[29] F. Fu and Q. Wang, "Removal of heavy metal ions from wastewaters: A review," *J Environ Manage*, vol. 92, no. 3, pp. 407–418, Mar. 2011, doi: 10.1016/j.jenvman.2010.11.011.

[30] Environment and Climate Change Canada., " Releases of harmful substances to water ," Government of Canada.

[31] B.C. Ministry of Environment and Climate Change Strategy 2019., " Copper Water Quality Guideline for the Protection of Freshwater Aquatic Life-Technical Report.," *Water Quality Guideline Series, , WQG-03-1. Prov. B.C., Victoria B.C*, 2019.

[32] Environment and Climate Change Canada (ECCC) (2021)., "Federal Environmental Quality Guidelines: Copper.," *Retrieved from: https://www.canada.ca/en/environment-climate-change/services/evaluating-existing-substances/federal-environmental-quality-guidelines-copper.html*, 2021.

[33] H. Schwartz *et al.*, "Metals in the drinking water of First Nations across Canada," *Canadian Journal of Public Health*, vol. 112, no. S1, pp. 113–132, Jun. 2021, doi: 10.17269/s41997-021-00497-5.

[34] Y. K. Chau and O. T. R. Kulikovsky-Cordeiro, "Occurrence of nickel in the Canadian environment," *Environmental Reviews*, vol. 3, no. 1, pp. 95–120, Jan. 1995, doi: 10.1139/a95-004.

[35] M. A. Barakat, "New trends in removing heavy metals from industrial wastewater," *Arabian Journal of Chemistry*, vol. 4, no. 4, pp. 361–377, Oct. 2011, doi: 10.1016/j.arabjc.2010.07.019.

[36] V. Subhashini and A. Swamy, "Subhashini and Swamy Phytoremediation of Pb and Ni Contaminated Soils Using Catharanthus roseus (L .)," *Universal Journal of Environmental Research and Technology*, vol. 3, pp. 465–472, 2013.

[37] M. Jaishankar, T. Tseten, N. Anbalagan, B. B. Mathew, and K. N. Beeregowda, "Toxicity, mechanism and health effects of some heavy metals," *Interdiscip Toxicol*, vol. 7, no. 2, pp. 60–72, Jun. 2014, doi: 10.2478/intox-2014-0009.

[38] S. Ismail, F. Khan, and M. Zafar Iqbal, "Phytoremediation: assessing tolerance of tree species against heavy metal (PB and CD) toxicity," *Pak J Bot*, vol. 45, pp. 2181–2186, 2013.

[39] A. H. Parizanganeh, V. Bijnavand, A. A. Zamani, and A. Hajabolfath, "Concentration, Distribution and Comparison of Total and Bioavailable Heavy Metals in Top Soils of Bonab District in Zanjan Province," *Open Journal of Soil Science*, vol. 02, no. 02, pp. 123–132, 2012, doi: 10.4236/ojss.2012.22018.

[40] P. B. Tchounwou, C. G. Yedjou, A. K. Patlolla, and D. J. Sutton, "Heavy Metal Toxicity and the Environment," 2012, pp. 133–164. doi: 10.1007/978-3-7643-8340-4_6.

[41] W. S. Wan Ngah and M. A. K. M. Hanafiah, "Removal of heavy metal ions from wastewater by chemically modified plant wastes as adsorbents: A review," *Bioresour Technol*, vol. 99, no. 10, pp. 3935–3948, Jul. 2008, doi: 10.1016/j.biortech.2007.06.011.

[42] F. S. A. Khan *et al.*, "A comprehensive review on magnetic carbon nanotubes and carbon nanotube-based buckypaper for removal of heavy metals and dyes," *J Hazard Mater*, vol. 413, p. 125375, Jul. 2021, doi: 10.1016/j.jhazmat.2021.125375.

[43] Y. P. Chen, Q. Liu, Y. J. Liu, F. A. Jia, and X. H. He, "Responses of soil microbial activity to cadmium pollution and elevated CO2," *Sci Rep*, vol. 4, no. 1, p. 4287, Mar. 2014, doi: 10.1038/srep04287.

[44] S. Biswas and U. Mishra, "Treatment of Copper Contaminated Municipal Wastewater by Using UASB Reactor and Sand-Chemically Carbonized Rubber Wood Sawdust Column," *Biomed Res Int*, vol. 2016, pp. 1–9, 2016, doi: 10.1155/2016/5762781.

[45] N. H. Ab Hamid *et al.*, "The Current State-Of-Art of Copper Removal from Wastewater: A Review," *Water (Basel)*, vol. 14, no. 19, p. 3086, Oct. 2022, doi: 10.3390/w14193086.

[46] H. Xiang, X. Min, C.-J. Tang, M. Sillanpää, and F. Zhao, "Recent advances in membrane filtration for heavy metal removal from wastewater: A mini review," *Journal of Water Process Engineering*, vol. 49, p. 103023, Oct. 2022, doi: 10.1016/j.jwpe.2022.103023.

[47] K. C. Khulbe and T. Matsuura, "Removal of heavy metals and pollutants by membrane adsorption techniques," *Appl Water Sci*, vol. 8, no. 1, p. 19, Mar. 2018, doi: 10.1007/s13201-018-0661-6.

[48] S. Bandehali, A. Moghadassi, F. Parvizian, J. Shen, and S. M. Hosseini, "Glycidyl POSS-functionalized ZnO nanoparticles incorporated polyether-imide based nanofiltration membranes for heavy metal ions removal from water," *Korean Journal of Chemical Engineering*, vol. 37, no. 2, pp. 263–273, Feb. 2020, doi: 10.1007/s11814-019-0441-5.

[49] B. Lam, S. Déon, N. Morin-Crini, G. Crini, and P. Fievet, "Polymer-enhanced ultrafiltration for heavy metal removal: Influence of chitosan and carboxymethyl cellulose on filtration performances," *J Clean Prod*, vol. 171, pp. 927–933, Jan. 2018, doi: 10.1016/j.jclepro.2017.10.090.

[50] J. Y. Sum, W. X. Kok, and T. S. Shalini, "The removal selectivity of heavy metal cations in micellar-enhanced ultrafiltration: A study based on critical micelle concentration," *Mater Today Proc*, vol. 46, pp. 2012–2016, 2021, doi: 10.1016/j.matpr.2021.02.683.

[51] J. Huang *et al.*, "Influence of pH on heavy metal speciation and removal from wastewater using micellar-enhanced ultrafiltration," *Chemosphere*, vol. 173, pp. 199–206, Apr. 2017, doi: 10.1016/j.chemosphere.2016.12.137.

[52] K. W. Soo, K. C. Wong, P. S. Goh, A. F. Ismail, and N. Othman, "Efficient heavy metal removal by thin film nanocomposite forward osmosis membrane modified with geometrically different bimetallic oxide," *Journal of Water Process Engineering*, vol. 38, p. 101591, Dec. 2020, doi: 10.1016/j.jwpe.2020.101591.

[53] M. F. Hamid *et al.*, "Effects of surface charge of thin-film composite membrane on copper (II) ion removal by using nanofiltration and forward osmosis process," *Journal of Water Process Engineering*, vol. 33, p. 101032, Feb. 2020, doi: 10.1016/j.jwpe.2019.101032.

[54] A. H. Algureiri and Y. R. Abdulmajeed, “Removal of Heavy Metals from Industrial Wastewater by Using RO Membrane,” *Iraqi Journal of Chemical and Petroleum Engineering*, vol. 17, no. 4, pp. 125–136, Dec. 2016, doi: 10.31699/IJCPE.2016.4.12.

[55] S. Bunani, G. Abbt-Braun, and H. Horn, “Heavy Metal Removal from Aqueous Solutions Using a Customized Bipolar Membrane Electrodialysis Process,” *Molecules*, vol. 29, no. 8, p. 1754, Apr. 2024, doi: 10.3390/molecules29081754.

[56] J. E. Efome, D. Rana, T. Matsuura, and C. Q. Lan, “Effects of operating parameters and coexisting ions on the efficiency of heavy metal ions removal by nano-fibrous metal-organic framework membrane filtration process,” *Science of The Total Environment*, vol. 674, pp. 355–362, Jul. 2019, doi: 10.1016/j.scitotenv.2019.04.187.

[57] S. Rajendran *et al.*, “A critical review on various remediation approaches for heavy metal contaminants removal from contaminated soils,” *Chemosphere*, vol. 287, p. 132369, Jan. 2022, doi: 10.1016/j.chemosphere.2021.132369.

[58] Q. Chen, Y. Yao, X. Li, J. Lu, J. Zhou, and Z. Huang, “Comparison of heavy metal removals from aqueous solutions by chemical precipitation and characteristics of precipitates,” *Journal of Water Process Engineering*, vol. 26, pp. 289–300, Dec. 2018, doi: 10.1016/j.jwpe.2018.11.003.

[59] X. Yan, L. Chai, and Q. Li, “Effect of Precipitant Additives on the Sludge Settling and Compacting Performance for Heavy Metal Wastewater Treatment,” *Sep Sci Technol*, vol. 48, no. 10, pp. 1442–1449, May 2013, doi: 10.1080/01496395.2012.753083.

[60] X. Chen, Y. Chen, T. Zhou, D. Liu, H. Hu, and S. Fan, “Hydrometallurgical recovery of metal values from sulfuric acid leaching liquor of spent lithium-ion batteries,” *Waste Management*, vol. 38, pp. 349–356, Apr. 2015, doi: 10.1016/j.wasman.2014.12.023.

[61] R. Abu-El-Halawa and S. A. Zabin, “Removal efficiency of Pb, Cd, Cu and Zn from polluted water using dithiocarbamate ligands,” *Journal of Taibah University for Science*, vol. 11, no. 1, pp. 57–65, Jan. 2017, doi: 10.1016/j.jtusci.2015.07.002.

[62] O. Tavakoli, V. Goodarzi, M. R. Saeb, N. M. Mahmoodi, and R. Borja, “Competitive removal of heavy metal ions from squid oil under isothermal condition by CR11 chelate ion exchanger,” *J Hazard Mater*, vol. 334, pp. 256–266, Jul. 2017, doi: 10.1016/j.jhazmat.2017.04.023.

[63] J. Bensalah *et al.*, “Investigation of the cationic resin Am®IRC-50 as a potential adsorbent of Co (II): Equilibrium isotherms and thermodynamic studies,” *Chemical Data Collections*, vol. 39, p. 100879, Jun. 2022, doi: 10.1016/j.cdc.2022.100879.

[64] J. P. Bezzina, L. R. Ruder, R. Dawson, and M. D. Ogden, “Ion exchange removal of Cu(II), Fe(II), Pb(II) and Zn(II) from acid extracted sewage sludge – Resin screening in weak acid media,” *Water Res*, vol. 158, pp. 257–267, Jul. 2019, doi: 10.1016/j.watres.2019.04.042.

[65] A. Ma, A. Abushaikha, S. J. Allen, and G. McKay, “Ion exchange homogeneous surface diffusion modelling by binary site resin for the removal of nickel ions from wastewater in fixed beds,” *Chemical Engineering Journal*, vol. 358, pp. 1–10, Feb. 2019, doi: 10.1016/j.cej.2018.09.135.

[66] P. Rudnicki, Z. Hubicki, and D. Kołodyńska, “Evaluation of heavy metal ions removal from acidic waste water streams,” *Chemical Engineering Journal*, vol. 252, pp. 362–373, Sep. 2014, doi: 10.1016/j.cej.2014.04.035.

[67] L. Ulloa, M. Martínez-Minchero, E. Bringas, A. Cobo, and M. F. San-Román, “Split regeneration of chelating resins for the selective recovery of nickel and copper,” *Sep Purif Technol*, vol. 253, p. 117516, Dec. 2020, doi: 10.1016/j.seppur.2020.117516.

[68] S.-P. Wu, X.-Z. Dai, J.-R. Kan, F.-D. Shilong, and M.-Y. Zhu, “Fabrication of carboxymethyl chitosan–hemicellulose resin for adsorptive removal of heavy metals from wastewater,” *Chinese Chemical Letters*, vol. 28, no. 3, pp. 625–632, Mar. 2017, doi: 10.1016/j.cclet.2016.11.015.

[69] E. I. Ugwu, A. Othmani, and C. C. Nnaji, “A review on zeolites as cost-effective adsorbents for removal of heavy metals from aqueous environment,” *International Journal of Environmental Science and Technology*, vol. 19, no. 8, pp. 8061–8084, Aug. 2022, doi: 10.1007/s13762-021-03560-3.

[70] E. Erdem, N. Karapinar, and R. Donat, “The removal of heavy metal cations by natural zeolites,” *J Colloid Interface Sci*, vol. 280, no. 2, pp. 309–314, Dec. 2004, doi: 10.1016/j.jcis.2004.08.028.

[71] N. Finish, P. Ramos, E. J. C. Borojovich, O. Zeiri, Y. Amar, and M. Gottlieb, “Zeolite performance in removal of multicomponent heavy metal contamination from wastewater,” *J Hazard Mater*, vol. 457, p. 131784, Sep. 2023, doi: 10.1016/j.jhazmat.2023.131784.

[72] N. Elboughdiri, “The use of natural zeolite to remove heavy metals Cu (II), Pb (II) and Cd (II), from industrial wastewater,” *Cogent Eng*, vol. 7, no. 1, p. 1782623, Jan. 2020, doi: 10.1080/23311916.2020.1782623.

[73] L. Velarde, M. S. Nabavi, E. Escalera, M.-L. Antti, and F. Akhtar, “Adsorption of heavy metals on natural zeolites: A review,” *Chemosphere*, vol. 328, p. 138508, Jul. 2023, doi: 10.1016/j.chemosphere.2023.138508.

[74] S. Gu, X. Kang, L. Wang, E. Lichtfouse, and C. Wang, “Clay mineral adsorbents for heavy metal removal from wastewater: a review,” *Environ Chem Lett*, vol. 17, no. 2, pp. 629–654, Jun. 2019, doi: 10.1007/s10311-018-0813-9.

[75] B. O. Otunola and O. O. Ololade, “A review on the application of clay minerals as heavy metal adsorbents for remediation purposes,” *Environ Technol Innov*, vol. 18, p. 100692, May 2020, doi: 10.1016/j.eti.2020.100692.

[76] E. A. Ashour and M. A. Tony, “Eco-friendly removal of hexavalent chromium from aqueous solution using natural clay mineral: activation and modification effects,” *SN Appl Sci*, vol. 2, no. 12, p. 2042, Dec. 2020, doi: 10.1007/s42452-020-03873-x.

[77] S. Barakan and V. Aghazadeh, “The advantages of clay mineral modification methods for enhancing adsorption efficiency in wastewater treatment: a review,” *Environmental Science and Pollution Research*, vol. 28, no. 3, pp. 2572–2599, Jan. 2021, doi: 10.1007/s11356-020-10985-9.

[78] A. E. Burakov *et al.*, “Adsorption of heavy metals on conventional and nanostructured materials for wastewater treatment purposes: A review,” *Ecotoxicol Environ Saf*, vol. 148, pp. 702–712, Feb. 2018, doi: 10.1016/j.ecoenv.2017.11.034.

[79] A. A. Attia, S. A. Khedr, and S. A. Elkholy, “Adsorption of chromium ion (VI) by acid activated carbon,” *Brazilian Journal of Chemical Engineering*, vol. 27, no. 1, pp. 183–193, Mar. 2010, doi: 10.1590/S0104-66322010000100016.

[80] R. Black, M. Sartaj, A. Mohammadian, and H. A. M. Qiblawey, “Biosorption of Pb and Cu using fixed and suspended bacteria,” *J Environ Chem Eng*, vol. 2, no. 3, pp. 1663–1671, Sep. 2014, doi: 10.1016/j.jece.2014.05.023.

[81] A. J. Mohammed, M. H. Ibrahim, S. Z. Zulkifli, and J. M. Salman, “Synthesis and Characterization of a Nano-Adsorbent Derivative Derived from Grape Seeds for Cadmium Ion Removal in an Aqueous Solution,” *Water (Basel)*, vol. 13, no. 20, p. 2896, Oct. 2021, doi: 10.3390/w13202896.

[82] A. M. Alkherraz, A. K. Ali, and K. M. Elsherif, “emoval of Pb(II), Zn(II), Cu(II) and Cd(II) from aqueous solutions by adsorption onto olive branches activated carbon: Equilibrium and thermodynamic studies,” *Chemistry International.*, 2020.

[83] Y. A. B. Neolaka *et al.*, “Potential of activated carbon from various sources as a low-cost adsorbent to remove heavy metals and synthetic dyes,” *Results Chem*, vol. 5, p. 100711, Jan. 2023, doi: 10.1016/j.rechem.2022.100711.

[84] M. Mariana *et al.*, “Recent advances in activated carbon modification techniques for enhanced heavy metal adsorption,” *Journal of Water Process Engineering*, vol. 43, p. 102221, Oct. 2021, doi: 10.1016/j.jwpe.2021.102221.

[85] Z. Zhang, T. Wang, H. Zhang, Y. Liu, and B. Xing, “Adsorption of Pb(II) and Cd(II) by magnetic activated carbon and its mechanism,” *Science of The Total Environment*, vol. 757, p. 143910, Feb. 2021, doi: 10.1016/j.scitotenv.2020.143910.

[86] V. K. Gupta, P. J. M. Carrott, M. M. L. Ribeiro Carrott, and Suhas, “Low-Cost Adsorbents: Growing Approach to Wastewater Treatment—a Review,” *Crit Rev Environ Sci Technol*, vol. 39, no. 10, pp. 783–842, Oct. 2009, doi: 10.1080/10643380801977610.

[87] R. Apiratikul and P. Pavasant, “Batch and column studies of biosorption of heavy metals by Caulerpa lentillifera,” *Bioresour Technol*, vol. 99, no. 8, pp. 2766–2777, May 2008, doi: 10.1016/j.biortech.2007.06.036.

[88] R. Black, M. Sartaj, A. Mohammadian, and H. A. M. Qiblawey, “Biosorption of Pb and Cu using fixed and suspended bacteria,” *J Environ Chem Eng*, vol. 2, no. 3, pp. 1663–1671, Sep. 2014, doi: 10.1016/j.jece.2014.05.023.

[89] Z. Raji, A. Karim, A. Karam, and S. Khalloufi, “Adsorption of Heavy Metals: Mechanisms, Kinetics, and Applications of Various Adsorbents in Wastewater Remediation—A Review,” *Waste*, vol. 1, no. 3, pp. 775–805, Sep. 2023, doi: 10.3390/waste1030046.

[90] C. Duan, T. Ma, J. Wang, and Y. Zhou, “Removal of heavy metals from aqueous solution using carbon-based adsorbents: A review,” *Journal of Water Process Engineering*, vol. 37, p. 101339, Oct. 2020, doi: 10.1016/j.jwpe.2020.101339.

[91] J. Dimitrijević, S. Jevtić, A. Marinković, M. Simić, M. Koprivica, and J. Petrović, “Ability of Deep Eutectic Solvent Modified Oat Straw for Cu(II), Zn(II), and Se(IV) Ions Removal,” *Processes*, vol. 11, no. 5, p. 1308, Apr. 2023, doi: 10.3390/pr11051308.

[92] Ł. Klapiszewski, P. Bartczak, T. Szatkowski, and T. Jesionowski, “Removal of lead(II) ions by an adsorption process with the use of an advanced SiO 2 /lignin biosorbent,” *Polish Journal of Chemical Technology*, vol. 19, no. 1, pp. 48–53, Mar. 2017, doi: 10.1515/pjct-2017-0007.

[93] X. Shi, Y. Qiao, X. An, Y. Tian, and H. Zhou, “High-capacity adsorption of Cr(VI) by lignin-based composite: Characterization, performance and mechanism,” *Int J Biol Macromol*, vol. 159, pp. 839–849, Sep. 2020, doi: 10.1016/j.ijbiomac.2020.05.130.

[94] C. O. Aniagor, M. A. Afifi, and A. Hashem, “Heavy metal adsorptive application of hydrolyzed corn starch,” *Journal of Polymer Research*, vol. 28, no. 11, p. 405, Nov. 2021, doi: 10.1007/s10965-021-02772-y.

[95] M. A. Akl, A. S. El-Zeny, M. A. Hashem, E.-S. R. H. El-Gharkawy, and A. G. Mostafa, “Flax fiber based semicarbazide biosorbent for removal of Cr(VI) and Alizarin Red S dye from wastewater,” *Sci Rep*, vol. 13, no. 1, p. 8267, May 2023, doi: 10.1038/s41598-023-34523-y.

[96] S. Liu, J. Gao, L. Zhang, Y. Yang, and X. Liu, “Diethylenetriaminepentaacetic acid–thiourea-modified magnetic chitosan for adsorption of hexavalent chromium from aqueous solutions,” *Carbohydr Polym*, vol. 274, p. 118555, Nov. 2021, doi: 10.1016/j.carbpol.2021.118555.

[97] L. Velarde, M. S. Nabavi, E. Escalera, M.-L. Antti, and F. Akhtar, “Adsorption of heavy metals on natural zeolites: A review,” *Chemosphere*, vol. 328, p. 138508, Jul. 2023, doi: 10.1016/j.chemosphere.2023.138508.

[98] H. Wang *et al.*, “Copper removal from wastewater and electricity generation using dual-chamber microbial fuel cells with shrimp shell as the substrate,” *Electrochim Acta*, vol. 441, p. 141849, Feb. 2023, doi: 10.1016/j.electacta.2023.141849.

[99] G. M. Mathew *et al.*, “Sustainable and eco-friendly strategies for shrimp shell valorization,” *Environmental Pollution*, vol. 267, p. 115656, Dec. 2020, doi: 10.1016/j.envpol.2020.115656.

[100] S. Shahabuddin, S. N. A. Baharin, N. F. Suhaimi, N. Yunus, and K. P. Sambasevam, “Preparation of shrimp-based chitin blend with polyaniline for chromium (VI) removal from aqueous solution,” *Mater Today Proc*, vol. 62, pp. 6940–6944, 2022, doi: 10.1016/j.matpr.2021.12.299.

[101] K. Kurita, “Chitin and Chitosan: Functional Biopolymers from Marine Crustaceans,” *Marine Biotechnology*, vol. 8, no. 3, pp. 203–226, Jun. 2006, doi: 10.1007/s10126-005-0097-5.

[102] J. Wang and S. Zhuang, “Removal of various pollutants from water and wastewater by modified chitosan adsorbents,” *Crit Rev Environ Sci Technol*, vol. 47, no. 23, pp. 2331–2386, Dec. 2017, doi: 10.1080/10643389.2017.1421845.

[103] E. S. Abdou, K. S. A. Nagy, and M. Z. Elsabee, “Extraction and characterization of chitin and chitosan from local sources,” *Bioresour Technol*, vol. 99, no. 5, pp. 1359–1367, Mar. 2008, doi: 10.1016/j.biortech.2007.01.051.

[104] S. Tokura and H. Tamura, “Chitin and Chitosan,” in *Comprehensive Glycoscience*, Elsevier, 2007, pp. 449–475. doi: 10.1016/B978-044451967-2/00127-6.

[105] A. Rahman, “Promising and Environmentally Friendly Removal of Copper, Zinc, Cadmium, and Lead from Wastewater Using Modified Shrimp-Based Chitosan,” *Water (Basel)*, vol. 16, no. 1, p. 184, Jan. 2024, doi: 10.3390/w16010184.

[106] G. Crini and P.-M. Badot, “Application of chitosan, a natural aminopolysaccharide, for dye removal from aqueous solutions by adsorption processes using batch studies: A review of recent literature,” *Prog Polym Sci*, vol. 33, no. 4, pp. 399–447, Apr. 2008, doi: 10.1016/j.progpolymsci.2007.11.001.

[107] J. Wang and C. Chen, “Chitosan-based biosorbents: Modification and application for biosorption of heavy metals and radionuclides,” *Bioresour Technol*, vol. 160, pp. 129–141, May 2014, doi: 10.1016/j.biortech.2013.12.110.

[108] Md. I. H. Mondal *et al.*, “Adsorbents from rice husk and shrimp shell for effective removal of heavy metals and reactive dyes in water,” *Environmental Pollution*, vol. 346, p. 123637, Apr. 2024, doi: 10.1016/j.envpol.2024.123637.

[109] H. El Knidri, R. Belaabed, A. Addaou, A. Laajeb, and A. Lahsini, “Extraction, chemical modification and characterization of chitin and chitosan,” *Int J Biol Macromol*, vol. 120, pp. 1181–1189, Dec. 2018, doi: 10.1016/j.ijbiomac.2018.08.139.

[110] S. Kaur and G. S. Dhillon, “Recent trends in biological extraction of chitin from marine shell wastes: a review,” *Crit Rev Biotechnol*, vol. 35, no. 1, pp. 44–61, Jan. 2015, doi: 10.3109/07388551.2013.798256.

[111] N. Özel and M. Elibol, “A review on the potential uses of deep eutectic solvents in chitin and chitosan related processes,” *Carbohydr Polym*, vol. 262, p. 117942, Jun. 2021, doi: 10.1016/j.carbpol.2021.117942.

[112] K. Morgan, C. Conway, S. Faherty, and C. Quigley, “A Comparative Analysis of Conventional and Deep Eutectic Solvent (DES)-Mediated Strategies for the Extraction of Chitin from Marine Crustacean Shells,” *Molecules*, vol. 26, no. 24, p. 7603, Dec. 2021, doi: 10.3390/molecules26247603.

[113] H. K. No and S. P. Meyers, “Application of Chitosan for Treatment of Wastewaters,” 2000, pp. 1–27. doi: 10.1007/978-1-4757-6429-1_1.

[114] G. Kaur, H. Kumar, and M. Singla, “Diverse applications of ionic liquids: A comprehensive review,” *J Mol Liq*, vol. 351, p. 118556, Apr. 2022, doi: 10.1016/j.molliq.2022.118556.

[115] H. Wang *et al.*, “Efficient removal of heavy metals from sewage sludge using a low-cost protic ionic liquid: Investigation of mechanism and ecological risk,” *J Environ Chem Eng*, vol. 12, no. 3, p. 112840, Jun. 2024, doi: 10.1016/j.jece.2024.112840.

[116] Y. Pei, Y. Zhang, J. Ma, M. Fan, S. Zhang, and J. Wang, “Ionic liquids for advanced materials,” *Mater Today Nano*, vol. 17, p. 100159, Mar. 2022, doi: 10.1016/j.mtnano.2021.100159.

[117] R. Goutham *et al.*, “Ionic liquids in wastewater treatment: A review on pollutant removal and degradation, recovery of ionic liquids, economics and future perspectives,” *J Mol Liq*, vol. 349, p. 118150, Mar. 2022, doi: 10.1016/j.molliq.2021.118150.

[118] E. S. Morais, A. M. da C. Lopes, M. G. Freire, C. S. R. Freire, J. A. P. Coutinho, and A. J. D. Silvestre, “Use of Ionic Liquids and Deep Eutectic Solvents in Polysaccharides Dissolution and Extraction Processes towards Sustainable Biomass Valorization,” *Molecules*, vol. 25, no. 16, p. 3652, Aug. 2020, doi: 10.3390/molecules25163652.

[119] Y. Qin, X. Lu, N. Sun, and R. D. Rogers, “Dissolution or extraction of crustacean shells using ionic liquids to obtain high molecular weight purified chitin and direct production of chitin films and fibers,” *Green Chemistry*, vol. 12, no. 6, p. 968, 2010, doi: 10.1039/c003583a.

[120] T. Setoguchi, T. Kato, K. Yamamoto, and J. Kadokawa, “Facile production of chitin from crab shells using ionic liquid and citric acid,” *Int J Biol Macromol*, vol. 50, no. 3, pp. 861–864, Apr. 2012, doi: 10.1016/j.ijbiomac.2011.11.007.

[121] H. Zhu *et al.*, “Advances and challenges in green extraction of chitin for food and agriculture applications: A review,” *Int J Biol Macromol*, vol. 297, p. 139762, Mar. 2025, doi: 10.1016/j.ijbiomac.2025.139762.

[122] I. Wazeer, H. F. Hizaddin, M. A. Hashim, and M. K. Hadj-Kali, “An overview about the extraction of heavy metals and other critical pollutants from contaminated water via hydrophobic deep eutectic solvents,” *J Environ Chem Eng*, vol. 10, no. 6, p. 108574, Dec. 2022, doi: 10.1016/j.jece.2022.108574.

[123] E. L. Smith, A. P. Abbott, and K. S. Ryder, “Deep Eutectic Solvents (DESs) and Their Applications,” *Chem Rev*, vol. 114, no. 21, pp. 11060–11082, Nov. 2014, doi: 10.1021/cr300162p.

[124] A. P. Abbott, K. J. Edler, and A. J. Page, “Deep eutectic solvents—The vital link between ionic liquids and ionic solutions,” *J Chem Phys*, vol. 155, no. 15, Oct. 2021, doi: 10.1063/5.0072268.

[125] H. Liu, J. Lv, and Y. Yang, “Recyclable water-modified deep eutectic solvents for removal of multiple heavy metals from soil,” *Chemosphere*, vol. 350, p. 141141, Feb. 2024, doi: 10.1016/j.chemosphere.2024.141141.

[126] L. A. Rodrigues, I. Radojčić Redovniković, A. R. C. Duarte, A. A. Matias, and A. Paiva, “Low-Phytotoxic Deep Eutectic Systems as Alternative Extraction Media for the Recovery of Chitin from Brown Crab Shells,” *ACS Omega*, vol. 6, no. 43, pp. 28729–28741, Nov. 2021, doi: 10.1021/acsomega.1c03402.

[127] A. P. Abbott, D. Boothby, G. Capper, D. L. Davies, and R. K. Rasheed, “Deep Eutectic Solvents Formed between Choline Chloride and Carboxylic Acids: Versatile Alternatives to Ionic Liquids,” *J Am Chem Soc*, vol. 126, no. 29, pp. 9142–9147, Jul. 2004, doi: 10.1021/ja048266j.

[128] P. Zhu, Z. Gu, S. Hong, and H. Lian, “One-pot production of chitin with high purity from lobster shells using choline chloride–malonic acid deep eutectic solvent,” *Carbohydr Polym*, vol. 177, pp. 217–223, Dec. 2017, doi: 10.1016/j.carbpol.2017.09.001.

[129] B. Bradić, U. Novak, and B. Likozar, “Crustacean shell bio-refining to chitin by natural deep eutectic solvents,” *Green Processing and Synthesis*, vol. 9, no. 1, pp. 13–25, Oct. 2019, doi: 10.1515/gps-2020-0002.

[130] P. S. Saravana *et al.*, “Deep eutectic solvent-based extraction and fabrication of chitin films from crustacean waste,” *Carbohydr Polym*, vol. 195, pp. 622–630, Sep. 2018, doi: 10.1016/j.carbpol.2018.05.018.

[131] J. Lei *et al.*, “Pretreatment of shrimp shells with an acidic deep eutectic solvent system for chitin extraction and its enhanced performance as a carrier for immobilized lipase,” *Int J Biol Macromol*, vol. 264, p. 130774, Apr. 2024, doi: 10.1016/j.ijbiomac.2024.130774.

[132] Y. Wang, H. Zhu, M. Qiao, and Y. Luo, “Glycerol/organic acid-based ternary deep eutectic solvents as a green approach to recover chitin with different molecular weight from seafood waste,” *Int J Biol Macromol*, vol. 257, p. 128714, Feb. 2024, doi: 10.1016/j.ijbiomac.2023.128714.

[133] I. Marzuki, R. S. Alwi, - Erniati, - Mudyawati, - Sinardi, and A. S. Iryani, “Chitosan Performance of Shrimp Shells in The Biosorption Ion Metal of Cadmium, Lead and Nickel Based on Variations Ph Interaction,” in *Proceedings of the First International Conference on Materials Engineering and Management - Engineering Section (ICMEMe 2018)*, Paris, France: Atlantis Press, 2019. doi: 10.2991/icmeme-18.2019.2.

[134] H. Charii *et al.*, “Phosphorylated chitin from shrimp shell waste: A robust solution for cadmium remediation,” *Int J Biol Macromol*, vol. 268, p. 131855, May 2024, doi: 10.1016/j.ijbiomac.2024.131855.

[135] C. Liu, H. Wen, K. Chen, and Y. Chen, “A Simple One-Step Modification of Shrimp Shell for the Efficient Adsorption and Desorption of Copper Ions,” *Molecules*, vol. 26, no. 18, p. 5690, Sep. 2021, doi: 10.3390/molecules26185690.

[136] D. W. Skaf, V. L. Punzi, C. F. Helenbrook, and E. H. Pozzuto, “Removal of copper contamination from simulated wastewater using chitosan and shrimp waste: Equilibrium analysis,” *J Environ Chem Eng*, vol. 11, no. 5, p. 110972, Oct. 2023, doi: 10.1016/j.jece.2023.110972.

[137] V. T. Le, M. U. Dao, H. S. Le, D. L. Tran, V. D. Doan, and H. T. Nguyen, “Adsorption of Ni(II) ions by magnetic activated carbon/chitosan beads prepared from spent coffee grounds, shrimp shells and green tea extract,” *Environ Technol*, vol. 41, no. 21, pp. 2817–2832, Sep. 2020, doi: 10.1080/09593330.2019.1584250.

[138] L. Zhang, Y. Zeng, and Z. Cheng, “Removal of heavy metal ions using chitosan and modified chitosan: A review,” *J Mol Liq*, vol. 214, pp. 175–191, Feb. 2016, doi: 10.1016/j.molliq.2015.12.013.

[139] J. Wang and C. Chen, “Biosorbents for heavy metals removal and their future,” *Biotechnol Adv*, vol. 27, no. 2, pp. 195–226, Mar. 2009, doi: 10.1016/j.biotechadv.2008.11.002.

[140] M. A. Al-Ghouti and D. A. Da’ana, “Guidelines for the use and interpretation of adsorption isotherm models: A review,” *J Hazard Mater*, vol. 393, p. 122383, Jul. 2020, doi: 10.1016/j.jhazmat.2020.122383.

[141] S. Brunauer, P. H. Emmett, and E. Teller, “Adsorption of Gases in Multimolecular Layers,” *J Am Chem Soc*, vol. 60, no. 2, pp. 309–319, Feb. 1938, doi: 10.1021/ja01269a023.

[142] O. Redlich and D. L. Peterson, “A Useful Adsorption Isotherm,” *J Phys Chem*, vol. 63, no. 6, pp. 1024–1024, Jun. 1959, doi: 10.1021/j150576a611.

[143] S. Debnath and R. Das, “Strong adsorption of CV dye by Ni ferrite nanoparticles for waste water purification: Fits well the pseudo second order kinetic and Freundlich isotherm model,” *Ceram Int*, vol. 49, no. 10, pp. 16199–16215, May 2023, doi: 10.1016/j.ceramint.2023.01.218.

[144] S. Senniappan *et al.*, “Exploring the adsorption efficacy of Cassia fistula seed carbon for Cd (II) ion removal: Comparative study of isotherm models,” *Environ Res*, vol. 235, p. 116676, Oct. 2023, doi: 10.1016/j.envres.2023.116676.

[145] A. Agrawal and K. K. Sahu, “Kinetic and isotherm studies of cadmium adsorption on manganese nodule residue,” *J Hazard Mater*, vol. 137, no. 2, pp. 915–924, Sep. 2006, doi: 10.1016/j.jhazmat.2006.03.039.

[146] M. A. Shaker, “Thermodynamics and kinetics of bivalent cadmium biosorption onto nanoparticles of chitosan-based biopolymers,” *J Taiwan Inst Chem Eng*, vol. 47, pp. 79–90, Feb. 2015, doi: 10.1016/j.jtice.2014.10.010.

[147] E. Repo, J. K. Warchol, T. A. Kurniawan, and M. E. T. Sillanpää, “Adsorption of Co(II) and Ni(II) by EDTA- and/or DTPA-modified chitosan: Kinetic and equilibrium modeling,” *Chemical Engineering Journal*, vol. 161, no. 1–2, pp. 73–82, Jul. 2010, doi: 10.1016/j.cej.2010.04.030.

[148] M. Ahmaruzzaman, “Industrial wastes as low-cost potential adsorbents for the treatment of wastewater laden with heavy metals,” *Adv Colloid Interface Sci*, vol. 166, no. 1–2, pp. 36–59, Aug. 2011, doi: 10.1016/j.cis.2011.04.005.

[149] M. E. A. Ali, M. M. S. Aboelfadl, A. M. Selim, H. F. Khalil, and G. M. Elkady, “Chitosan nanoparticles extracted from shrimp shells, application for removal of Fe(II) and Mn(II) from aqueous phases,” *Sep Sci Technol*, vol. 53, no. 18, pp. 2870–2881, Dec. 2018, doi: 10.1080/01496395.2018.1489845.

[150] Y. Xiang *et al.*, “Fabrication of sustainable manganese ferrite modified biochar from vinasse for enhanced adsorption of fluoroquinolone antibiotics: Effects and mechanisms,” *Science of The Total Environment*, vol. 709, p. 136079, Mar. 2020, doi: 10.1016/j.scitotenv.2019.136079.

[151] C. Gerente, V. K. C. Lee, P. Le Cloirec, and G. McKay, “Application of Chitosan for the Removal of Metals From Wastewaters by Adsorption—Mechanisms and Models Review,” *Crit Rev Environ Sci Technol*, vol. 37, no. 1, pp. 41–127, Jan. 2007, doi: 10.1080/10643380600729089.

[152] B. Zhao, J. Zhang, W. Yan, X. Kang, C. Cheng, and Y. Ouyang, “Removal of cadmium from aqueous solution using waste shells of golden apple snail,” *Desalination Water Treat*, vol. 57, no. 50, pp. 23987–24003, Oct. 2016, doi: 10.1080/19443994.2016.1140078.

[153] V. M. Boddu, K. Abburi, J. L. Talbott, and E. D. Smith, “Removal of Hexavalent Chromium from Wastewater Using a New Composite Chitosan Biosorbent,” *Environ Sci Technol*, vol. 37, no. 19, pp. 4449–4456, Oct. 2003, doi: 10.1021/es021013a.

[154] M. Ahmadi, H. Rahmani, B. Ramavandi, and B. Kakavandi, “Removal of nitrate from aqueous solution using activated carbon modified with Fenton reagents,” *Desalination Water Treat*, vol. 76, pp. 265–275, May 2017, doi: 10.5004/dwt.2017.20705.

[155] S. Tamjidi and H. Esmaeili, “Chemically Modified CaO/Fe 3 O 4 Nanocomposite by Sodium Dodecyl Sulfate for Cr(III) Removal from Water,” *Chem Eng Technol*, vol. 42, no. 3, pp. 607–616, Mar. 2019, doi: 10.1002/ceat.201800488.

[156] Y.-T. Zhou, C. Branford-White, H.-L. Nie, and L.-M. Zhu, “Adsorption mechanism of Cu2+ from aqueous solution by chitosan-coated magnetic nanoparticles modified with α-ketoglutaric acid,” *Colloids Surf B Biointerfaces*, vol. 74, no. 1, pp. 244–252, Nov. 2009, doi: 10.1016/j.colsurfb.2009.07.026.

[157] A. Maleki, E. Pajootan, and B. Hayati, “Ethyl acrylate grafted chitosan for heavy metal removal from wastewater: Equilibrium, kinetic and thermodynamic studies,” *J Taiwan Inst Chem Eng*, vol. 51, pp. 127–134, Jun. 2015, doi: 10.1016/j.jtice.2015.01.004.

[158] J. W. Miller, “Adsorption Technology: A Step-by-Step Approach to Process Evaluation and Application,” *J Environ Qual*, vol. 15, no. 1, pp. 94–94, Jan. 1986, doi: 10.2134/jeq1986.00472425001500010024x.

[159] S. H. Chien and W. R. Clayton, “Application of Elovich Equation to the Kinetics of Phosphate Release and Sorption in Soils,” *Soil Science Society of America Journal*, vol. 44, no. 2, pp. 265–268, Mar. 1980, doi: 10.2136/sssaj1980.03615995004400020013x.

[160] A. , Bonilla-Petriciolet, D. I. Mendoza-Castillo, and H. E. Reynel-Ávila, *Adsorption Processes for Water Treatment and Purification*. Cham: Springer International Publishing, 2017. doi: 10.1007/978-3-319-58136-1.

[161] E. D. Revellame, D. L. Fortela, W. Sharp, R. Hernandez, and M. E. Zappi, “Adsorption kinetic modeling using pseudo-first order and pseudo-second order rate laws: A review,” *Clean Eng Technol*, vol. 1, p. 100032, Dec. 2020, doi: 10.1016/j.clet.2020.100032.

[162] Y. S. Ho and G. McKay, “Pseudo-second order model for sorption processes,” *Process Biochemistry*, vol. 34, no. 5, pp. 451–465, Jul. 1999, doi: 10.1016/S0032-9592(98)00112-5.

[163] “Zur Theorie der sogenannten Adsorption gelöster Stoffe,” *Zeitschrift für Chemie und Industrie der Kolloide*, vol. 2, no. 1, pp. 15–15, Jul. 1907, doi: 10.1007/BF01501332.

[164] R. Shahrokhi-Shahraki, C. Benally, M. G. El-Din, and J. Park, “High efficiency removal of heavy metals using tire-derived activated carbon vs commercial activated carbon: Insights into the adsorption mechanisms,” *Chemosphere*, vol. 264, p. 128455, Feb. 2021, doi: 10.1016/j.chemosphere.2020.128455.

[165] I. J. Kim, W. Zhao, J. G. Park, and Z. Meng, “Carbon nanotube filter for heavy metal ion adsorption,” *Ceram Int*, vol. 47, no. 23, pp. 33280–33285, Dec. 2021, doi: 10.1016/j.ceramint.2021.08.230.

[166] H. Qin, T. Hu, Y. Zhai, N. Lu, and J. Aliyeva, “The improved methods of heavy metals removal by biosorbents: A review,” *Environmental Pollution*, vol. 258, p. 113777, Mar. 2020, doi: 10.1016/j.envpol.2019.113777.

[167] Z. Xiao, D. Li, F. Wang, Z. Sun, and Z. Lin, “Simultaneous removal of NO and SO2 with a new recycling micro-nano bubble oxidation-absorption process based on HA-Na,” *Sep Purif Technol*, vol. 242, p. 116788, Jul. 2020, doi: 10.1016/j.seppur.2020.116788.

[168] H. Musarurwa and N. T. Tavengwa, “Advances in the application of chitosan-based metal organic frameworks as adsorbents for environmental remediation,” *Carbohydr Polym*, vol. 283, p. 119153, May 2022, doi: 10.1016/j.carbpol.2022.119153.

[169] D. Saravanan, T. Gomathi, and P. N. Sudha, “Sorption studies on heavy metal removal using chitin/bentonite biocomposite,” *Int J Biol Macromol*, vol. 53, pp. 67–71, Feb. 2013, doi: 10.1016/j.ijbiomac.2012.11.005.

[170] G. Ali, M. Sharma, E.-S. Salama, Z. Ling, and X. Li, “Applications of chitin and chitosan as natural biopolymer: potential sources, pretreatments, and degradation pathways,” *Biomass Convers Biorefin*, vol. 14, no. 4, pp. 4567–4581, Feb. 2024, doi: 10.1007/s13399-022-02684-x.

[171] P. Sirajudheen, N. C. Poovathumkuzhi, S. Vigneshwaran, B. M. Chelaveettil, and S. Meenakshi, “Applications of chitin and chitosan based biomaterials for the adsorptive removal of textile dyes from water — A comprehensive review,” *Carbohydr Polym*, vol. 273, p. 118604, Dec. 2021, doi: 10.1016/j.carbpol.2021.118604.

[172] W. Boulaiche, B. Hamdi, and M. Trari, “Removal of heavy metals by chitin: equilibrium, kinetic and thermodynamic studies,” *Appl Water Sci*, vol. 9, no. 2, p. 39, Mar. 2019, doi: 10.1007/s13201-019-0926-8.

[173] R. Kh. Khamizov, “A Pseudo-Second Order Kinetic Equation for Sorption Processes,” *Russian Journal of Physical Chemistry A*, vol. 94, no. 1, pp. 171–176, Jan. 2020, doi: 10.1134/S0036024420010148.

[174] R. Ezzati, “A new insight into the pseudo-second-order model and the physical meaning of its rate constant in adsorption,” *J Dispers Sci Technol*, pp. 1–8, Nov. 2023, doi: 10.1080/01932691.2023.2288090.

[175] A. A. Mohammed, O. A. Abdel Moamen, S. S. Metwally, A. M. El-Kamash, I. Ashour, and M. S. Al-Geundi, “Utilization of Modified Attapulgite for the Removal of Sr(II), Co(II), and Ni(II) Ions

from Multicomponent System, Part I: Kinetic Studies," *Environmental Science and Pollution Research*, vol. 27, no. 7, pp. 6824–6836, Mar. 2020, doi: 10.1007/s11356-019-07292-3.

[176] S. Shahabuddin, S. N. A. Baharin, N. F. Suhaimi, N. Yunus, and K. P. Sambasevam, "Preparation of shrimp-based chitin blend with polyaniline for chromium (VI) removal from aqueous solution," *Mater Today Proc*, vol. 62, pp. 6940–6944, 2022, doi: 10.1016/j.matpr.2021.12.299.

[177] T. A. Salah, A. M. Mohammad, M. A. Hassan, and B. E. El-Anadouli, "Development of nano-hydroxyapatite/chitosan composite for cadmium ions removal in wastewater treatment," *J Taiwan Inst Chem Eng*, vol. 45, no. 4, pp. 1571–1577, Jul. 2014, doi: 10.1016/j.jtice.2013.10.008.

[178] Y. Ren, H. A. Abbood, F. He, H. Peng, and K. Huang, "Magnetic EDTA-modified chitosan/SiO2/Fe3O4 adsorbent: Preparation, characterization, and application in heavy metal adsorption," *Chemical Engineering Journal*, vol. 226, pp. 300–311, Jun. 2013, doi: 10.1016/j.cej.2013.04.059.

[179] T. Shahnaz, M. M. F. S., P. V.C., and S. Narayanasamy, "Surface modification of nanocellulose using polypyrrole for the adsorptive removal of Congo red dye and chromium in binary mixture," *Int J Biol Macromol*, vol. 151, pp. 322–332, May 2020, doi: 10.1016/j.ijbiomac.2020.02.181.

[180] A. Babakhani and M. Sartaj, "Competitive adsorption of nickel(II) and cadmium(II) ions by chitosan cross-linked with sodium tripolyphosphate," *Chem Eng Commun*, vol. 209, no. 10, pp. 1348–1366, Oct. 2022, doi: 10.1080/00986445.2021.1966424.

[181] N. Conte and J. M. Gómez, "Improving the sorption properties of mesoporous carbons for the removal of cobalt, nickel and manganese from spent lithium-ion batteries effluent," *Sep Purif Technol*, vol. 328, p. 125095, Jan. 2024, doi: 10.1016/j.seppur.2023.125095.

[182] X. Peng, J. Yan, C. He, R. Liu, and Y. Liu, "Sustainable triethylenetetramine modified sulfonated graphene oxide/chitosan composite for enhanced adsorption of Pb(II), Cd(II), and Ni(II) ions," *Int J Biol Macromol*, vol. 261, p. 129741, Mar. 2024, doi: 10.1016/j.ijbiomac.2024.129741.

[183] A. Rahman, M. A. Haque, S. Ghosh, P. Shinu, M. Attimarad, and G. Kobayashi, "Modified Shrimp-Based Chitosan as an Emerging Adsorbent Removing Heavy Metals (Chromium, Nickel, Arsenic, and Cobalt) from Polluted Water," *Sustainability*, vol. 15, no. 3, p. 2431, Jan. 2023, doi: 10.3390/su15032431.

[184] A. Rahman, "Promising and Environmentally Friendly Removal of Copper, Zinc, Cadmium, and Lead from Wastewater Using Modified Shrimp-Based Chitosan," *Water (Basel)*, vol. 16, no. 1, p. 184, Jan. 2024, doi: 10.3390/w16010184.

[185] M. Kavisri *et al.*, "Adsorption isotherm, kinetics and response surface methodology optimization of cadmium (Cd) removal from aqueous solution by chitosan biopolymers from cephalopod waste," *J Environ Manage*, vol. 335, p. 117484, Jun. 2023, doi: 10.1016/j.jenvman.2023.117484.

[186] S. Boddu, A. Chandra, and A. Ali Khan, "Biosorption of Cu(II), Pb(II) from electroplating industry effluents by treated shrimp shell," *Mater Today Proc*, vol. 57, pp. 1520–1527, 2022, doi: 10.1016/j.matpr.2021.12.052.

[187] X. Liu, X. Zhao, Y. Liu, and T. Zhang, "Review on preparation and adsorption properties of chitosan and chitosan composites," *Polymer Bulletin*, vol. 79, no. 4, pp. 2633–2665, Apr. 2022, doi: 10.1007/s00289-021-03626-9.

[188] A. Babakhani and M. Sartaj, "Optimization of Nickel(II) adsorption by sodium tripolyphosphate crosslinked chitosan using response surface methodology (RSM)," *Sustainable Chemistry for the Environment*, vol. 2, p. 100019, Aug. 2023, doi: 10.1016/j.scenv.2023.100019.

[189] Amrutha, G. Jeppu, C. R. Girish, B. Prabhu, and K. Mayer, "Multi-component Adsorption Isotherms: Review and Modeling Studies," *Environmental Processes*, vol. 10, no. 2, p. 38, Jun. 2023, doi: 10.1007/s40710-023-00631-0.

[190] J. W. Miller, "Adsorption Technology: A Step-by-Step Approach to Process Evaluation and Application," *J Environ Qual*, vol. 15, no. 1, pp. 94–94, Jan. 1986, doi: 10.2134/jeq1986.00472425001500010024x.

[191] M. Horsfall, A. A. Abia, and A. I. Spiff, "Kinetic studies on the adsorption of Cd2+, Cu2+ and Zn2+ ions from aqueous solutions by cassava (Manihot sculenta Cranz) tuber bark waste," *Bioresour Technol*, vol. 97, no. 2, pp. 283–291, Jan. 2006, doi: 10.1016/j.biortech.2005.02.016.

[192] E. Igberase, P. Osifo, and A. Ofomaja, "The Adsorption of Pb, Zn, Cu, Ni, and Cd by Modified Ligand in a Single Component Aqueous Solution: Equilibrium, Kinetic, Thermodynamic, and Desorption Studies," *Int J Anal Chem*, vol. 2017, pp. 1–15, 2017, doi: 10.1155/2017/6150209.

[193] J. Qu *et al.*, "Multi-component adsorption of Pb(II), Cd(II) and Ni(II) onto microwave-functionalized cellulose: Kinetics, isotherms, thermodynamics, mechanisms and application for electroplating wastewater purification," *J Hazard Mater*, vol. 387, p. 121718, Apr. 2020, doi: 10.1016/j.jhazmat.2019.121718.

[194] K. Kayalvizhi *et al.*, "Adsorption of copper and nickel by using sawdust chitosan nanocomposite beads – A kinetic and thermodynamic study," *Environ Res*, vol. 203, p. 111814, Jan. 2022, doi: 10.1016/j.envres.2021.111814.

[195] A. Babakhani and M. Sartaj, "Synthesis, characterization, and performance evaluation of ion-imprinted crosslinked chitosan (with sodium tripolyphosphate) for cadmium biosorption," *J Environ Chem Eng*, vol. 10, no. 2, p. 107147, Apr. 2022, doi: 10.1016/j.jece.2022.107147.

[196] A. Babakhani and M. Sartaj, "Optimization of Nickel(II) adsorption by sodium tripolyphosphate crosslinked chitosan using response surface methodology (RSM)," *Sustainable Chemistry for the Environment*, vol. 2, p. 100019, Aug. 2023, doi: 10.1016/j.scenv.2023.100019.

[197] E. D. Revellame, D. L. Fortela, W. Sharp, R. Hernandez, and M. E. Zappi, "Adsorption kinetic modeling using pseudo-first order and pseudo-second order rate laws: A review," *Clean Eng Technol*, vol. 1, p. 100032, Dec. 2020, doi: 10.1016/j.clet.2020.100032.

[198] J. S. Piccin, T. R. S. Cadaval, L. A. A. de Pinto, and G. L. Dotto, "Adsorption Isotherms in Liquid Phase: Experimental, Modeling, and Interpretations," in *Adsorption Processes for Water Treatment and Purification*, Cham: Springer International Publishing, 2017, pp. 19–51. doi: 10.1007/978-3-319-58136-1_2.

[199] X. S. Wang, H. H. Miao, W. He, and H. L. Shen, "Competitive Adsorption of Pb(II), Cu(II), and Cd(II) Ions on Wheat-Residue Derived Black Carbon," *J Chem Eng Data*, vol. 56, no. 3, pp. 444–449, Mar. 2011, doi: 10.1021/je101079w.

[200] I. Marzuki, R. S. Alwi, - Erniati, - Mudyawati, - Sinardi, and A. S. Iryani, "Chitosan Performance of Shrimp Shells in The Biosorption Ion Metal of Cadmium, Lead and Nickel Based on Variations Ph Interaction," in *Proceedings of the First International Conference on Materials Engineering and Management - Engineering Section (ICMEMe 2018)*, Paris, France: Atlantis Press, 2019. doi: 10.2991/icmeme-18.2019.2.

[201] N. You, X.-F. Wang, J.-Y. Li, H.-T. Fan, H. Shen, and Q. Zhang, "Synergistic removal of arsanilic acid using adsorption and magnetic separation technique based on Fe3O4@ graphene nanocomposite," *Journal of Industrial and Engineering Chemistry*, vol. 70, pp. 346–354, Feb. 2019, doi: 10.1016/j.jiec.2018.10.035.

[202] Y.-X. Song, S. Chen, N. You, H.-T. Fan, and L.-N. Sun, "Nanocomposites of zero-valent Iron@Activated carbon derived from corn stalk for adsorptive removal of tetracycline antibiotics," *Chemosphere*, vol. 255, p. 126917, Sep. 2020, doi: 10.1016/j.chemosphere.2020.126917.

[203] H. Basu, S. Saha, I. A. Mahadevan, M. V. Pimple, and R. K. Singhal, "Humic acid coated cellulose derived from rice husk: A novel biosorbent for the removal of Ni and Cr," *Journal of Water Process Engineering*, vol. 32, p. 100892, Dec. 2019, doi: 10.1016/j.jwpe.2019.100892.

[204] D. Dou *et al.*, "Adsorption of copper (II) and cadmium (II) ions by in situ doped nano-calcium carbonate high-intensity chitin hydrogels," *J Hazard Mater*, vol. 423, p. 127137, Feb. 2022, doi: 10.1016/j.jhazmat.2021.127137.

[205] G. Gök, H. Kocyigit, O. Gök, and H. Celebi, "The use of raw shrimp shells in the adsorption of highly polluted waters with Co2+," *Chemical Engineering Research and Design*, vol. 186, pp. 229–240, Oct. 2022, doi: 10.1016/j.cherd.2022.07.041.

[206] D. Yadav and J. Dutta, "Development and characterization of novel CS-ZnO-Alg polyelectrolyte complex for enhanced removal of Cd(II), Cu(II), and Ni(II) from simulated paint industrial

wastewater," *Colloids and Surfaces C: Environmental Aspects*, vol. 2, p. 100043, Nov. 2024, doi: 10.1016/j.colsuc.2024.100043.

[207] A. Rahmatpour and A. H. Alizadeh, "Biofilm hydrogel derived from physical crosslinking (self-assembly) of xanthan gum and chitosan for removing Cd2+, Ni2+, and Cu2+ from aqueous solution," *Int J Biol Macromol*, vol. 266, p. 131394, May 2024, doi: 10.1016/j.ijbiomac.2024.131394.

Appendices

Appendix A: Complementary Results

A1: Kinetic study

The following Figure shows the kinetic study for Cu(II), Cd(II) and Ni(II) adsorption onto Ch-C in a single-component system.

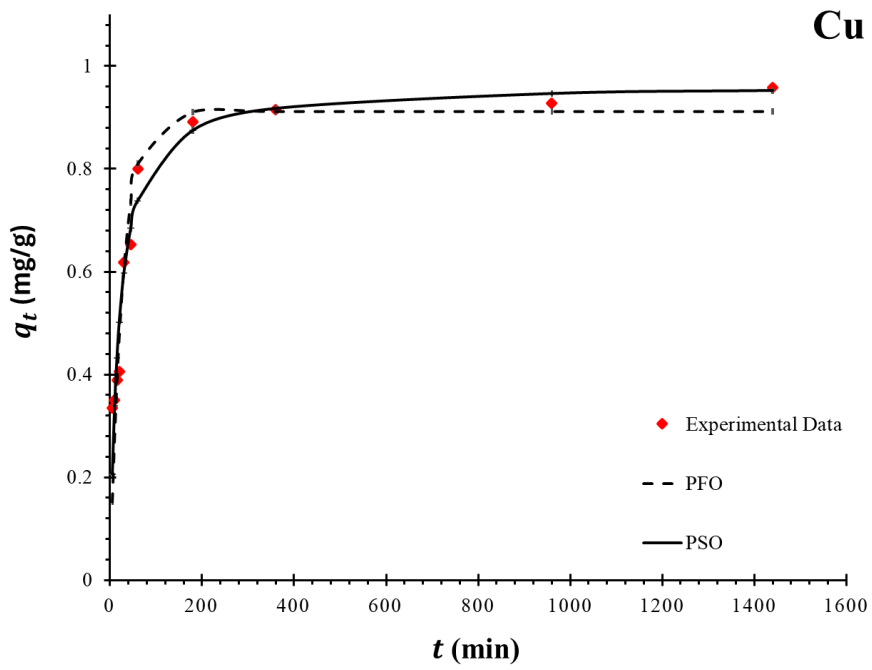

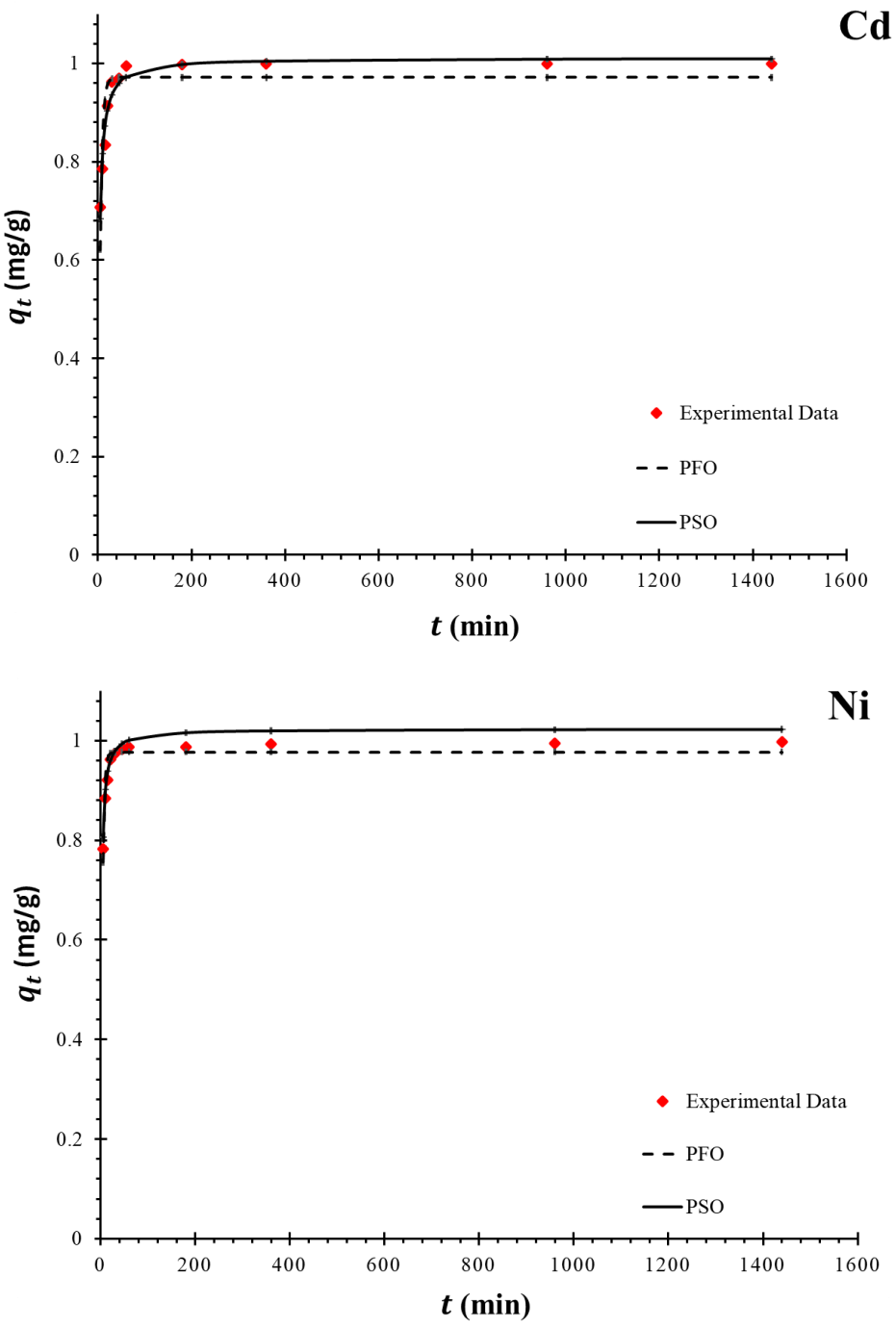

Fig A1- 1 Kinetic study for HMs' adsorption onto Ch-C in a single-component system.

The following Figures show the kinetic study for Cu(II), Cd(II) and Ni(II) adsorption onto Ch-C and Ch-DES in a multi-component system.

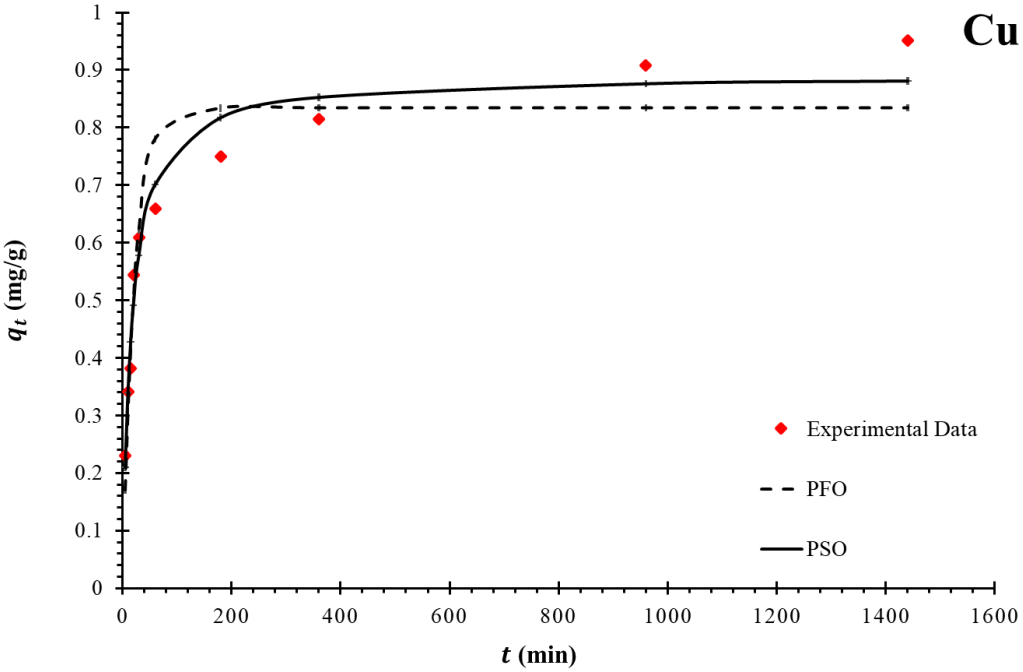
Cu
q_t (mg/g)
t (min)
Experimental Data
PFO
PSO
0
0.1
0.2
0.3
0.4
0.5
0.6
0.7
0.8
0.9
1
0
200
400
600
800
1000
1200
1400
1600

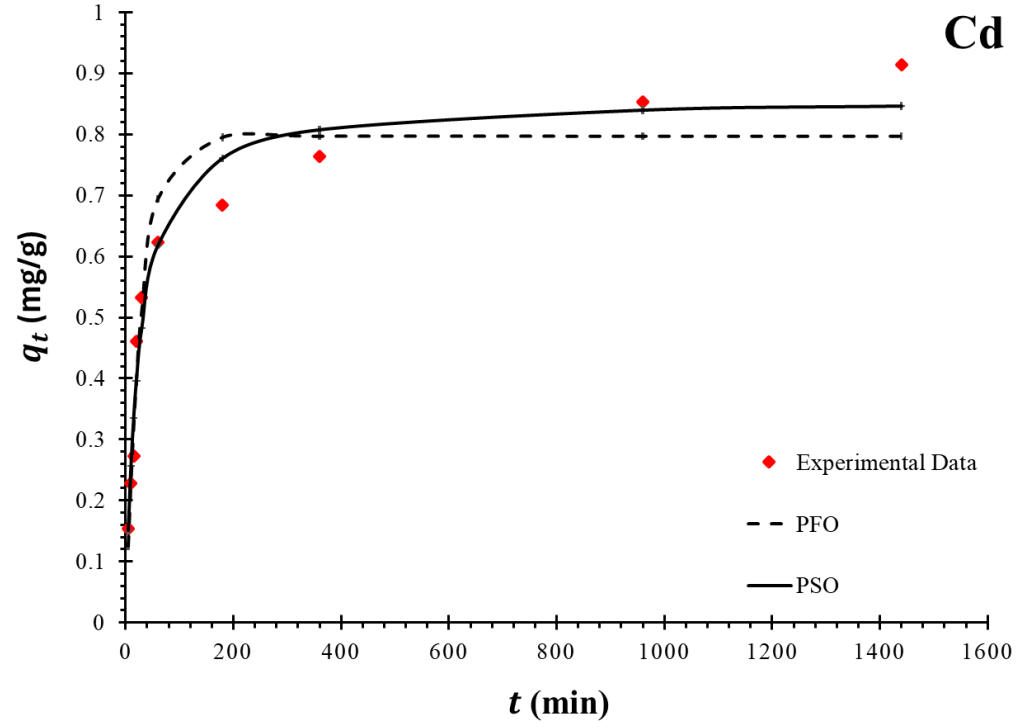
Cd
q_t (mg/g)
t (min)
Experimental Data
PFO
PSO
0
0.1
0.2
0.3
0.4
0.5
0.6
0.7
0.8
0.9
1
0
200
400
600
800
1000
1200
1400
1600

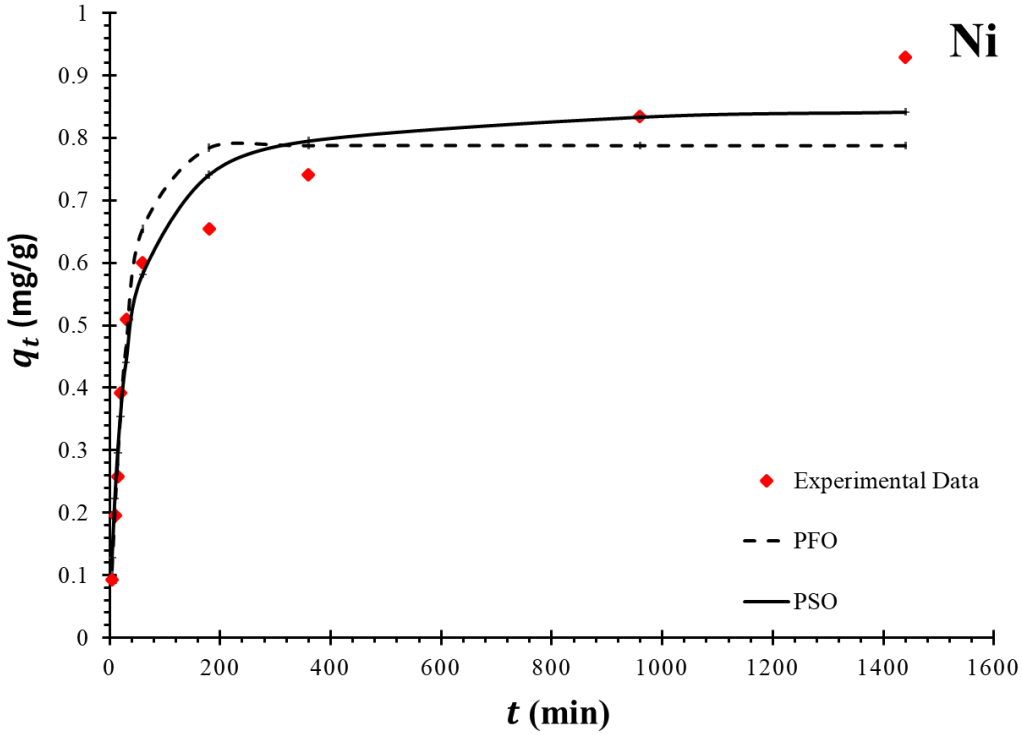

Fig A1- 2 Kinetic study for HMs' adsorption onto Ch-C in a multi-component system.

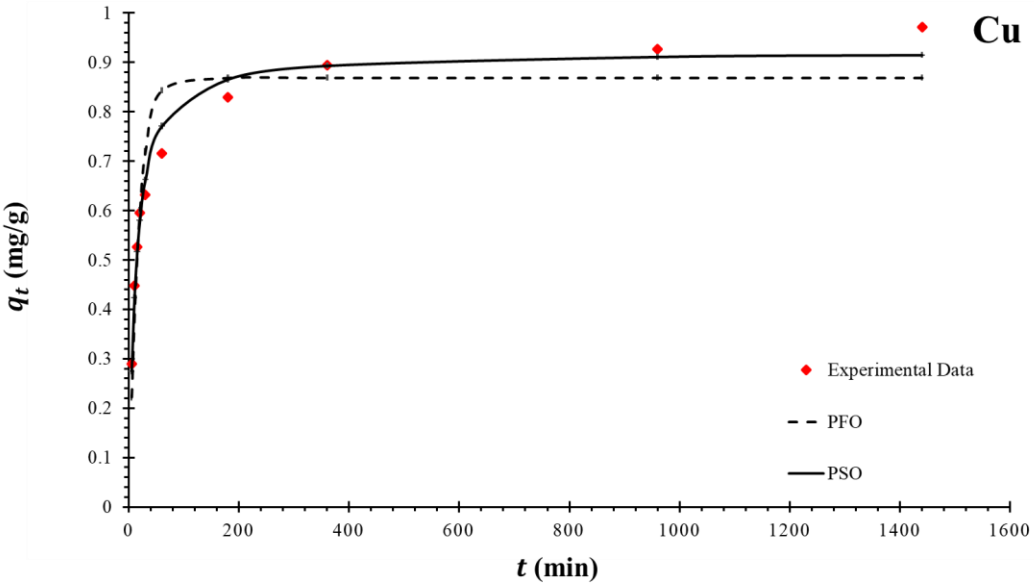

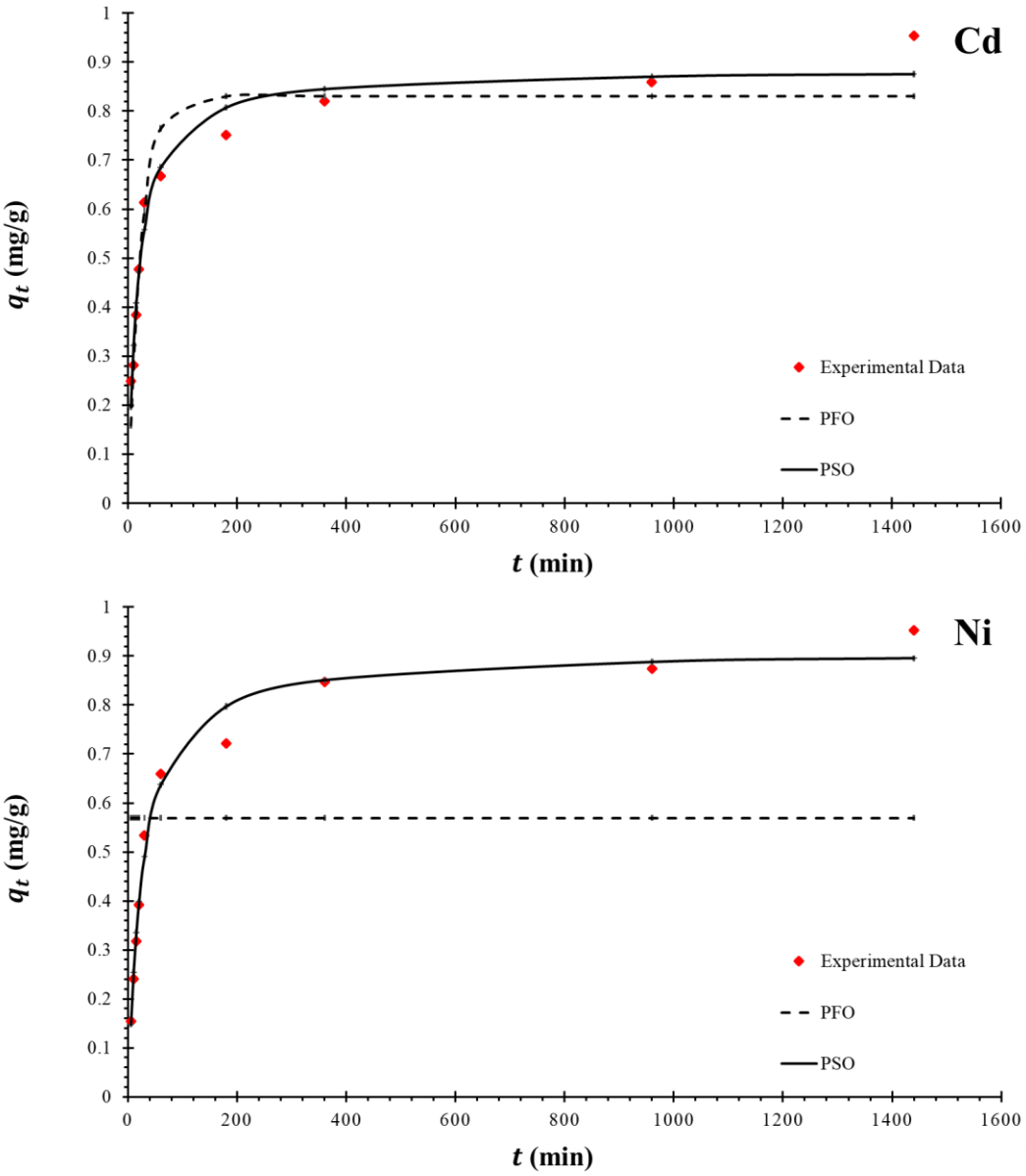

Fig A1-3 Kinetic study for HMs' adsorption onto Ch-DES in a multi-component system.

A2: Freundlich Isotherm study of multi-component systems onto Ch-C and Ch-DES

The following Figure shows the isotherm study for Cu(II), Cd(II) and Ni(II) adsorption onto Ch-C and Ch-DES in a multi-component system.

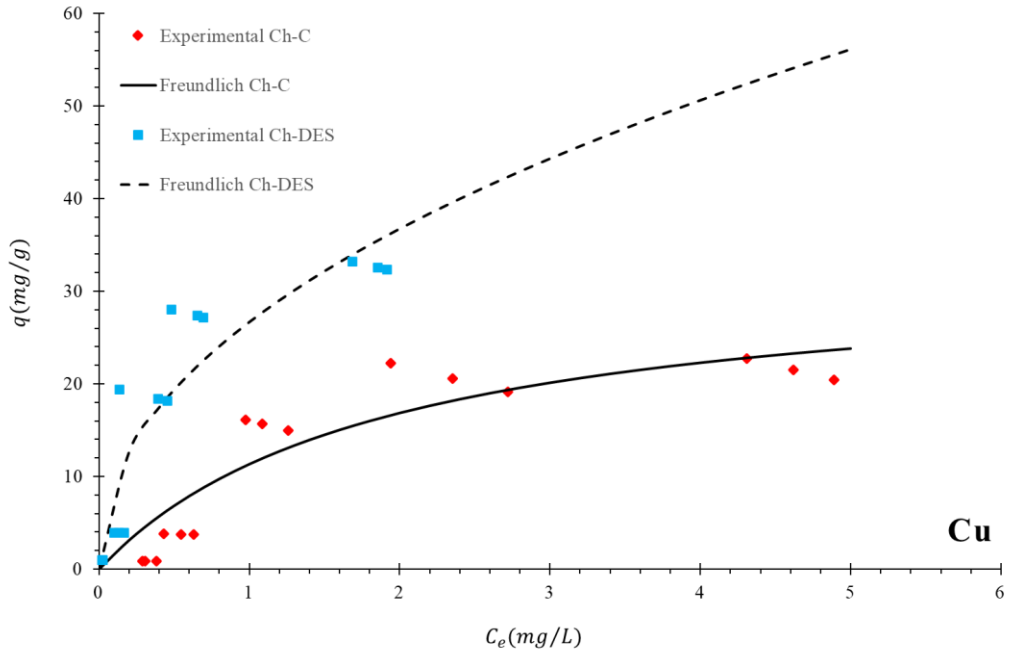
Experimental Ch-C
Freundlich Ch-C
Experimental Ch-DES
Freundlich Ch-DES
$q(mg/g)$
$C_e(mg/L)$
Cu

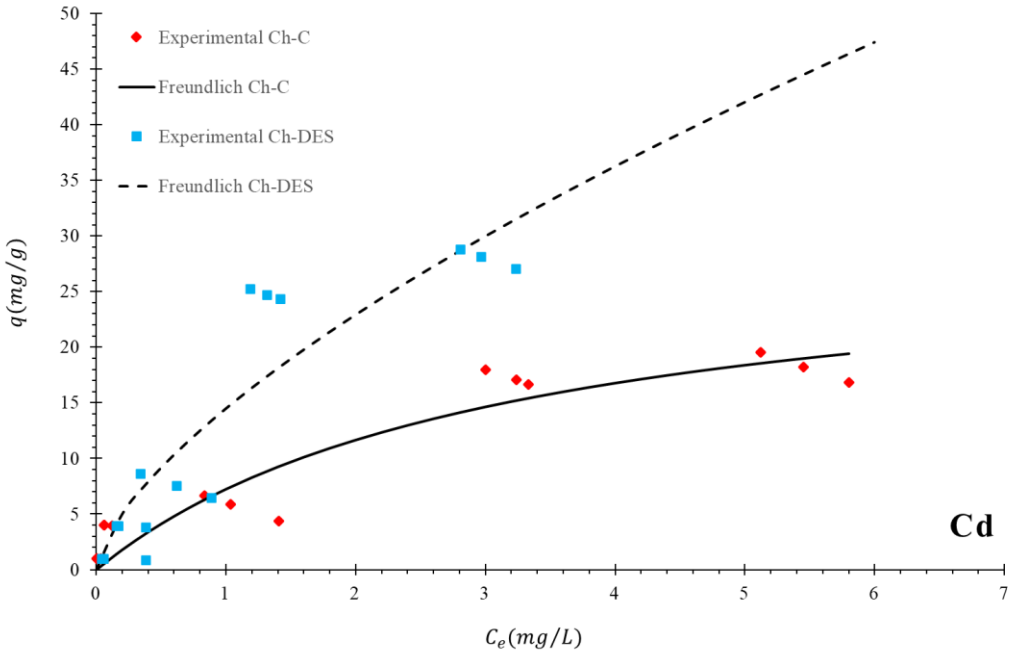
Experimental Ch-C
Freundlich Ch-C
Experimental Ch-DES
Freundlich Ch-DES
$q(mg/g)$
$C_e(mg/L)$
Cd

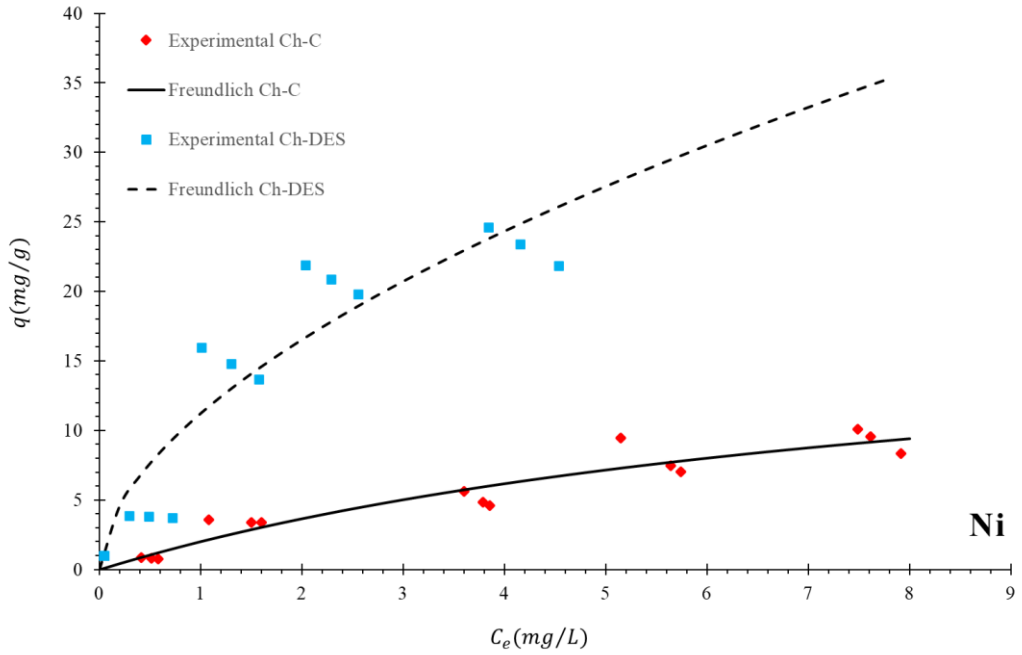

Fig A2- 1 Experimental data and Freundlich model for initial concentration 2.5, 10, 50, 75 and 100 ppm of Cu(II), Cd(II) and Ni(II) on Ch-C and Ch-DES with dosage 2.5 g/L at 20 °C in a competitive environment.

A3: FT-IR analysis of Ch-C and SSW in a single-component system

The following Figures shows the FT-IR study for Cu(II), Cd(II) and Ni(II) adsorption onto Ch-C and SSW in a single-component system and Ch-DES in a single-component system. The samples' condition for FT-IR analysis were, initial concentration of 25 ppm, 24 hours, room temperature, pH=6 for Cd and 5 for both Cu and Ni adsorption onto Ch-C and SSW.

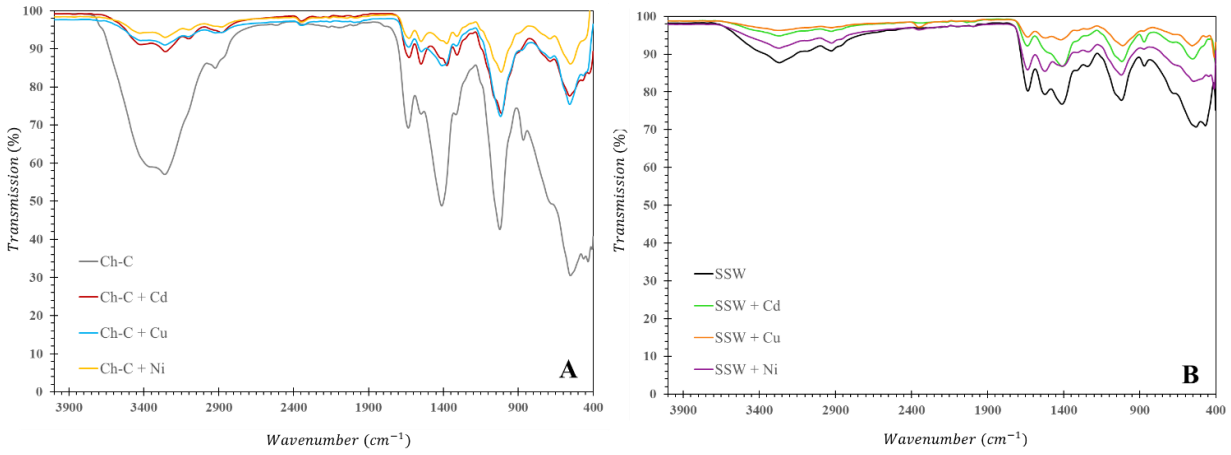

Fig A3-1 FT-IR analysis on (A) Ch-C and Ch-C loaded with Cd(II), Cu(II), and Ni(II); (B) SSW and SSW loaded with Cd(II), Cu(II), and Ni(II).

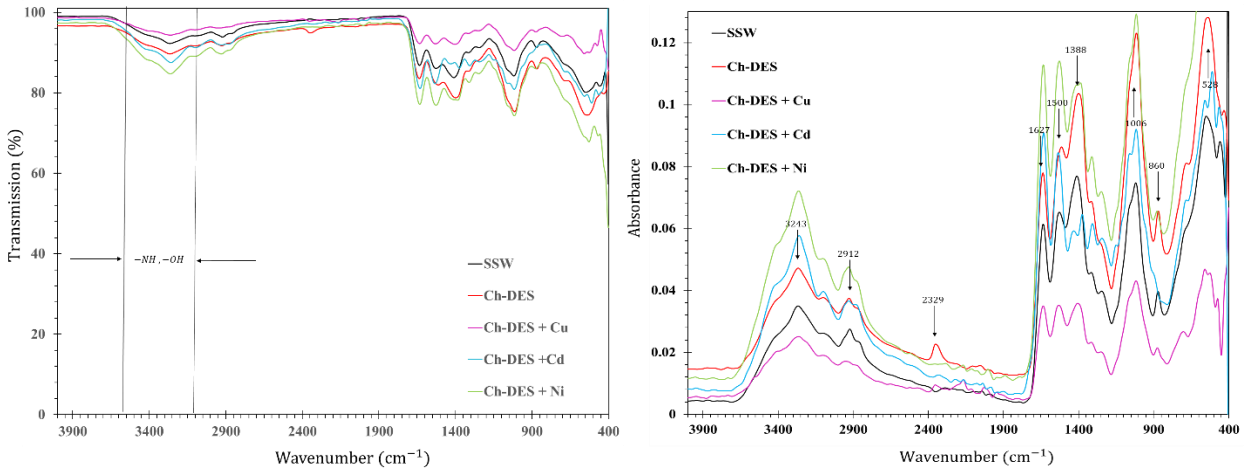

Figure A3-2 FT-IR analysis on Ch-DES and Ch-DES loaded with Cd(II), Cu(II), and Ni(II).

A4: SEM-EDS analysis on Ch-DES in a single-component system

The SEM-EDS analysis of Ch-DES after Cu, Cd and Ni adsorption in a single-component system is shown in Fig. AP 2-1 (a), (b) and (c), respectively. The EDS analysis showed the presence of carbon and oxygen, both of which are components of the chitin structure; plus, the Au and Pd peaks in the obtained spectra were caused by the samples being coated with gold-palladium. The EDS data confirmed the presence of Cu(II), Cd(II) and Ni(II) signals, with Cu showing the highest peak which confirms the highest removal

efficiency. Moreover, the chloride peak has also appeared in the EDS spectrum which is due to the choline chloride (HBA) in the DES synthesis.

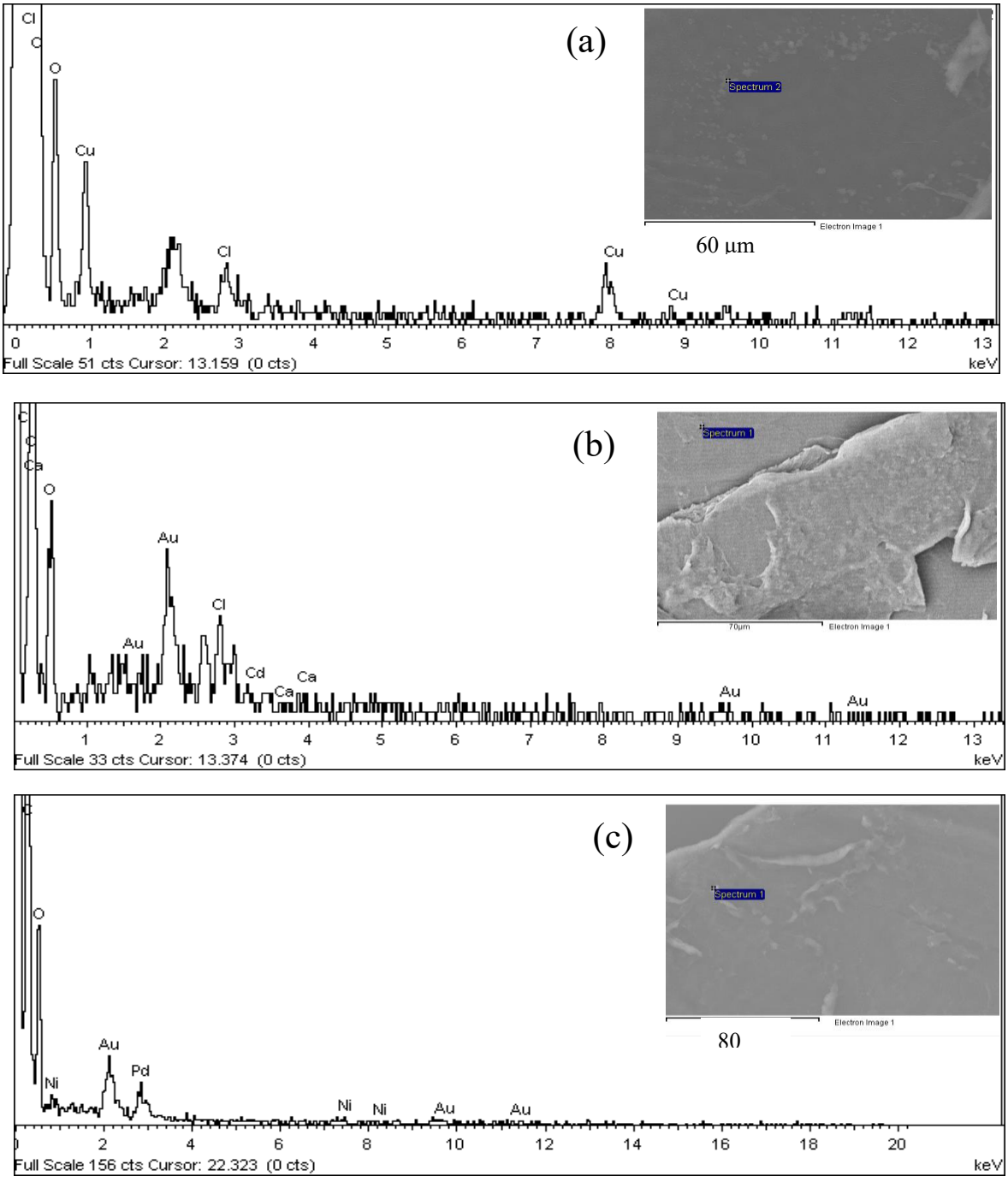

Figure A4-1 SEM-EDS analysis; (a) Cu, (b) Cd, and (c) Ni.